Ohio Water Resources Center
Annual Technical Report
FY 2013

Introduction

Pursuant to the Water Resources Research Act of 1964, the Ohio Water Resources Center (Ohio WRC) is the federally-authorized and state-designated Water Resources Research Institute (WRRI) for the State of Ohio.

The Ohio WRC was originally established at The Ohio State University (OSU) in 1959 as part of the College of Engineering's Engineering Experiment Station and it conducted an extensive program of research on water and wastewater treatment processes. The Center continues to be administered through the College of Engineering and has maintained a tradition of placing special emphasis on encouraging and supporting research in the area of physical, chemical, and biological treatment processes for water and wastewater. The mission of Ohio WRC is to promote innovative, water-related research in the State of Ohio through research grant competitions, coordination of interdisciplinary research proposals, and educational outreach activities.

Research Program Introduction

Over this past year's reporting period we sponsored seven new research projects conducted at five different Ohio universities totaling $393,518 in research funding (direct and cost share). The PI's for these projects are four Assistant Professors, two Research Scientists and one Full Professor. They advise in total eleven students majoring in environmental engineering, chemical engineering, biochemistry, chemistry, biology and other water related fields.

The funded research projects entail studies of important Ohio water resources problems. For example, Dr. Christopher Spiese from Ohio Northern University investigated the proportion of nutrient stream pollution resulting from on-site wastewater treatment units. Three projects were not yet finalized and will be ongoing in the next year. They include Dr. George Bullerjahn's investigation of methods for source tracking of Microcystin blooms, Dr. Ishi Buffam's research on the effectiveness of biochar use in vegetative roofs and Dr. Paula Mouser's research on limiting biofouling of ceramic membranes. Three projects sponsored from funds different than the 104 USGS funds were initiated this reporting period. One to support Dr. Isabel Escobar's research on novel biologically inspired membranes and two small seed grants to Dr. Mary Ann Thomas at the USGS to measure methane presence in groundwater wells and to Dr. Chin-Ming Chen to test a novel coal combustion byproduct-based media for treating agricultural wastewater. Several projects from previous years (four funded by USGS and one funded by other source) were successfully concluded during this reporting period.

In summary we administered 12 research projects this reporting period, 8 of which were funded by USGS 104 base grants. In total this resulted in the training of 20 students, 6 manuscripts in development, submitted or accepted in peer-review journals and 27 presentations or posters at local, national or international conferences. In this reporting period our PI's have been able to secure an additional $1,128,307 in research awards using data generated with Center funding.

The Constructed Wetland Dilemma: Nitrogen Removal at the Expense of Methane Generation?

Basic Information

Title:	The Constructed Wetland Dilemma: Nitrogen Removal at the Expense of Methane Generation?
Project Number:	2011OH205B
Start Date:	3/1/2011
End Date:	8/31/2013
Funding Source:	104B
Congressional District:	OH-12
Research Category:	Engineering
Focus Category:	Nitrate Contamination, Wetlands, Ecology
Descriptors:	
Principal Investigators:	Paula J Mouser, Gil Bohrer

Publications

1. Mouser, Paula, Michael Brooker, William Mitsch, Gil Bohrer, 2012, Factors Influencing Microbial Gas Production Rates in a Constructed Wetland Ecosystem. Oral Presentation, 5/2012, In 30th AMS Conference on Agricultural and Forest Meteorology, Boston, MA.
2. Bohrer, Gil; Liel Naor-Azrieli; Scott Mesi; Paula Mouser; K Stefanik; KV Schafer; William Mitsch, 2012, Determining the meteorological forcing that affect seasonal and diurnal dynamics of methane emissions at a constructed urban wetland in Ohio. Oral Presentation, 5/2012, In 30th AMS Conference on Agricultural and Forest Meteorology, Boston, MA.
3. Shafer, KV; Gil Bohrer, Liel Naor-Azrieli, Paula Mouser, William Mitch, M Wu, 2011, Temporal Dynamics of Methane Fluxes in Temperate Urban Wetlands, Poster Presentation B12C-05, 12/2011, In American Geophysical Annual Meeting, San Francisco, CA.
4. Naor-Azrieli, Liel; Gil Bohrer, William Mitsch, 2011, Collaborative research: Greenhouse gas balance of urban temperate wetlands. Oral presentation, 5/2011, In Annual Meeting of the American Ecological Engineering Society, Ashville, NC.
5. Mouser, PJ, Brooker, M, Bohrer, G. (2012), Factors Influencing Microbial Gas Production Rates in Wetland Sediments. Oral Presentation, 10/2012. 4th International EcoSummit Ecological Sustainability: Restoring the Planet's Ecosystem Services, Columbus, OH.
6. Brooker, M, Mitsch, W, Bohrer, G, Mouser, PJ. (2012), Factors Influencing Methane Emission Potential from Wetland Sediments. Oral Presentation, 6/2012. 2012 Ohio River Basin Consortium for Research and Education Symposium, Athens, OH.
7. Brooker, M., Bohrer, G., Mouser, P.J. (2012) Factors Influencing Microbial Carbon Emission Potential from Wetland Sediments and its Relation to Surface- and Plot-Scale Measurements, B33C-0536, poster presentation at Fall Meeting, AGU, San Francisco, Calif., 3-7 Dec.
8. Mouser, PJ, Brooker, M, Bohrer, G. (2012), Factors Influencing Microbial Gas Production Rates in Wetland Sediments. Oral Presentation, 10/2012. 4th International EcoSummit Ecological Sustainability: Restoring the Planet's Ecosystem Services, Columbus, OH.
9. Brooker, M, Mitsch, W, Bohrer, G, Mouser, PJ. (2012), Factors Influencing Methane Emission Potential from Wetland Sediments. Oral Presentation, 6/2012. 2012 Ohio River Basin Consortium for

Research and Education Symposium, Athens, OH.
10. Brooker, M., Bohrer, G., Mouser, P.J. (2012) Factors Influencing Microbial Carbon Emission Potential from Wetland Sediments and its Relation to Surface- and Plot-Scale Measurements, B33C-0536, poster presentation at Fall Meeting, AGU, San Francisco, Calif., 3-7 Dec.
11. *Brooker, M.R., Bohrer, G., Mouser, P.J. (2014) Variations in Potential CH4 Flux and CO2 Respiration from Freshwater Wetland Sediments that Differ by Microsite Location, Depth, and Temperature. Ecological Engineering (in review).

Final Report 2011-2013

Contract Information

Title	The Constructed Wetland Dilemma: Nitrogen Removal at the Expense of Methane Generation?
Project Number	60030648
Start Date	6/1/2011
End Date	9/21/2013
Focus Category	Methanogenesis, Denitrification, Wetlands, Ecology
Keywords	Microbial Ecology, Biogeochemistry, Methanogenesis, Constructed Wetlands
Lead Institute	The Ohio State University
Principle Investigators	Paula Mouser and Gil Bohrer

Abstract

Fixed nitrogen (N) is required for the growth for all biological organisms, and agriculture is dependent upon nitrogen for fertilizer. When present at elevated levels in water resources, however, nitrate-N concentrations present human and environmental health risks, including contributing to the eutrophication of some water bodies and coastal zones. Ohio exports significant levels of nitrogen in its surface waters and groundwater to Lake Erie and the Mississippi Basin due to its geology and agricultural land management techniques. Constructed wetlands can be used for nitrogen removal through the biologically-mediated process of denitrification, where nitrite is reduced to nitrogen gas and released to the atmosphere. Unfortunately, denitrification in wetlands comes with the tradeoff of increased Green House Gas (GHG) production. Wetlands sequester large amounts of carbon (C) from the atmosphere, removing the most common GHG - CO_2 but produce another and more potent GHG – methane (CH_4). In order to allow development of wetlands as a solution for N removal without concerns of GHG emissions, it is critical to understand what factors control methane production, and how they relate to wetland aquatic conditions. The proposed work will examine the interaction between environmental factors (temperature, depth, and microsite) based on inocula-based laboratory experiments. Microcosms constructed from the sediments from distinct horizons within each microsite will serve as different sources of microbial communities and chemical substrates. Anaerobic incubation will determine maximum levels of methane and carbon dioxide production from biogeochemical processes. This will direct which factors should be incorporated as parameters in GHG emission models to predict carbon budgets at the ORWRP, and other wetlands.

Methodology

We used anaerobic microcosm experiments developed from wetland sediment and source water to measure the production of methane and carbon dioxide gases, while monitoring solution geochemistry. Two incubation temperatures were used on sediment collected from three distinct microsites across a 1-ha wetland and from two depth horizons. Microsite locations include: (1) an upland area, (2) an edge zone with emergent vegetation, and (3) an unvegetated, central basin. Headspace gas productions during a temporal incubation were used to develop linear gas

production rates which were used to predict maximum gas flux. Statistical methods were used to identify the key factors related to maximum gas production.

Major Activities

We completed a series of experiments over a two-year period that tested the effect of environmental conditions on methane flux from sediment cores. Samples cores were taken in the dormant-season of vegetation growth (November) when water levels were low, and during the growing-season (July) when water levels were high. For the dormant-season experiment, composite 30-cm cores were sample within a 1-m^2 area for the upland, vegetated, and open-water sites (Figure 1). Cores were sampled again during the growing-season experiment at the vegetated and open-water microsites, but split into two 15-cm lengths (Figure 2). Samples were stored under an anaerobic atmosphere until bottles could be constructed using 25-g of sediment and 75-ml of intake water. Carbon amendment was made in a subset of bottles to test for carbon limitation of methanogenic activities. Bottles were placed under an atmosphere of pure N_2 gas and incubated for 77 days. Methane and carbon dioxide concentrations within the headspace were measured using gas chromatography to calculate linear rates of production. Based on sediment density, these rates were translated into equivalent maximum anaerobic flux on a surficial area basis. A linear fit model incorporating random effects to handle the pseudoreplication of samples was used to determine the significant factors acting on the maximum potential GHG fluxes. Concurrent microcosms were used to analyze the solution geochemistry through time.

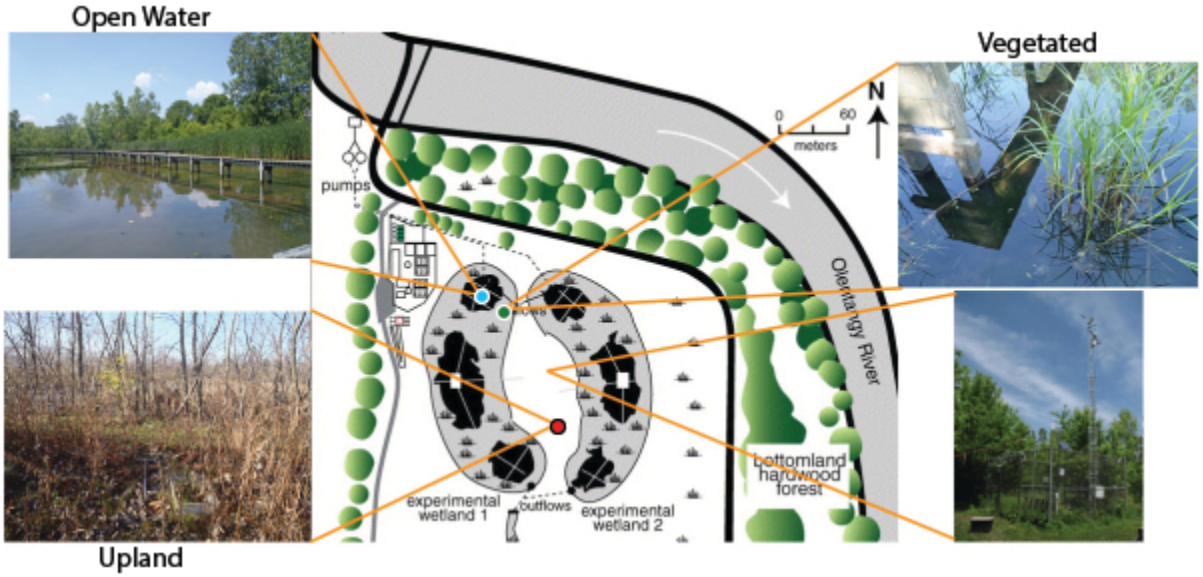

Figure 1. Samping locations used for collection of cores at the ORWRP wetland site. Images show the areas from which cores were taken through the course of both experiments. The location of the eddy flux meteorological tower used for flux comparisons is also shown.

In addition to the above described experiments, we characterized the microbial communities initially present within the four sediments collected during the growing-season (open-water/vegetated microsites at the shallow/deep horizons). High-throughput 454-pyrotagged sequencing was used to obtain >1000 sequence reads of the V4 region of 16S rRNA gene for the

prokaryotic community. These DNA primers target both *Bacteria* and *Archaeal* members in order to identify the most prevalent operational taxonomic units (OTUs). The virtual QIIME pipeline was used to align sequences to the Greengenes database for a taxonomic analysis. A directed approach was taken to analyze the microbial community members that, based on sequence alignment to genus-level OTUs, have been identified within the literature as belonging to a functional guild critical to methanogenesis and GHG flux.

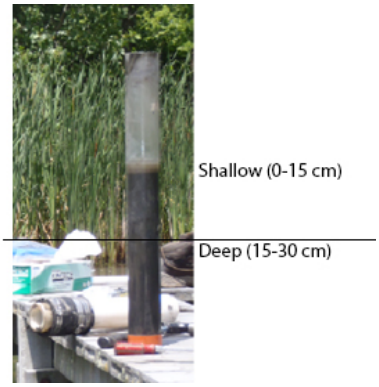

Figure 2. Open-water microsite core from the ORWRP. The shallow and deep horizon depths are indicated by the black line.

Findings

In dormant season experiments, average potential methane flux rate for open-water samples was 3- to 5-fold greater than the VEG and UP wetland microsites (Figure 3). Rates for bottles held at 30ºC were about 3-fold higher than methane and carbon dioxide fluxes from bottles kept at 20ºC. A positive linear correlation was observed between potential carbon dioxide and methane fluxes within microcosms (r^2 = 0.28, p = 0.025, Pearson correlation analysis). Average potential methane flux in growing-season treatments was 70% higher than the dormant-season, while average potential carbon dioxide flux, on the other hand, was 20% lower in growing-season treatments than the dormant-season (Figure 2C-D, respectively). Microsite, temperature, and depth had no significant independent effects on mean potential methane flux during the growing season. However, the interaction between depth and temperature was significant, indicating the increased potential methane flux from shallow microsites was caused by temperature. Mean rates at 30ºC were approximately double those at 20ºC for both potential methane and carbon dioxide flux. Sodium acetate amendment to deep open-water sediments significantly increased production of methane and carbon dioxide compared to ambient samples (Figure 3). Methane flux estimate measured in microcosms were found to be comparable to upper range measurements previously recorded by chambers and eddy flux covariance at the site.

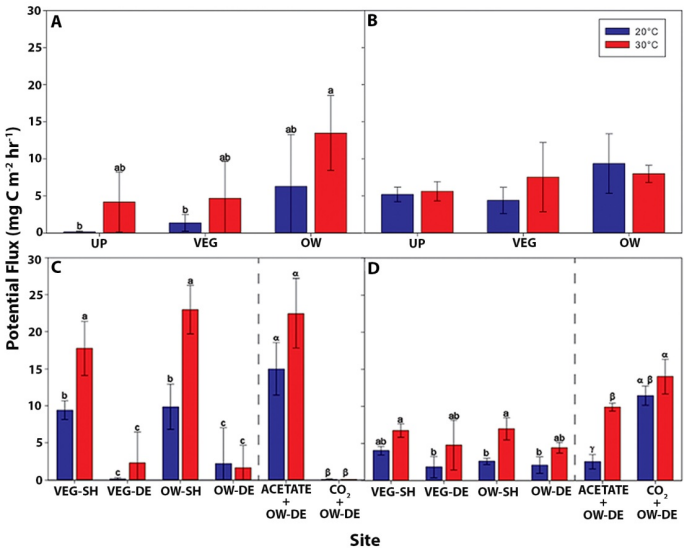

Figure 3. Methane and carbon dioxide flux for dormant season (A and B, n=3) and growing season (C and D, n=5) experimental treatments, respectively. Bars show the standard deviations upland = UP; vegetate = VEG; open-water = OW) microsites at shallow (SH) or deep (DE) horizons. Lower case letters represent significant difference in mean fluxes between treatments. Dashed line indicates the bottles containing acetate or carbon dioxide amendments, with Greek letters indicating significant differences in mean flux.

A comparison of the microbial community members at the phylum hierarchal classification level revealed differences in dominant taxa between the four sediments (Figure 4). Higher richness was observed in the shallow vegetated sediments while lower richness was seen in open-water, deep sediments. The *Proteobacteria,* primarily the α- and δ-*proteobacteria,* were the most dominant group in site sediments. The *Euryarchaeota* (containing methanogens) were of greatest abundance at the open-water microsite. The vegetated microsite contained a greater number of *Nitrospirae* relative to the open-water microsite. Other dominant taxa include: *Bacteroidetes*, *Chloroflexi*, *Verrucomicrobia*, *Acidobacteria*, and *Actinobacteria*.

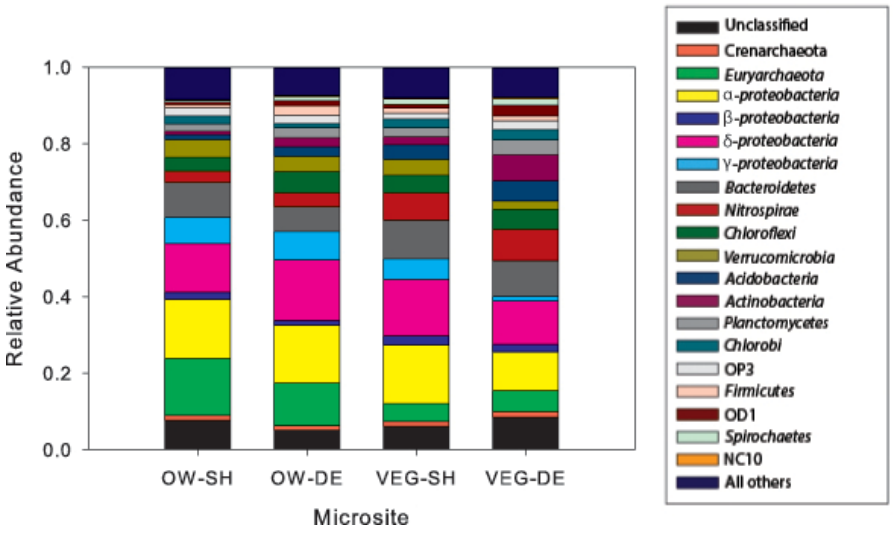

Figure 4. Dominant phyla (with *Proteobacteria* divided into class) for the four sediments sampled detected for the 16S rRNA gene using 454-pyrosequencing. Samples include the vegetated (VEG) and open-water (OW) microsites at the shallow (SH) or deep (DE) horizon. "All Others" represents phyla which were present at <1% across the site.

Significance

A microcosm approach was useful to show that temperature caused an increase in methane flux from temperate freshwater wetlands. Fold changes measured in the laboratory were consistent with those measured *in situ* by chambers and eddy flux across a similar temperature range. Results suggest that although deep sediments contain microbial members associated with methanogenesis, they have weak methanogenic capabilities as a result of substrate availability and competition by bacteria utilizing other electron acceptors. Open water and vegetative microsites had similar potential methane flux from shallow sediments during the growing season, and as hypothesized, fell along the upper range of fluxes measured in the field. If methanogens are respiring at similar rates across microsites, this suggests that larger-scale processes (e.g. redox boundaries, vegetation piping) greatly alters overall emission rates across these wetland microsites.

Publications/Conferences (since 6/2011)
(*Denotes the student working on the project)

<u>Publications</u>
*Brooker, M.R., Bohrer, G., Mouser, P.J. (2014) Variations in Potential CH_4 Flux and CO_2 Respiration from Freshwater Wetland Sediments that Differ by Microsite Location, Depth, and Temperature. *Ecological Engineering* (in review).

Conference Presentations

*Brooker, M.R., Bohrer, G., Mitsch, W.J., Mouser, P.J. Factors Influencing Methane Flux Potential from Wetland Sediments. Oral presentation *Ohio River Basin Consortium for Research and Education 2012 Scientific Symposium*, July 18-20, 2012, Athens, OH.

Mouser, PJ, *Brooker, M., Mitsch, W., Bohrer, G. Factors Influencing Microbial Gas Production Rates in a Constructed Wetland Ecosystem. Oral presentation *American Meteorological Society, First Conference on Atmospheric Biogeosciences,* May 29-June 1, 2012, Boston, MA.

Mouser, PJ, *Brooker, M., and Bohrer, G. Factors Influencing Microbial Gas Production Rates in Wetland Sediments. Oral presentation *4th International EcoSummit on Ecological Sustainability: Restoring the Planet's Ecosystem Services,* Sept 30-Oct 5, 2012, Columbus, OH.

*Brooker, M.R.; Mouser, P.J. and Bohrer, G. Quantifying *in situ* rates of methanogenesis and denitrification in wetland sediments. Poster, *4th International EcoSummit on Ecological Sustainability: Restoring the Planet's Ecosystem Services,* Sept 30-Oct 5, 2012, Columbus, OH.

Students Supported By Project 6/2011--9/2013

One student worked on the project: Michael Brooker – who completed a MS degree through Environmental Sciences Graduate Program in 9/2013.

Awards or Achievements

1. Department of the Interior, USDA, "An integrated approach to foster science-based management of agricultural drainage channels in the Western Lake Erie basin", 2013-2016. PI Jon Witter, co-PI Paula Mouser. $659,979.

Professional Placement of Graduates

Michael Brooker has graduated and continued on to the Ph.D. track of the Environmental Sciences Graduate Program at The Ohio State University.

Generating Renewable Energy on Lake Erie with Wave Energy Converters: A Feasibility Study

Basic Information

Title:	Generating Renewable Energy on Lake Erie with Wave Energy Converters: A Feasibility Study
Project Number:	2011OH239B
Start Date:	3/1/2011
End Date:	2/28/2014
Funding Source:	104B
Congressional District:	15
Research Category:	Engineering
Focus Category:	Models, Surface Water, Water Quality
Descriptors:	
Principal Investigators:	Ethan John Kubatko

Publications

1. Dibling, Dave; Ethan Kubatko, Generating Renewable Energy on Lake Erie with wave energy converters: a feasibility study, Great Lakes Research, in preparation.
2. Kubatko, Ethan, 2011, Development of a high-resolution, nearshore model for Lake Erie, The 10th International Workshop on Multiscale (Un-)structured Mesh Numerical Modelling for coastal, shelf and global ocean dynamics, August 2011.
3. Kubatko, Ethan, 2012, Validation of a high-resolution finite element model for Lake Erie, In World Congress on Computational Mechanics, July 2012.
4. Kubatko, Ethan, 2013, Introducing DG-Wave: A discontinuous Galerkin-based wave prediction model, The ADCIRC Annual Workshop, April 2013.
5. Kubatko, Ethan, 2013, Development and Validation of DG-Wave, US National Congress on Computational Mechanics.
6. Kubatko, Ethan, 2013, Introducing DG-Wave: A discontinuous Galerkin-based wave prediction model, The ADCIRC Annual Workshop, April 2013.
7. Kubatko, Ethan, 2013, Development and Validation of DG-Wave, US National Congress on Computational Mechanics.
8. Nappi, A., Kubatko, E.J., Conroy, C.J., “Development and validation of a discontinuous Galerkin-based wave prediction model,” Advances in Water Resources, to be submitted
9. A. Nappi, Development and application of a discontinuous Galerkin-based wave prediction model, World Congress on Computational Mechanics (WCCM10), Sao Paulo, Brazil, July 2012
10. D. Dibling, Development and validation of a nearshore model for Lake Erie, World Congress on Computational Mechanics (WCCM10), Sao Paulo, Brazil, July 2012

GENERATING RENEWABLE ENERGY ON LAKE ERIE WITH WAVE ENERGY CONVERTERS: A FEASIBILITY STUDY

Principal Investigator:

Ethan J. Kubatko, Assistant Professor
Department of Civil & Environmental Engineering & Geodetic Science
The Ohio State University

1 Research Objectives

The primary objective of this research is to investigate the feasibility of generating clean, renewable energy on Lake Erie by harnessing the Lake's wave energy through the use of a novel kinetic energy harvesting technology called nPower® developed by Tremont Electric, LLC, a Cleveland-based alternative energy company. Specifically, feasibility of this idea will be investigated by performing wave energy simulations that make use of two critical modeling components described in detail below: 1) a *high-resolution*, *unstructured mesh* of Lake Erie that provides highly accurate measurements of the bathymetry and the shoreline of the Lake, see Figure 1; and 2) a *computational model* that consists of a tightly coupled two-dimensional shallow water circulation/spectral wave energy evolution model.

2 Methodology

The current hydrodynamic model used by the Lake Erie Operational Forecast System or LEOFS is the Princeton Oceanic Model or POM. The POM model was developed primarily by Dr. Alan Blumberg and Dr. George Mellor in the late 1970's and uses and sigma coordinate (vertical), curvilinear coordinate (horizontal), free surface, ocean model that also uses a turbulent sub-model. The current POM version used by GLOFS has been modified by Dr. David Schwab of NOAA's Great Lakes Environmental Research Laboratory (GLERL) and by researchers from The Ohio State University. As its input, The model takes surface meteorological data, such as surface wind speed and air temperature, which are obtained from, for example, U.S. and Canadian meteorological buoys (nowcast mode) and the National Weather Services operational North American Mesoscale (NAM) weather forecast model (forecast mode). However, the current models inability to accurately model the nearshore region of Lake Erie has induced the idea that a new model may need to be used to capture this region of Lake Erie.

Besides POM, other potential hydrodynamic models include ADCIRC, GEMSS, QUODDY, ROMS, and DYNLET. However, the flexibility of ADCIRC to be coupled with a wave model(SWAN) makes it the easiest to use. It has been tested and validated in a variety of

different applications such as modeling tides & wind driven circulation, analysis of hurricane storm surge & flooding, dredging feasibility & material disposal studies, larval transport studies, and nearshore marine operations. The ability of ADCIRC to model wind driven circulation in the nearshore region makes it a reputable choice for usage on Lake Erie because Lake Erie is driven by wind.

2.1 Governing Equations

The three main equations that govern the ADCIRC model are the shallow water equations which are the depth-averaged continuity equation($\mathcal{L}$) and the 2D momentum equation($\mathcal{M}$). These hyperbolic PDEs are derived from the Navier-Stokes equations which are the general equations for fluid motion and are:

$$\mathcal{L} \equiv \frac{\partial \zeta}{\partial t} + \nabla \cdot \mathbf{q} = 0 \tag{1}$$

$$\mathcal{M} \equiv \frac{\partial \mathbf{q}}{\partial t} + \nabla \cdot \left(\mathbf{q}\mathbf{q}/H\right) + \tau_{bf}\mathbf{q} + \mathbf{f}_c \times \mathbf{q} + gH\nabla\zeta - \varepsilon\Delta\mathbf{q} - \mathbf{F} = \mathbf{0} \tag{2}$$

The equations above are able to solve the 3 unknowns ζ, u and v. From Equation 1, ζ is the height or elevation of the free surface and $\mathbf{q} \equiv (Hu, Hv)$,where the total height of the water column, $\zeta + h_b$, is H and where u and v are the depth-integrated horizontal velocities or currents. The distance from the datum to the bottom or bathymetric depth(positive downward) is h_b. The constant surface elevation or datum in the case of Lake Erie is set at 184 meters above sea level. The reference datums for bodies of water are generally taken when the water is still. From Equation 2, the bottom friction factor is τ_{bf}, the Coriolis force is $\mathbf{f}_c$, acceleration due to gravity is g, the eddy viscosity coefficient is ε, and $\mathbf{F}$ can potentially, depending on the inputs, contain multiple stresses and forces such as wave radiation stresses, wind radiation stresses, variable atmospheric pressure, and tidal potential forces.

2.2 ADCIRC

The *ADvanced CIRCulation model for oceanic, coastal and estuarine water* or ADCIRC was created as a means of solving 2D and 3D time dependent, free surface circulation and transport problems. ADCIRC offers the user the ability to run in serial or in parallel which allows for faster simulation run times. It also uses the continuous Galerkin method in solving the finite element mesh.

ADCIRC uses the 2D Momentum Equations as they appear in Equations 2; however, they make various manipulations of the Continuity Equation in 1 to create the Generalized Wave Continuity Equation or GWCE, and can be written as:

$$\frac{\partial \mathcal{L}}{\partial t} + \nabla \cdot \mathcal{M} + \tau_0 \mathcal{L} = 0 \tag{3}$$

The GWCE is a weak weighted residual that is solved by ADCIRC along with the 2D momentum equation. During the manipulations of these equations, a user-defined weighting

factor,τ_0, is created. This weighting factor weights the relative contribution of the primitive wave portions of the GWCE. τ_0 is basically a factor that needs to be adjusted and fine tuned to disperse the solution enough as to not cause oscillatory solutions in your model so it runs smoothly. The τ_0 variable is something that only exists in the continuous Galerkin method, CG, version of ADCIRC and not the discontinuous Galerkin method, DG, version of ADCIRC.

Carrying out the partial time derivative of $\mathcal{L}$ and and the $\nabla \cdot \mathcal{M}$ from Equation 3, the GWCE is expanded into:

$$\frac{\partial^2 \zeta}{\partial t^2} + \tau_0 \frac{\partial \zeta}{\partial t} + \frac{\partial J_x}{\partial x} + \frac{\partial J_y}{\partial y} - uH\frac{\partial \tau_0}{\partial x} - vH\frac{\partial \tau_0}{\partial y} = 0, \tag{4}$$

where:

$$\begin{aligned} J_x = -uH\frac{\partial u}{\partial x} - vH\frac{\partial u}{\partial y} + \mathbf{f}_c vH - \frac{g}{2}\frac{\partial \zeta^2}{\partial x} - gH\frac{\partial}{\partial x}\left(\frac{P_{H_20}}{g\rho_0} - \alpha\eta\right) \\ + \frac{\tau_{sx,winds} + \tau_{sx,waves} - \tau_{bx}}{\rho_0} + (M_x - D_x) + u\frac{\partial \zeta}{\partial t} + \tau_0 uH - gH\frac{\partial \zeta}{\partial x}, \end{aligned} \tag{5}$$

$$\begin{aligned} J_y = -uH\frac{\partial v}{\partial x} - vH\frac{\partial v}{\partial y} + \mathbf{f}_c uH - \frac{g}{2}\frac{\partial \zeta^2}{\partial y} - gH\frac{\partial}{\partial y}\left(\frac{P_{H_20}}{g\rho_0} - \alpha\eta\right) \\ + \frac{\tau_{sy,winds} + \tau_{sy,waves} - \tau_{by}}{\rho_0} + (M_y - D_y) + v\frac{\partial \zeta}{\partial t} + \tau_0 vH - gH\frac{\partial \zeta}{\partial y}, \end{aligned} \tag{6}$$

and the vertically-integrated momentum equations determine the currents by:

$$\begin{aligned} \frac{\partial u}{\partial t} + u\frac{\partial u}{\partial x} + v\frac{\partial u}{\partial y} - \mathbf{f}_c v = -g\frac{\partial}{\partial x}\left(\zeta + \frac{P_{H_20}}{g\rho_0} - \alpha\eta\right) + \\ + \frac{\tau_{sx,winds} + \tau_{sx,waves} - \tau_{bx}}{\rho_0 H} + \left(\frac{M_x - D_x}{H}\right), \end{aligned} \tag{7}$$

and:

$$\begin{aligned} \frac{\partial v}{\partial t} + u\frac{\partial v}{\partial x} + v\frac{\partial v}{\partial y} - \mathbf{f}_c u = -g\frac{\partial}{\partial y}\left(\zeta + \frac{P_{H_20}}{g\rho_0} - \alpha\eta\right) + \\ + \frac{\tau_{sy,winds} + \tau_{sy,waves} - \tau_{by}}{\rho_0 H} + \left(\frac{M_y - D_y}{H}\right), \end{aligned} \tag{8}$$

where the atmospheric pressure at the water surface is P_{H_20}, the reference density of water is ρ_0, the Newtonian equilibrium tidal potential is η, and the effective earth elasticity factor is α; the surface stresses caused by winds and waves are $\tau_{sx,winds}$, $\tau_{sy,winds}$, $\tau_{sx,waves}$, and $\tau_{sy,waves}$; the bottom stresses are τ_{bx} and τ_{by}; the lateral stress gradients are M_x and M_y, and the momentum dispersion terms are D_x and D_y. The unknown water level(ζ) and currents (u and v) can be computed by ADCIRC using a linear Lagrange interpolation and solving these expanded Equations 4, 7, and 8 for the three degrees of freedom at every node of the finite element mesh.

2.2.1 ADCIRC Inputs

There are 5 input files that are read by ADCIRC in which 2 of them are required and the other 3 are conditional depending on what your simulation needs are. The *Grid and Boundary Information File* or fort.14 is required and is the the actual finite element mesh that you wish to use. The finite element mesh and the boundary conditions types need to be established in this file. The *Model Parameter and Periodic Boundary Condition File* or fort.15 is the other required input file. The fort.15 file contains most of the parameters required to run ADCIRC. Some of these parameters include the timestep interval, run duration, ramping function options, the τ_0 value you wish to use, meteorological wind/pressure interval, normal flow boundary flow rates, and the station's longitude & latitude for which you would like to have data written for and the interval at which the data should be written. The *Single File Meteorological Forcing Input* or fort.22 is used to inform ADCRIC the number the meteorological fields to be used, the offset that the meteorological data starts in comparison to the start time of the ADCIRC run(if there is one), and the wind velocity multiplication factor. The *Multiple File Meteorological Forcing Input* or fort.221 & fort.222 are the methods used to force the Lake Erie model other than river flows. The fort.221 contains atmospheric pressure recorded by stations around Lake Erie and are measured in units of Pascals(millibars). The fort.222 contains wind velocity in the u and v components from recording stations around Lake Erie at 10 meter heights above the water surface and are in units of m/s.

Once the pressure and wind velocities are read into ADCIRC, the following relationships are computed;

$$P_{H_20} = \frac{P}{100 \times g \times \ \gamma_{H_20}} \tag{9}$$

$$W_S = \|W_V\| \tag{10}$$

$$D_C \ = \ 0.001 \times (0.75 \ + \ 0.067 \times W_S) \tag{11}$$

$$W_{ST} \ = \ D_C \times 0.001293 \times W_V \times W_S \tag{12}$$

where P is the atmospheric pressure read from the fort.221, γ_{H_20} is the density of water, W_S is the wind speed, W_V is the wind velocity read from the fort.222, D_C is the drag coefficient, and W_{ST} is the wind stress. If the calculated D_C is greater than 0.003, then the D_C is set to 0.003.

2.2.2 ADCIRC Outputs

ADCIRC has multiple outputs from which we can use to verify against recorded data at specified meteorological that the model is working; such as, the elevation time series or surface elevation (fort.61), the atmospheric pressure time series(fort.71), and the wind velocity time series(fort.72). The elevation time series is the most important output from ADCIRC, because unlike the atmospheric pressure and wind velocity, the change in the water surface elevation is not an input into ADCIRC. Because of this, matching the recorded surface elevation to the ADCIRC results goes a long way into verifying the model. The depth-averaged

velocity time series(fort.62) cannot be compared with recorded data because there are no recordings for depth averaged velocity in Lake Erie; however, it can be used to compare the differences in the depth-averaged velocity the ADCRIC+SWAN results.

Another way of validating the model is comparing the significant wave heights recorded at the 3 meteorological buoys that are all located in the open water. However ADCIRC only solves the modified forms of the Shallow Water Equations so it is unable to determine the significant wave heights. This is why the SWAN model, one that can model the wave heights, is coupled with ADCIRC so this validation is possible.

2.3 ADCIRC + SWAN

Simulating WAves Nearshore or SWAN was developed to determine wave propagation in time and space, shoaling, refraction due to current and depth, frequency shifting due to currents and non-stationary depth. For our model, the most important physics that SWAN accounts for is the wave generation by wind because as mentioned before, Lake Erie is primarily a wind driven lake. Other physics that SWAN accounts for are white capping, depth-induced breaking, dissipation due to vegetation, and diffraction. The SWAN equation, $\mathcal{S}$, accounts for the wave action density $N(\lambda, \varphi, \sigma, \theta, t)$ as it moves through geographic space (λ, φ) and spectral space (with relative frequencies σ and direction θ), in time (t),the action balance equation is governed by:

$$\begin{aligned} \mathcal{S} \equiv \frac{\partial N}{\partial t} \; + \; \frac{\partial}{\partial \lambda}\left[\left(c_\lambda + u\right) N\right] \; + \; \arccos\varphi \frac{\partial}{\partial \varphi}\left[\left(c_\varphi + v\right) N \cos\varphi\right] \\ + \; \frac{\partial}{\partial \theta}\left[c_\theta N\right] \; + \; \frac{\partial}{\partial \sigma}\left[c_\sigma N\right] \; = \; \frac{S_{tot}}{\sigma} \end{aligned} \tag{13}$$

where (u, v) are the ambient current, (c_λ, c_φ) are the group velocities, c_θ is the propagation velocity in the θ-space, and c_σ is the propagation velocity in the σ-space. S_{tot} is the source term that represents how the wind determines the growth of the waves by:

- surf breaking and bottom friction,
- action lost due to whitecapping,
- and action in deep water and shallow water of the exchange between spectral components caused by nonlinear effects.

SWAN communicates with ADCIRC in order to obtain the necessary wind speeds, water levels, and currents that ADCIRC calculates at each node. These three components are essentially what drives the SWAN model. For a given timestep, these components are first calculated by ADCIRC, then they are passed onto SWAN where it recalculates the water level and all related wave processes. These SWAN values are then read back into ADCIRC at each node where the process repeats itself for the next timestep. When running ADCIRC+SWAN, only one of the models can run at once because each model needs information from the other in order to force it. The radiation stress gradients, $\tau_{sx,waves}$ & $\tau_{sy,waves}$, partially drive and force ADCIRC and are computed by SWAN by the following equations;

$$\tau_{sx,waves} \; = \; -\frac{\partial S_{xx}}{\partial x} \; - \; \frac{\partial S_{xy}}{\partial y}, \tag{14}$$

$$\tau_{sy,waves} \;=\; -\frac{\partial S_{xy}}{\partial x} \;-\; \frac{\partial S_{yy}}{\partial y}, \tag{15}$$

where the wave radiation stresses are S_{xx}, S_{xy} and S_{yy}. The radiation stresses, which are constant on each element, are interpolated into the space of continuous, piecewise linear functions and differentiated to obtain the radiation stress gradients in Equations 14 & 15. The wave radiation stresses are computed at the mesh node and are defined as;

$$S_{xx} \;=\; \rho_0 g \int\int \left(\left(n\ cos^2\theta + n - \frac{1}{2}\right)\sigma N\right) d\sigma d\theta, \tag{16}$$

$$S_{xy} \;=\; \rho_0 g \int\int \left(n\ sin\theta\ cos\theta\ \sigma N\right) d\sigma d\theta, \tag{17}$$

$$S_{yy} \;=\; \rho_0 g \int\int \left(\left(n\ sin^2\theta + n - \frac{1}{2}\right)\sigma N\right) d\sigma d\theta, \tag{18}$$

where n is the ratio of group velocity to phase velocity. Equations 16 – 18 are computed before Equations 14 & 15. An area-weighted average of the gradients is used to project the element-based gradients to the elements adjacent to each mesh node.

There are many outputs from SWAN which include average wave direction, directional spreading, wave energy, and dissipation but the most useful output is the significant wave height. This value can be compared to the recorded results from the 3 Lake Erie buoys, thus adding another comparison to help validate the model. Once validation has occurred, the wave energy can be used to determine locations for the wave energy converters.

2.4 The GLERL-Donelan Wave model

While the coupled ADCIRC + SWAN model has performed well for a number of applications, spectral wave models are known to be prohibitively expensive in terms the computational effort required; see, for example, (Mellor, 2008), which claims the SWAN model required 86 times the computer run time as the Princeton Ocean circulation model. This motivates our interest in the investigation of a simpler wave model, that has come to be known as the GLERL–Donelan wave model. Originally formulated at the Canadian Centre for Inland Waters and the US National Oceanic and Atmospheric Administrations Great Lakes Environmental Research Laboratory (GLERL), the GLERL–Donelan model is a relatively simple parametric wave model that has historically formed the basis of the US National Weather Services Great Lakes wave forecasts. In contrast to spectral and most other parametric wave models, which are based on the action balance equation, the GLERLDonelan wave model is based on the conservation of total wave momentum. This formulation avoids the need to solve the action balance equation over a (usually large) set of discrete frequency components, which is one factor that makes spectral-based models, such as SWAN, prohibitively expensive from a computational perspective.

Therefore, as part of this project we explored the development and application of a discontinuous Galerkin (DG) finite element method for a relatively simple parametric wave model, the so-called GLERL–Donelan wave model, originally developed by Mark A. Donelan

and subsequently revised by Schwab, et al, at the Great Lakes Environmental Research Laboratory (GLERL). Unlike spectral-based model, which are based on the action balance equation, the model is based on a conservation of wave momentum equation, i.e.,

$$\frac{\partial \mathbf{M}}{\partial t} + \nabla \cdot \mathbf{T} = \frac{\boldsymbol{\tau}_w}{\rho_w g}, \tag{19}$$

where $\mathbf{M} = (M_x, M_y)^\intercal$ is the total wave momentum vector with components in the horizontal, x and y directions, $\mathbf{T}$ is the (symmetric) momentum flux tensor, $\boldsymbol{\tau}_w$ is the wind stress vector, g is the gravitational constant, and ρ_w is the density of water. Starting with the right-hand side of (19), the wind forcing is parameterized by

$$\frac{\boldsymbol{\tau}^w}{\rho_w} = 0.028 D_f \left|\mathbf{U} - 0.83\mathbf{C}_p\right| \left(\mathbf{U} - 0.83\mathbf{C}_p\right),$$

where $\mathbf{U} = (u_w, v_w)^\intercal$ is the wind velocity vector at 10 meters above the sea surface, $\mathbf{C}_p$ is the wave phase velocity vector, and D_f is the form drag coefficient given by an empirical relationship.

Under the assumption of deep water linear wave theory (applicable for most wind waves on the lake surface), the momentum flux tensor has components

$$\begin{aligned} T_{xx} &= \frac{g}{2}\int_0^{2\pi}\int_0^{\infty} E\left(f,\theta\right)\cos^2\theta \, df\, d\theta, \\ T_{xy} &= T_{yx} = \frac{g}{2}\int_0^{2\pi}\int_0^{\infty} E\left(f,\theta\right)\sin\theta\cos\theta \, df\, d\theta, \\ T_{yy} &= \frac{g}{2}\int_0^{2\pi}\int_0^{\infty} E\left(f,\theta\right)\sin^2\theta \, df\, d\theta, \end{aligned} \tag{20}$$

where $E(f,\theta)$ is the wave energy spectrum, which is a function of wave frequency f and direction θ. In the GLERL–Donelan model, it is assumed that the wave energy spectrum is separable in frequency and direction, i.e., $E(f,\theta) = \tilde{E}(f)S(\theta)$, where $S(\theta)$ is assumed to have a cosine-squared angular dependence about some mean wave direction θ_0, i.e., $S(\theta) \propto \cos^2(\theta - \theta_0))$ and $\tilde{E}(f)$ is given by the Joint North Sea Wave Project (JONSWAP) energy spectrum. Under these assumptions, the moment flux tensor components given by (20) take a relatively simple form. Preliminary numerical results obtained with a "stand-alone" DG implementation of the GLERL–Donelan model on Lake Erie are very promising in terms of both accuracy and computational efficiency (see the next section, in particular, Figure 11)

3 Principal Findings & Significance

3.1 ADCIRC+SWAN Results

The mesh on which ADCIRC+SWAN runs on was created using up-to-date shoreline that was traced and the newest bathymetry data. The resulting mesh contains 401,547 nodes connecting 782,650 elements and can be seen in Figure 1. The size of individual elements ranges from 10 meter in rivers/channels/marinas to 3 kilometers in the open water where there is little to no change in bathymetry.

Monthly simulations were run from May through October because these are the months that have the weather buoy data available to compare the model simulations to. The years that the simulations were run for were 2009, 2010, and 2011. A comparison of the weather buoys 45005, 45132, and 45142 to the ADCIRC+SWAN output for both May 2009 and August 2009 is shown in Figures 2 - 7. The gaps in the Recorded Data(blue line) indicate times in which the station was not recording. Overall the model has shown it's ability to capture the peaks and general trends of the recorded data.

The maximum monthly waves heights for May 2009 and August 2009 are shown in figures 8 & 9. Computing the max height values for the entire lake at every node provides us with information on where the max elevation is most likely to occur and therefor be the best place to implement the wave energy converters.

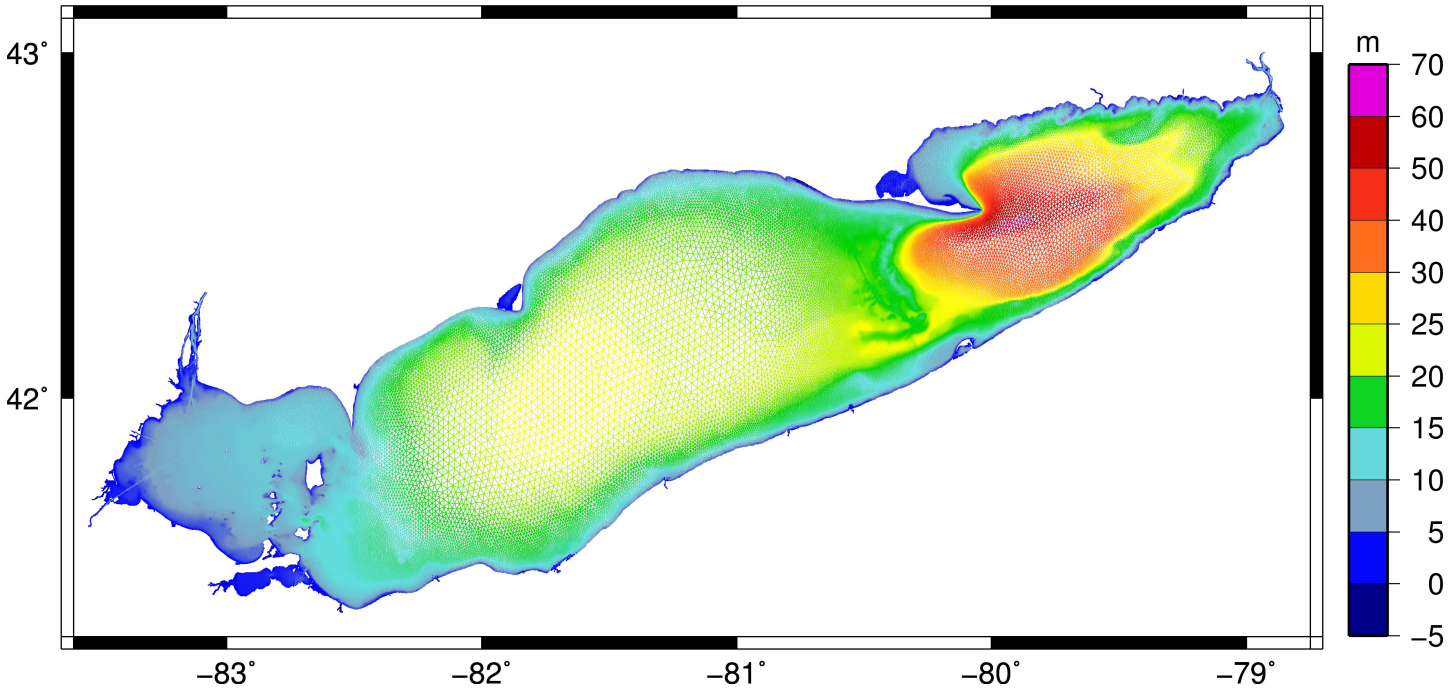

Figure 1: Lake Erie Mesh with Bathymetry

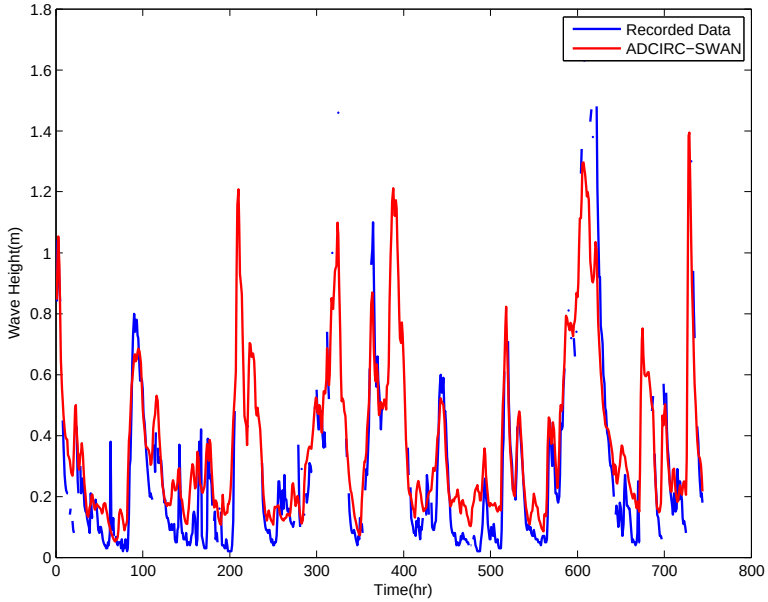

Figure 2: May 2009 Significant Wave Height at Buoy 45005

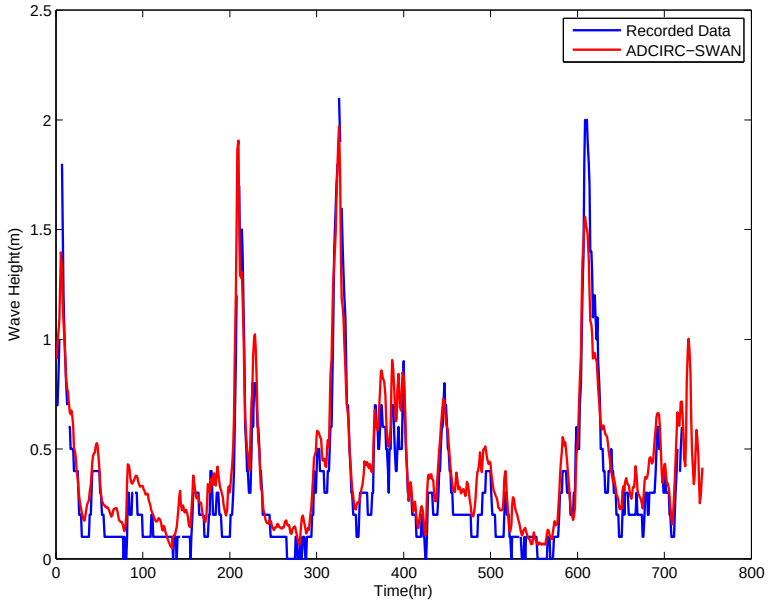

Figure 3: May 2009 Significant Wave Height at Buoy 45132

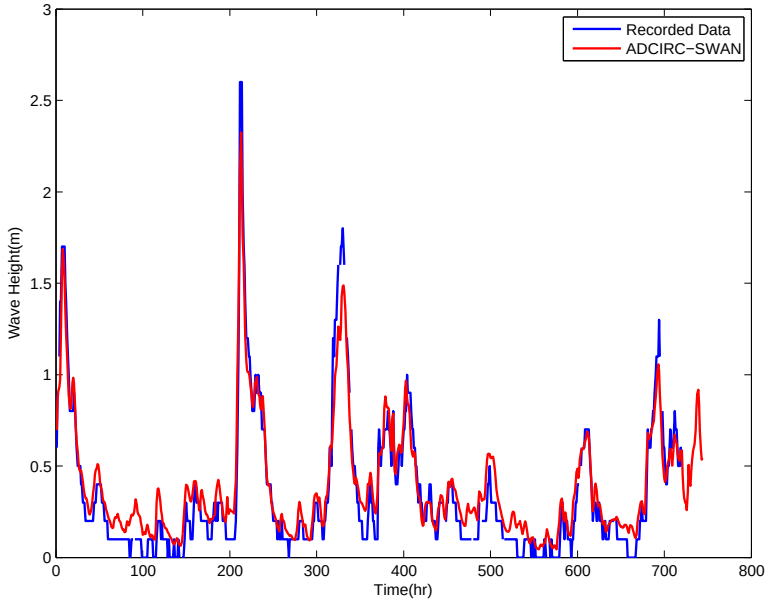

Figure 4: May 2009 Significant Wave Height at Buoy 45142

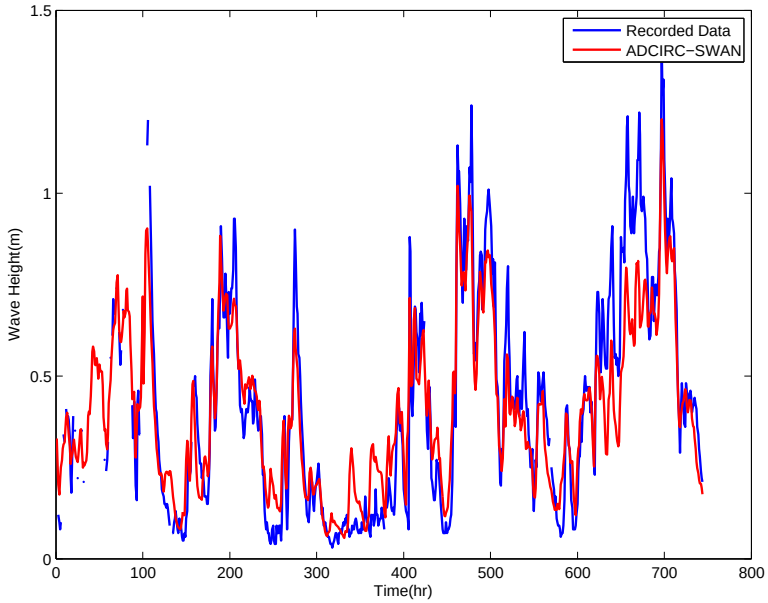

Figure 5: August 2009 Significant Wave Height at Buoy 45005

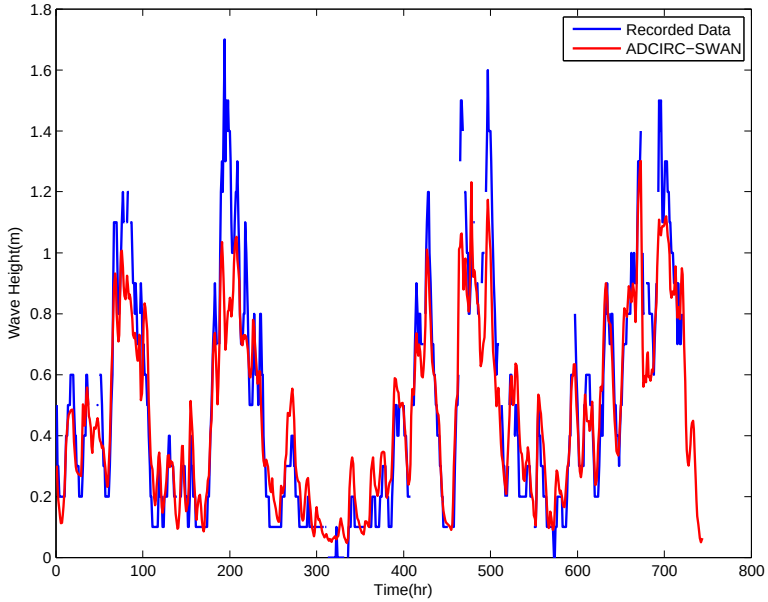

Figure 6: August 2009 Significant Wave Height at Buoy 45132

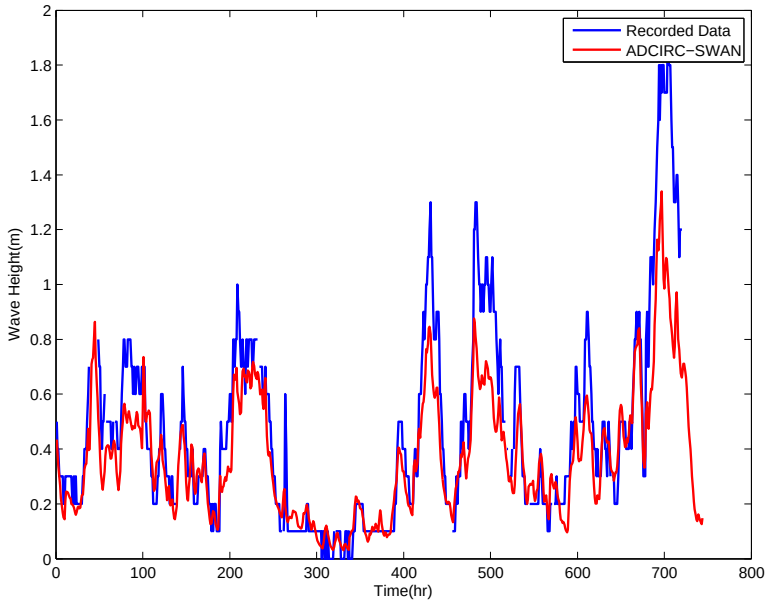

Figure 7: August 2009 Significant Wave Height at Buoy 45142

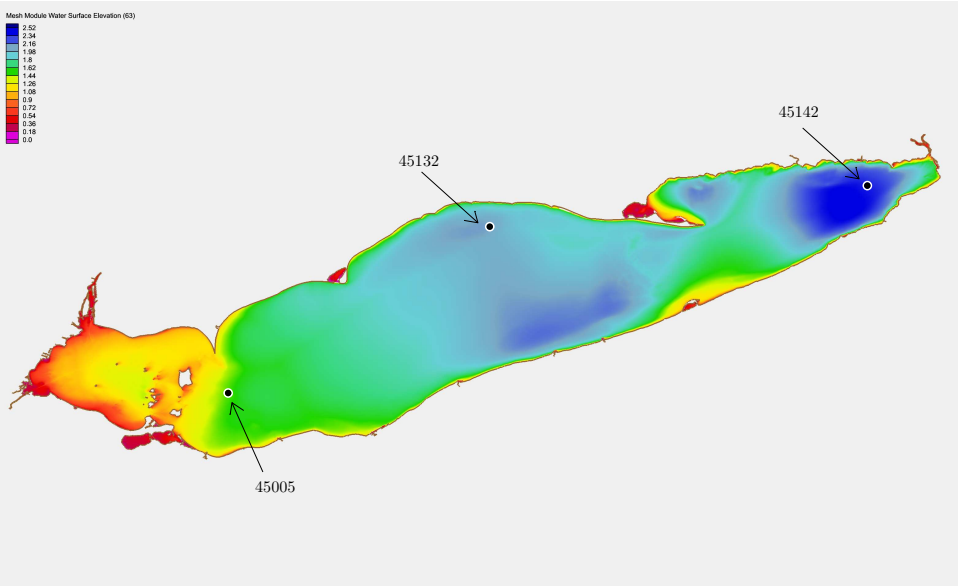

Figure 8: May 2009 Maximum Wave Heights

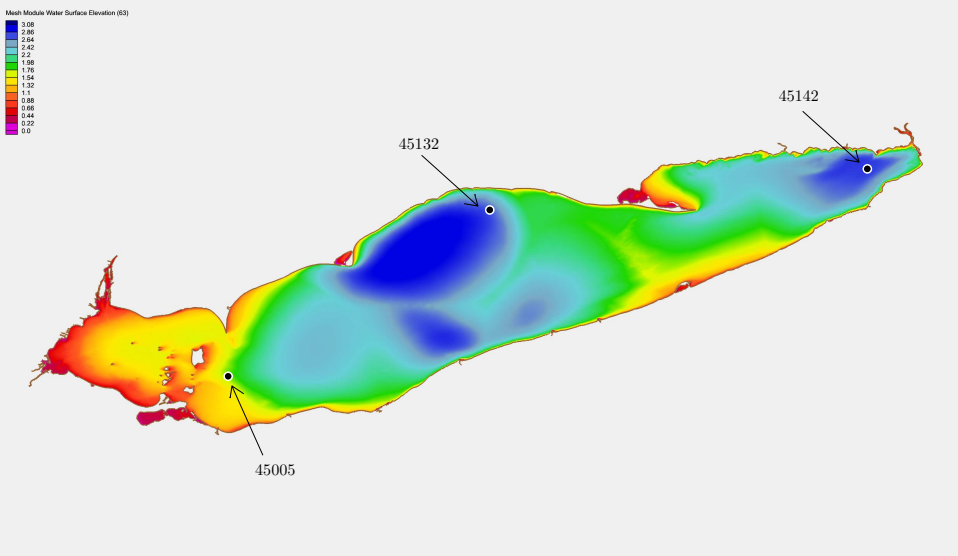

Figure 9: August 2009 Maximum Wave Heights

3.2 DG-Wave Results

Graduate student Angela Nappi is working with PI Kubatko on the development and application of the aforementioned DG method for the GLERL–Donelan wave model. Preliminary numerical results obtained with the DG GLERL–Donelan model are very promising. Verification and initial validation of the model are shown in Figures (8) and (9), respectively. The model was verified on a simple test case presented in Schwab, 1984. The domain of the test case is a 100-km diameter circular basin discretized using the mesh shown in Figure (8). A constant wind of 10 m/s is applied in the positive x direction for a duration of 24 hours. Donelan developed the following empirical relationship for characteristic wave height, H_c, as a function of fetch X, namely,

$$H_c = 0.00366 g^{-0.62} X^{0.38} \left(U \cos\theta\right)^{1.24},$$

where θ is the angle between the wind and wave vectors found by maximizing the effective fetch

$$F_e = X \left(\cos\theta\right)^{2.35}.$$

A comparison of the DG solution to the empirical formula for characteristic wave height along the centerline of the circular basin ($y = 50$ km) is displayed in Figure (8). The computed correlation coefficient between the solutions is 0.944. In terms of model validation, the DG GLERL–Donelan model is applied to an unstructured mesh of Lake Erie. The mesh used for this preliminary validation test has approximately 2500 elements with a maximum element size of 5 km and a minimum size of 4 km; see Figure (8). The mesh was generated automatically using the advanced mesh generator ADMESH.

Wind forcing data is obtained from a number of recording stations around and on the Lake. Three buoys on Lake Erie record significant wave height hourly. The results for a simulation of the first full week of May 2010 are presented in Figure (9). Results from the DG GLERL–Donelan are compared to both recorded buoy data and simulation results from a SWAN simulation. In general, the model shows very good agreement with the recorded data and even out-performs SWAN in general. This is especially promising considering the relative simplicity and computational cost of the model compared to third-generation wave models.

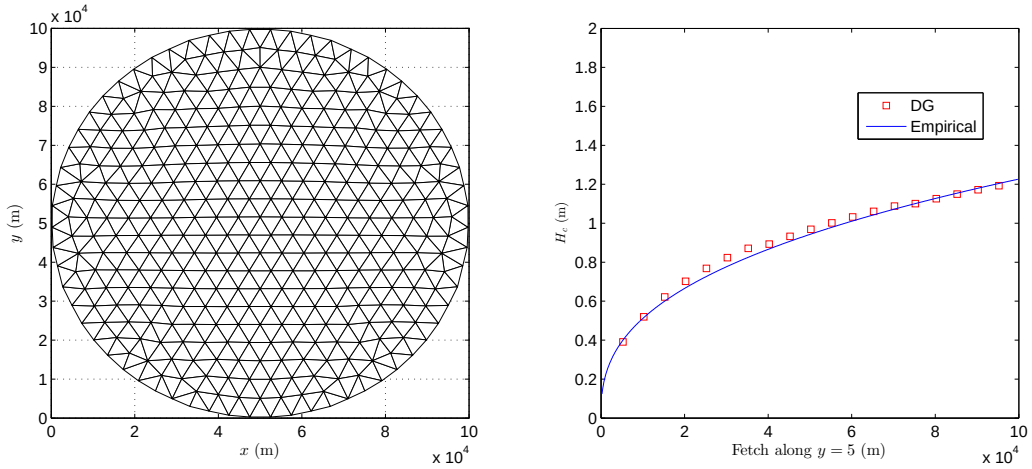

Figure 10: Plot of the finite element mesh used for the verification test case (left) and a comparison of the DG and empirical solutions along $y = 50$ km (right).

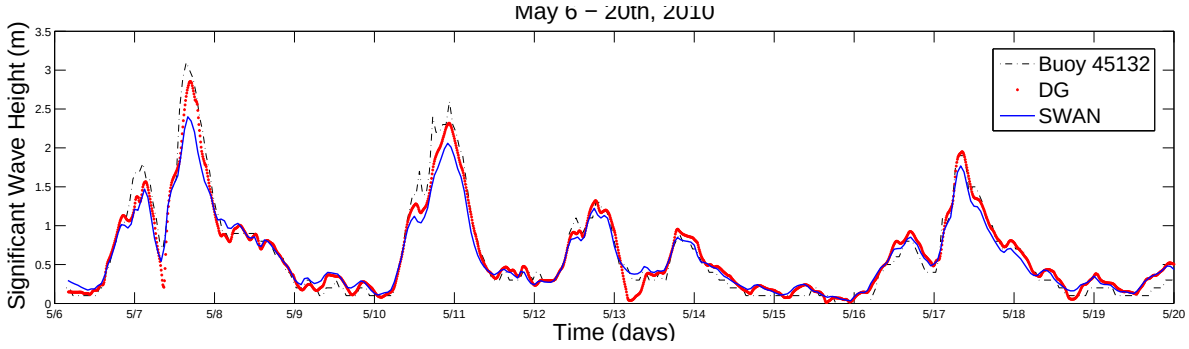

Figure 11: Numerical predictions of significant wave height in meters comparing the SWAN model (blue line) and the DG GLERL–Donelan model (red squares) to recorded buoy data.

Research Information
1. WRC 104(b) or 104(g) or OWDA Grant including (1) Project number; (2) Number of faculty involved; (3) Number of students supported; (4) Degree type and major or specialization
(1) 60030647, (2) 1, (3) 3 different students partially funded, (4) MS in Civil Engineering with a specialization in computational water resources.
2. Research Publications including (1) Complete citation; (2) Whether publication was peer-reviewed; (3) Whether publication was funded by WRRAA §104
(1) Nappi, A., Kubatko, E.J., Conroy, C.J., "Development and validation of a discontinuous Galerkin-based wave prediction model," Advances in Water Resources, to be submitted.
3. Conference Presentation including (1) Complete citation; (2) Conference title; (3) Whether presentation is based on research funded by WRRAA §104 (4) Number of students attending who were sponsored by the institute
(1) (i) A. Nappi, Development and application of a discontinuous Galerkin-based wave prediction model, (ii) D. Dibling, Development and validation of a nearshore model for Lake Erie; (iii) Nappi, A., Kubatko, E.J., "Development and Validation of DG WAVE: a Discontinuous Galerkin-Based Numerical WAVe Prediction Model" (iv) Nappi, A., Kubatko, E.J., "Introducing DG-WAVE: A discontinuous Galerkin-based wave prediction model" (2) (i) and (ii) were given at World Congress on Computational Mechanics (WCCM10), Sao Paulo, Brazil, July 2012; (iii) was given at the 12th U.S. National Congress on Computational Mechanics, Raleigh, NC, July 22–25, 2013, and (iv) at The 17th Annual ADCIRC Model Workshop, U.S. Army Engineering Research and Development Center, Vicksburg, MS, April 29–30, 2013. (3) In part; (4) 1
4. Research Award or Other Recognition including (1) Award title; (2) Name of organization giving award; (3) Brief summary of the work that was recognized; (4) Who received the award (student name etc.)
NA
5. Patent or Copyright including (1) Title of intellectual property; (2) Brief description of the property; (3) Whether the property is patented or copyrighted; (4) Whether property was funded by WRRAA §104
NA
6. Profession Placement of Graduates including (1) Economic sector; (2) Number of placements

Student Angela Nappi is currently a Marine Structures Engineer at AECOM, NY, NY.
7. Teaching Assistantship including (1) Number of assistantships; (2) number of these assistantships funded using WRRAA §104 funds
Three students were partially funded with research assistantships under this project.

Microbial Modulation of Acidic Coal Mine Drainage Chemistry: Implications for Passive Treatment of Minewater

Basic Information

Title:	Microbial Modulation of Acidic Coal Mine Drainage Chemistry: Implications for Passive Treatment of Minewater
Project Number:	2012OH250B
Start Date:	3/1/2012
End Date:	8/31/2013
Funding Source:	104B
Congressional District:	OH-013
Research Category:	Biological Sciences
Focus Category:	None, None, None
Descriptors:	
Principal Investigators:	John M. Senko

Publications

1. Brantner, J.S., Hotchkiss, S.T., Senko, J.M. 2013. Adaptation of soil-associated microbial communities to intrusion of acidic coal mine drainage: implications for Fe(II) removal. Environmental Science & Technology. In preparation.
2. Brantner, J.S., Milsted, A., Senko, J.M. Microbial modulation of acidic coal mine drainage chemistry: implications for passive treatment of minewater. American Society for Microbiology General Meeting Abstracts. Denver, CO. May 2013.
3. Senko, J.M. Microbially mediated iron cycling in acid mine drainage. Department of Biological Sciences Seminar. Missouri University of Science & Technology. Rolla, MO. November, 2013.
4. Senko, J.M. Microbially mediated iron cycling in acid mine drainage. Department of Geological Sciences Seminar. Ohio University. Athens, OH. May, 2012
5. Senko, J.M. Adaptation of soil-associated microbial communities to intrusion of acid mine drainage. Invited talk. Society for Industrial Microbiology Annual Meeting. San Diego, CA. August 2012.
6. Brantner, J.S., Hotchkiss, S.T., Senko, J.M. 2013. Adaptation of soil-associated microbial communities to intrusion of acidic coal mine drainage: implications for Fe(II) removal. Environmental Science & Technology. In preparation.
7. Brantner, J.S., Milsted, A., Senko, J.M. Microbial modulation of acidic coal mine drainage chemistry: implications for passive treatment of minewater. American Society for Microbiology General Meeting Abstracts. Denver, CO. May 2013.
8. Senko, J.M. Microbially mediated iron cycling in acid mine drainage. Department of Biological Sciences Seminar. Missouri University of Science & Technology. Rolla, MO. November, 2013.
9. Senko, J.M. Microbially mediated iron cycling in acid mine drainage. Department of Geological Sciences Seminar. Ohio University. Athens, OH. May, 2012
10. Senko, J.M. Adaptation of soil-associated microbial communities to intrusion of acid mine drainage. Invited talk. Society for Industrial Microbiology Annual Meeting. San Diego, CA. August 2012.

Microbial Modulation of Acidic Coal Mine Drainage Chemistry: Implications for Passive Treatment of Minewater

John Senko (PI)
Department of Geoscience
The University of Akron
senko@uakron.edu

PRINCIPAL FINDINGS AND SIGNIFICANCE

Background and Research Objectives

We have identified several acid mine drainage (AMD)-impacted systems in which the acidic, dissolved Fe(II)-rich fluids emerge at the terrestrial surface from underground coal mine works. At these systems, AMD flows over the surface in a "sheet-flow" fashion with a water depth of approximately 0.5 cm. The AMD sheet flow characteristic of these systems facilitates the aeration of the initially anoxic AMD, and enhances the activities of aerobic Fe(II) oxidizing bacteria (FeOB). FeOB catalyze the oxidation of Fe(II) to Fe(III) at greater rates than could be achieved via the abiotic reaction between Fe(II) and O_2 at the pH associated with these systems (pH = 3.0 – 4.5). The biogenic Fe(III) subsequently hydrolyzes and precipitates as a variety of Fe(III) (hydr)oxide phases, giving rise to extensive Fe(III) (hydr)oxides that are referred to as iron mounds. In some cases, the oxidative precipitation of Fe from AMD leads to removal of ≥90% of dissolved Fe from AMD. Since removal of Fe from AMD is one of the most pressing treatment objectives of AMD treatment, the activities associated with these iron mounds could be exploited to achieve this goal. These sheet flow systems are quite remarkable, since none of these sites have received human intervention to stimulate Fe removal. As such, iron mounds could serve as inexpensive and sustainable approaches to AMD treatment. Implicit in the development of these iron mounds is the fact that at some point in time, "pristine" soil (i.e. unimpacted by AMD) was infiltrated by AMD, inducing shifts in the microbial communities associated with the systems that culminated in the microbial communities that are currently capable of robust Fe(II) oxidizing activity.

However, the dynamics of this adaptation is unclear. In this 2012 OWRC-USGS-funded project, we sought to answer the following questions:

1) Is the robust Fe(II) oxidizing activity associated with iron mounds attributable mostly to a) microorganisms that are suspended in AMD and "delivered" to the formerly pristine soil, b) microorganisms associated with pristine soil, or c) synergistic interaction between microorganisms associated with both AMD and pristine soil?
2) Do microbial communities associated with AMD and pristine soil develop robust Fe(II) oxidizing activities that are comparable to those of mature iron mound sediments?
3) What changes in microbial community composition accompany the development of robust Fe(II) oxidizing bacterial activities?

With an eye toward the development of "designed" iron mounds for AMD treatment, it has been suggested that "seeding" sediments with material (and associated microorganisms) from mature iron mounds could enhance the development of robust Fe(II) oxidizing microbial activities, so we asked the additional question:

4) Does the addition of iron mound sediment (and associated microorganisms) to pristine soil facilitate the more rapid development of robust Fe(II) oxidizing activities?

Methodology

AMD, iron mound sediments, and pristine soil (nearby soil that was unimpacted by AMD) were collected from an AMD-impacted system in North Lima, OH that is referred to as the Mushroom Farm (Figure 1). All experiments were conducted as semi-continuous reactor experiments, in which 5 g of iron mound sediment and/or soil were suspended in 50 ml of AMD and incubated under oxic conditions. For experiments to evaluate the relative contributions of AMD- and soil-associated microorganisms to the development of Fe(II) oxidizing activities, incubations were conducted using non-sterile AMD and non-sterile soil, filter-sterilized AMD and non-sterile soil, non-sterile AMD and heat-deactivated soil, and filter-sterilized AMD and heat-deactivated soil, as a negative control. To roughly approximate the continuous infiltration of AMD into sediments/soil, 25 ml of fluid was periodically removed from reactors and replaced with fresh AMD. Dissolved Fe(II) and pH were periodically measured throughout the experiments. Experiments to determine whether rates of Fe(II) oxidation increased with continuous incubation of AMD with pristine soil were conducted as described above, and included reactors that contained 5 g of iron mound sediment, 5 g of pristine soil, or 4 g pristine soil with 1 g of iron mound sediment suspended in 50 ml of AMD. In addition to dissolved Fe(II) and pH, FeOB abundances (as colony forming units per unit volume in reactor; CFU/ml) were determined in periodically removed samples using a solid medium that specifically targets aerobic microorganisms capable of using Fe(II) as an electron donor. First-order rate constants for Fe(II) oxidation (k) were calculated by linear least squares regression fitting of ln[Fe(II)] vs. time (t) using the equation:

$$\ln[Fe(II)_t] = -kt + \ln[Fe(II)_{initial}]$$

Samples were also periodically removed from the reactors, and genomic DNA was extracted for evaluation of microbial communities associated with the sediments/soil using nucleic acid-based approach targeting partial sequences of 16S rRNA genes of microorganisms associated with the soils/sediments.

Principal Findings

AMD- and soil-associated microbial contributions to Fe(II) oxidation. Initial rates of Fe(II) oxidation were highest in incubations containing non-sterile soil and non-sterile AMD, and oxidative precipitation of Fe was incomplete in incubations containing filter-sterilized AMD and heat-deactivated soil after 28 d of incubation (Figure 2 and Table 1). While initial rates of Fe(II) oxidation in incubations containing either non-sterile soil and filter-sterilized AMD or heat-deactivated soil and non-sterile soil than those that contained non-sterile soil and AMD (Figure 2), the rates of Fe(II) oxidation in all incubations except the sterile controls reached comparable levels in all incubations after three exchanges with fresh AMD (Table 1). Based on these results, it appears that the development of robust Fe(II) oxidizing bacterial activity is due to synergistic activities of microorganisms associated with soil and AMD.

Development of Fe(II) oxidizing activities. The rates of biological Fe(II) oxidation far exceeded abiotic oxidation of Fe(II) in all incubations (Figure 3). Fe(II) oxidation was incomplete in incubations containing pristine soil and pristine soil amended with iron mound sediment, and did

not occur in incubations containing iron mound sediment only (Figure 3), suggesting that the majority of oxidative precipitation of Fe(II) was attributable to microbiological activity. In incubations containing pristine soil or pristine soil with iron mound sediment, pH decreased as Fe(II) oxidation proceeded, due to hydrolysis and precipitation of biogenic Fe(III) (Figures 3 and 4). Incubations were reamended with fresh AMD 11 times, and with successive replacements of AMD, the rates of Fe(II) oxidation increased (Table 2), suggesting that the microbial communities associated with the soils/sediments adapted to continuous intrusion of AMD. The amendment of soil with iron mound material appeared to decrease the number of exchanges required to achieve maximal rates of Fe(II) oxidation (Table 2), suggesting that the use of material from existing iron mounds could be a useful approach to enhance the development of robust Fe(II) oxidizing activity in "engineered" iron mounds.

Characterization of microbial communities associated with soil/sediment incubations. After 24 d of incubation, abundances of FeOB were highest in incubations containing iron mound sediment and soil amended with iron mound sediment (1×10^4 and 6×10^3, respectively). While FeOB could not initially be detected in incubations containing pristine soil only, their abundance increased to approximately 1×10^3 after 24 d of incubation. After 0, 6, 12, 18, and 24 d of incubation, DNA was extracted from incubations after washing of soils and sediments with ammonium oxalate, to remove Fe(III) (hydr)oxides. Additionally, DNA was extracted from organisms associated with pristine soil, iron mound sediment, and AMD. High quality genomic DNA was recovered from all samples. DNA recovered from each sample was shipped to Molecular Research LP (Shallowater, TX) for 454 pyrosequencing of 16S rRNA genes. Analysis of these sequences revealed a shift in microbial community composition, whereby microbial communities in incubations that contained soil and AMD developed characteristics that were similar to those of the "mature" iron mound sediments (Figure 5). Furthermore, "seeding" soil with mature iron mound sediment enhanced the development of robust Fe(II) oxidizing activities (Figure 5).

Significance

The results that we report here are quite striking in that they illustrate the rapid rate at which microbial communities associated with pristine soil adapt to intrusion of AMD, resulting in rapid rates of Fe(II) oxidation. The robust Fe(II) oxidizing activities appear to be attributable to some type of synergistic activities of microorganisms associated with the formerly pristine soil and microorganisms suspended in the AMD that may colonize the soil. We observed that this adaptation is quite rapid, with combined soil- and AMD-associated microorganisms catalyzing Fe(II) oxidation at rates comparable to iron mound sediment after one exchange with fresh AMD. This response appears to be enhanced by the addition of iron mound material (with associated microorganisms). Analysis of microbial communities indicates that soil-associated microbial communities develop characteristics of "mature" iron mound sediments quite rapidly, and indicate that relatively simple approaches to mimic the hydrologic characteristics of iron mounds may lead to the development of robust Fe(II) oxidizing microbial communities in soils that had not previously been impacted by AMD.

PUBLICATION CITATIONS

Brantner, J.S., Hotchkiss, S.T., Senko, J.M. 2013. Adaptation of soil-associated microbial communities to intrusion of acidic coal mine drainage: implications for Fe(II) removal. *Environmental Science & Technology.* submitted.

Brantner, J.S., Milsted, A., Senko, J.M. Microbial modulation of acidic coal mine drainage chemistry: implications for passive treatment of minewater. American Society for Microbiology General Meeting Abstracts. Denver, CO. May 2013.

Senko, J.M. Microbially mediated iron cycling in acid mine drainage. Department of Biological Sciences Seminar. Missouri University of Science & Technology. Rolla, MO. November, 2013.

Senko, J.M. Microbially mediated iron cycling in acid mine drainage. Department of Geological Sciences Seminar. Ohio University. Athens, OH. May, 2012.

Senko, J.M. Adaptation of soil-associated microbial communities to intrusion of acid mine drainage. Invited talk. Society for Industrial Microbiology Annual Meeting. San Diego, CA. August 2012.

NUMBER OF STUDENTS SUPPORTED

This grant supported the work of two students at The University of Akron. It is anticipated that both students will be included as co-authors of the manuscript that is in preparation for *Environmental Science & Technology*.

Justin Brantner (PhD, Integrated Biosciences; in progress; justin3@zips.uakron.edu) received salary (Summer 2012) and material support through this project.

Shane Hotchkiss (BS, Biology; May 2013; sth8@zips.uakron.edu) received material support through this project. Shane is pursuing opportunities as a high school teacher.

AWARDS OR ACHIEVEMENTS

No awards of achievements have resulted from this work, thus far.

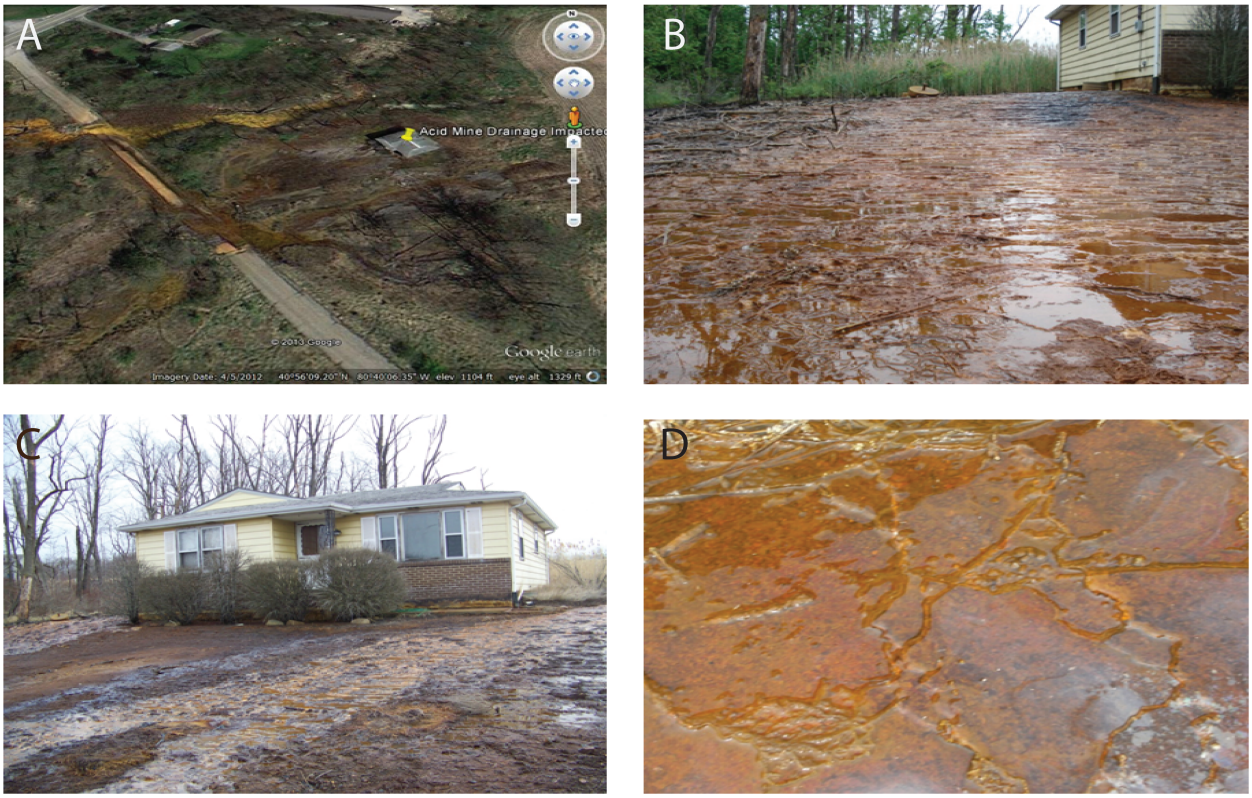

Figure 1. Various field site photographs of the Mushroom Farm. A) Google Earth image of the Mushroom Farm. B) Iron hydroxide crust and 'sheet flow' conditions of the Mushroom farm. C) Abandoned residence front yard view of iron hydroxide 'sheet flow.' D) Close-up image of the iron hydroxide mound formed under 'sheet flow' conditions.

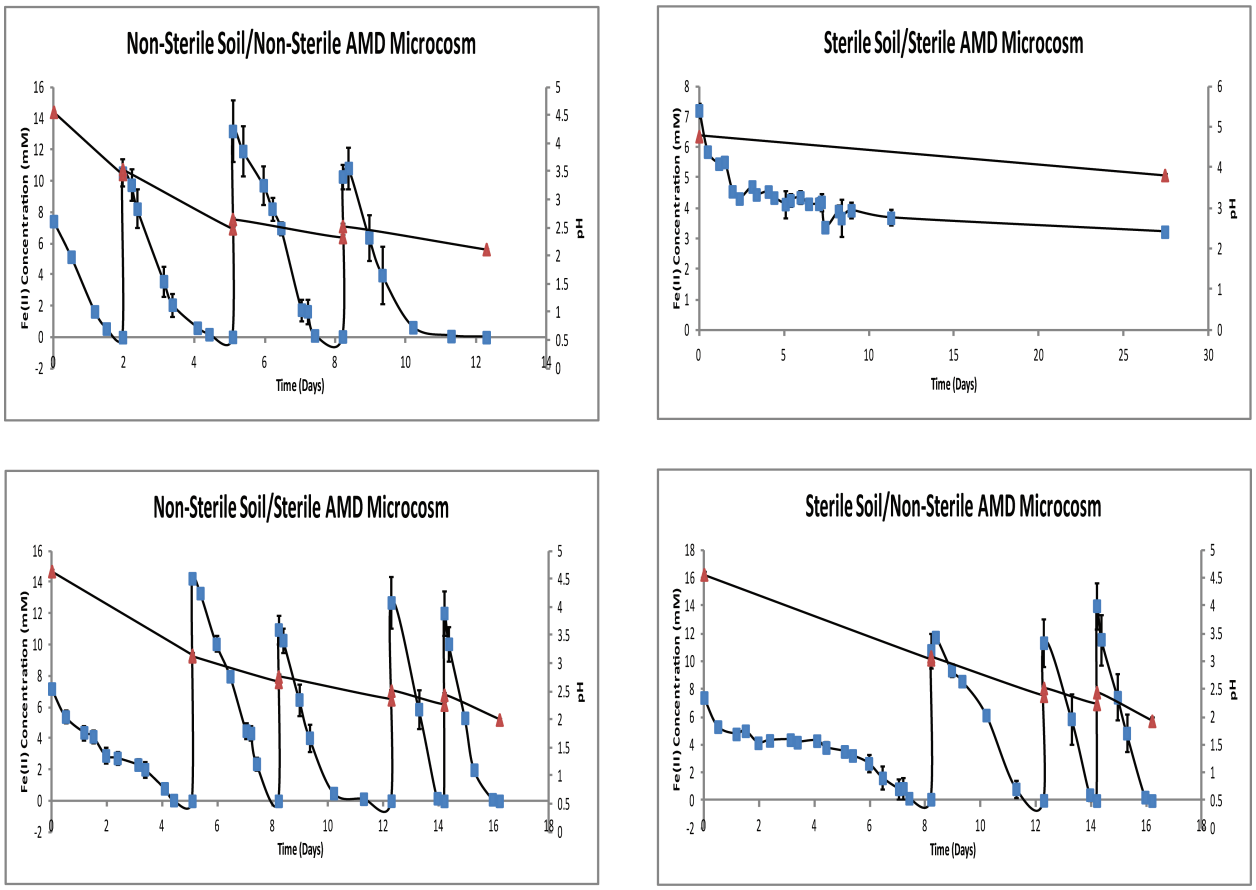

Figure 2. Dissolved Fe(II) (blue squares) and pH (red triangles) in four different microcosm incubations including pristine soil and AMD from the Mushroom Farm. Error bars = one standard deviation.

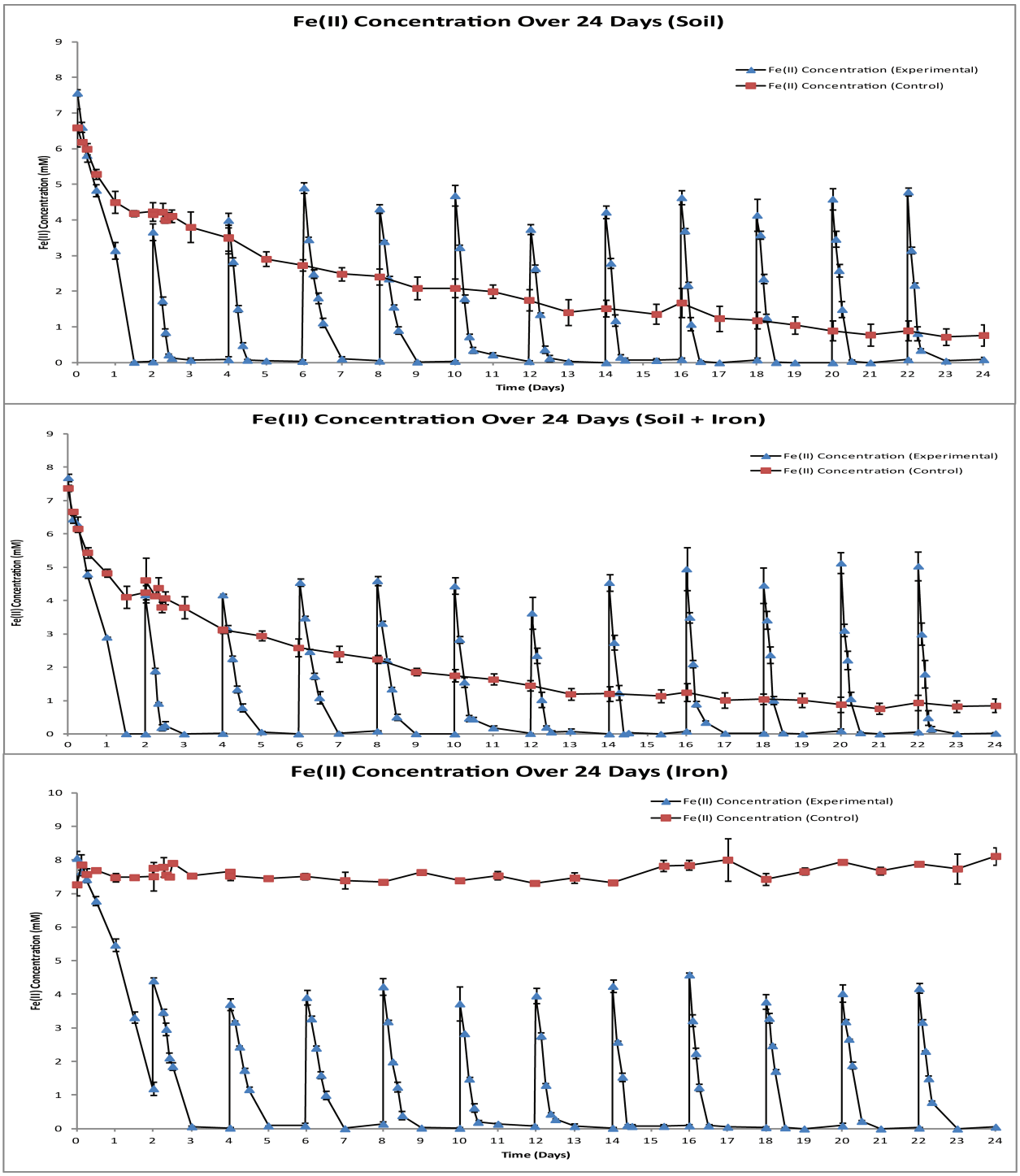

Figure 3. Dissolved Fe(II) concentrations in three different microcosm incubations over 24 days. Microcosms included: pristine soil (top panel), pristine soil amended with iron mound sediment (middle panel), and iron mound sediment (bottom panel). Blue triangles represent Fe(II) concentrations in non-sterile incubations. Red squares represent Fe(II) concentrations in formaldehyde-deactivated controls. Error bars = one standard deviation of triplicate incubations.

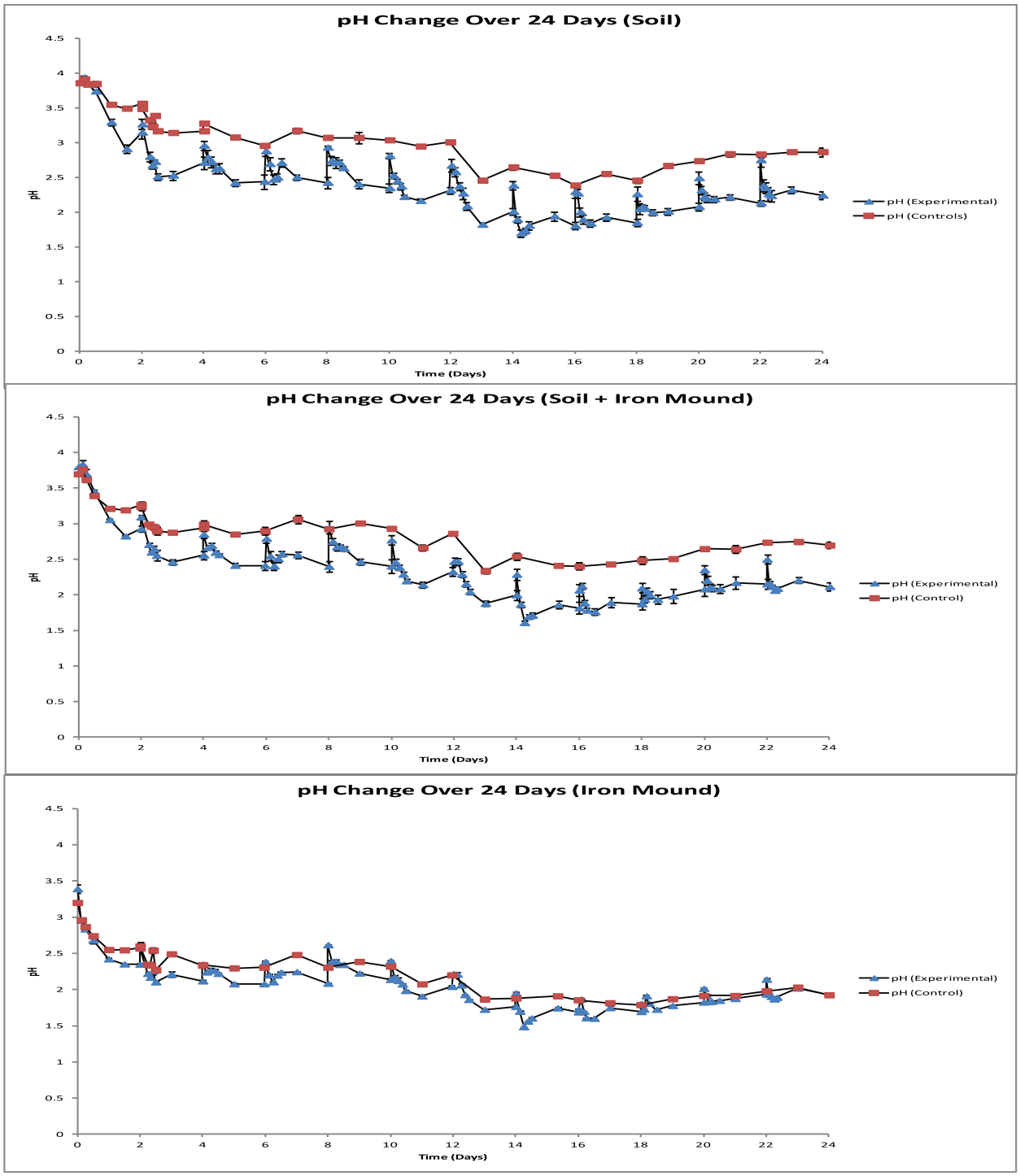

Figure 4. pH of three different microcosm incubations over 24 days. Microcosms included: pristine soil (top panel), pristine soil amended with iron mound sediment (middle panel), and iron mound sediment (bottom panel). Blue triangles represent pH of non-sterile incubations. Red squares represent pH of formaldehyde-deactivated controls. Error bars = one standard deviation of triplicate incubations.

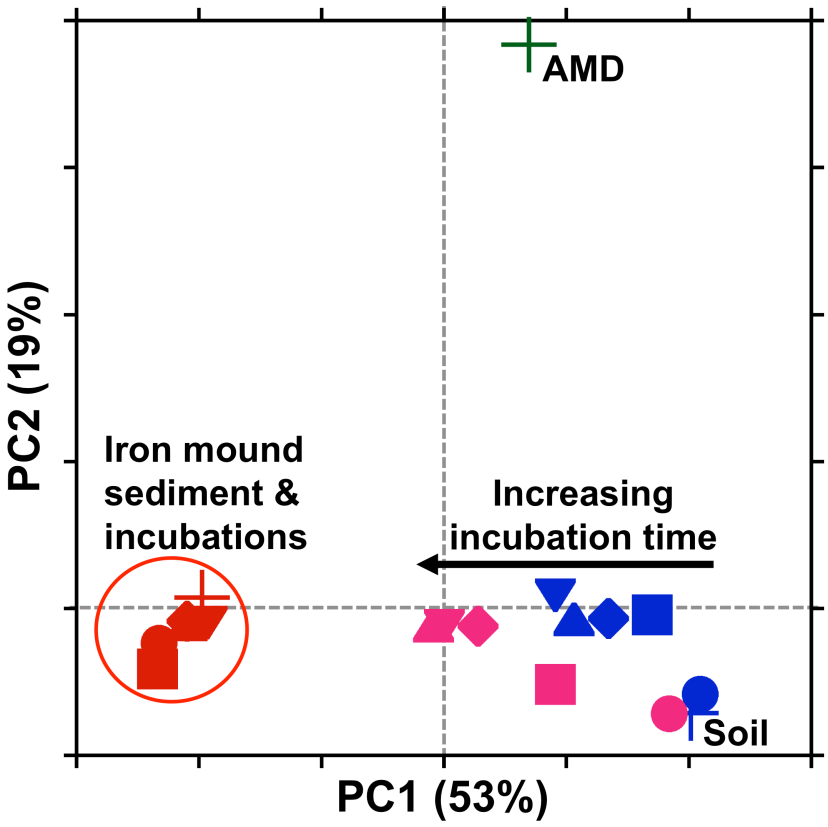

Figure 5. PCoA analysis of microbial communities associated with iron mound sediment, AMD-unimpacted soil, and AMD (red, blue, and green +, respectively) and iron mound sediment (red shapes), AMD-unimpacted soil (blue shapes), and iron mound-seeded AMD-unimpacted soil mixed (purple shapes) incubated with AMD for (●) 0, (■) 6, (◆) 12, (▲) 18, and (▼) 24 days using weighted UniFrac (Lozupone and Knight, 2005; Lozupone et al., 2007). Oval is to aid in visualizing clustering of IM-associated microbial communities. Arrow is to aid in visualizing the separation of soil-associated microbial communities from AMD-unimpacted soil with continuing exposure to AMD.

Lozupone, C.; Knight, R. UniFrac: a new phylogenetic method for comparing microbial communities. *Appl. Environ. Microbiol*. **2005**, *71*, 8228-8235.

Lozupone, C.; Hamady, M.; Kelly, S. T.; Knight, R. Quantitative and qualitative β diversity measures lead to different insights into factors that structure microbial communities. *Appl. Environ. Microbiol*. **2007**, *73*, 1576-1585.

Green-House-Gas budget of constructed wetlands: Understanding the sources to maximize benefits

Basic Information

Title:	Green-House-Gas budget of constructed wetlands: Understanding the sources to maximize benefits
Project Number:	2012OH259B
Start Date:	4/1/2012
End Date:	2/28/2014
Funding Source:	104B
Congressional District:	OH-12
Research Category:	Climate and Hydrologic Processes
Focus Category:	Wetlands, Ecology, Nitrate Contamination
Descriptors:	
Principal Investigators:	Gil Bohrer

Publications

1. Bohrer G, Zhu K, Jones RL, Curtis PS. (2013) Optimizing wind power generation while minimizing wildlife impacts in an urban area. Plos One 8:e56036.
2. Barr AG, Richardson AD, Hollinger DY, Papale D, Arain MA, Black TA, Bohrer G, Dragoni D, Fischer ML, Gu L, Law BE, Margolis HA, McCaughey JH, Munger JW, Oechel W, Schaeffer K. (2013) Use of change-point detection for friction-velocity threshold evaluation in eddy-covariance studies. Agricultural & Forest Meteorology 171:31-45.
3. Bohrer, G, Naor-Azieli, L, Mesi, S, Mouser, PJ, Stefanik, K, Schafer, KVR, and Mitsch, W 5/2012, Determining the meteorological forcing that affect seasonal and diurnal dynamics of methane emissions at a constructed urban wetland in Ohio. Oral Presentation, 30th AMS Conference on Agricultural and Forest Meteorology, Boston, MA.
4. Bohrer G, Naor-Azrieli L, Mesi S, Schäfer KVR, Mouser P, Stefanik K, Mitsch WJ, Morin T. 10/2012. Eddy flux measurements of methane at the Oletangy River Wetland Research Park wetland - Determining the seasonal and diurnal dynamics of methane emissions. Oral presentation, 4th International EcoSummit on Ecological Sustainability, Columbus, OH.
5. Schäfer KVR, Bohrer G. 10/2012. Effect of restoration on the carbon balance in the Meadowlands of New Jersey. 4th International EcoSummit on Ecological Sustainability, Columbus, OH.
6. Schäfer KVR, Bohrer G, Reid M, Tripathee R, Jaffe P. 10/2012. Temporal and spatial dynamics of methane fluxes in a temperate urban wetland. Oral presentation, 4th International EcoSummit on Ecological Sustainability, Columbus, OH.
7. Schäfer KVR, Bohrer G, Tripathee R. 4/2012. Carbon sequestration by Phragmites australis. Northeast Natural History Conference 2012, Syracuse, NY.
8. Bohrer G, Morin T, Naor-Azrieli L, Mouser PJ, Mitsch WJ, Schafer KVR. 12/2012. Determining the meteorological forcing that affect seasonal and diurnal dynamics of respiration and GPP in a constructed urban wetland in Ohio. Oral Presentation. American Geophysical Union Meeting 2012, San Francisco, CA.
9. Schafer KVR, Tripathee R, Bohrer G. 12/2012. Effect of restoration on carbon fluxes in urban temperate wetlands. Poster, American Geophysical Union Meeting 2012, San Francisco, CA.

10. Morin T, Bohrer G, Naor-Azrieli L, Mesi S, Schafer KVR, Stefanik K, Mitsch WJ. 11/2012. Effects of environmental conditions on an urban wetland's methane fluxes. Poster, 41st Annual Water Management Association of Ohio Conference, Columbus, OH.
11. Mesi S, Bohrer G, Naor-Azrieli L, Brooker M, Mouser P. 6/2012. Spatial-temporal intermittency of methane flux in an urban temperate wetland. Poster, 12th Annual American Ecological Engineering Society Meeting, Syracuse, NY.
12. Scannell GS, Bohrer G, Jones RL. 9/2012. Green solutions for wet weather management. Poster, 4th International EcoSummit on Ecological Sustainability, Columbus, OH.
13. Bohrer G, Zhu K, Jones RL, Curtis PS. (2013) Optimizing wind power generation while minimizing wildlife impacts in an urban area. Plos One 8:e56036.
14. Barr AG, Richardson AD, Hollinger DY, Papale D, Arain MA, Black TA, Bohrer G, Dragoni D, Fischer ML, Gu L, Law BE, Margolis HA, McCaughey JH, Munger JW, Oechel W, Schaeffer K. (2013) Use of change-point detection for friction-velocity threshold evaluation in eddy-covariance studies. Agricultural & Forest Meteorology 171:31-45.
15. Bohrer, G, Naor-Azieli, L, Mesi, S, Mouser, PJ, Stefanik, K, Schafer, KVR, and Mitsch, W 5/2012, Determining the meteorological forcing that affect seasonal and diurnal dynamics of methane emissions at a constructed urban wetland in Ohio. Oral Presentation, 30th AMS Conference on Agricultural and Forest Meteorology, Boston, MA.
16. Bohrer G, Naor-Azrieli L, Mesi S, Schäfer KVR, Mouser P, Stefanik K, Mitsch WJ, Morin T. 10/2012. Eddy flux measurements of methane at the Oletangy River Wetland Research Park wetland - Determining the seasonal and diurnal dynamics of methane emissions. Oral presentation, 4th International EcoSummit on Ecological Sustainability, Columbus, OH.
17. Schäfer KVR, Bohrer G. 10/2012. Effect of restoration on the carbon balance in the Meadowlands of New Jersey. 4th International EcoSummit on Ecological Sustainability, Columbus, OH.
18. Schäfer KVR, Bohrer G, Reid M, Tripathee R, Jaffe P. 10/2012. Temporal and spatial dynamics of methane fluxes in a temperate urban wetland. Oral presentation, 4th International EcoSummit on Ecological Sustainability, Columbus, OH.
19. Schäfer KVR, Bohrer G, Tripathee R. 4/2012. Carbon sequestration by Phragmites australis. Northeast Natural History Conference 2012, Syracuse, NY.
20. Bohrer G, Morin T, Naor-Azrieli L, Mouser PJ, Mitsch WJ, Schafer KVR. 12/2012. Determining the meteorological forcing that affect seasonal and diurnal dynamics of respiration and GPP in a constructed urban wetland in Ohio. Oral Presentation. American Geophysical Union Meeting 2012, San Francisco, CA.
21. Schafer KVR, Tripathee R, Bohrer G. 12/2012. Effect of restoration on carbon fluxes in urban temperate wetlands. Poster, American Geophysical Union Meeting 2012, San Francisco, CA.
22. Morin T, Bohrer G, Naor-Azrieli L, Mesi S, Schafer KVR, Stefanik K, Mitsch WJ. 11/2012. Effects of environmental conditions on an urban wetland's methane fluxes. Poster, 41st Annual Water Management Association of Ohio Conference, Columbus, OH.
23. Mesi S, Bohrer G, Naor-Azrieli L, Brooker M, Mouser P. 6/2012. Spatial-temporal intermittency of methane flux in an urban temperate wetland. Poster, 12th Annual American Ecological Engineering Society Meeting, Syracuse, NY.
24. Scannell GS, Bohrer G, Jones RL. 9/2012. Green solutions for wet weather management. Poster, 4th International EcoSummit on Ecological Sustainability, Columbus, OH.
25. Morin* TH, Bohrer G, Naor-Azrieli* L, Mesi* S, Kenny WT, Mitsch WJ, Schäfer KVR. (2014) The seasonal and diurnal dynamics of methane flux at a created urban wetland. Ecological Engineering (in press, available on-line http://dx.doi.org/10.1016/j.ecoleng.2014.02.002).

Green-House-Gas budget of constructed wetlands: Understanding the sources to maximize benefits

Principal Investigator: Gil Bohrer

Abstract

Fixed nitrogen (N) is required for the growth for all biological organisms, and agriculture is dependent upon nitrogen for fertilizer. Ohio exports significant levels of nitrogen in its surface waters to Lake Erie and the Mississippi Basin due to its geology and agricultural land management techniques. Constructed wetlands can be used for nitrogen removal through the biologically-mediated process of denitrification, where nitrite is reduced to nitrogen gas and released to the atmosphere. Unfortunately, denitrification in wetlands comes with the tradeoff of increased Green House Gas (GHG) production. Wetlands sequester large amounts of carbon (C) from the atmosphere, removing the most common GHG – CO_2 but produce another and more potent GHG – methane (CH_4). In order to allow development of wetlands as a solution for N removal without concerns of GHG emissions, it is critical to understand how methane production in the wetland responds to different environmental conditions such as water and soil temperature, water chemistry. GHG emission rates and water and meteorological conditions can be measured simultaneously over wetlands using eddy-flux sensors that measure the combined emissions from a broad flux footprint area, and chamber measurements at specific points and provide spatially anecdotal and temporally sparse information. Highly variable rates of methane production and carbon sequestration at different sub-ecosystems within the wetland at a very small scale (meters) prohibits the generalization of measured environmental relationships from either eddy-flux or chamber measurements. The proposed work will use a combination of meteorological, water, and GHG flux and chamber measurements in a constructed wetland at the Olentagy River Wetland Research Center (ORWRP) over 2 years to parameterize a novel high-resolution flux footprint model. The model will be used to determine the atmospheric exchange rates of methane sources and carbon sinks at different sub-ecosystem components of the wetland. This will allow determining the strength of different environmental variables that control methane production, and will facilitate the parameterization of an empirical model to predict whole-wetland GHG budgets at ORWRP, and ultimately GHG budgets in other constructed and urban wetland ecosystems.

Methodology

We use continuous long-term eddy-covariance flux measurements to observe the rates of methane flux and the corresponding meteorological, water and soil conditions. We use a probabilistic footprint model to determine which of the tower-top observation has originated primarily from the wetland area and not from the surrounding grass, river or forest. We use an advanced neural-network model to gap-fill the flux data when an observation is missing or was filtered out. We look for empirical relationships between the meteorological, ecological and water variables in the wetland and the rates of methane flux emissions and use these observations to explain the drivers of methane flux.

Major Activity

General achievements for the whole project: We completed the eddy flux tower to for continuous methane and carbon flux measurements and the corresponding meteorological data. We have completed 3 years of continuous observations, and on-going. We installed a network of soil temperature sensors in various locations and depths across the wetland floor. We have completed the software for meteorological and flux data analysis from the wetland site. This includes the processing of the raw data, development of a new approach for despiking and data quality control, and an improved footprint model. We also completed the software and calibration of the post-processing of the data and specifically the gap-filling using an automated neural network (ANN) approach which was customized specifically for our site. We have registered the site with Ameriflux – a national open and free database of carbon and methane flux measurements and a component of a global FLUXNET database. We became the second site nationwide to report methane flux data to Ameriflux.

Specifically to the last reporting period: We conducted a detailed ground-based survey and airborne imaging of the vegetation in the wetland and developed high resolution detailed vegetation and patch type map of the wetland, and developed a procedure to repeat the survey and update the map every summer (Figure 1). We installed 5 pore-water peepers to conduct continuous measurements of methane and CO2 concentrations at the pore water in the sediments under the wetland. We completed a study of the diurnal and seasonal dynamics of flux from the wetlands (Morin et al 2014, *Ecological Engineering*, in press). We developed a neural-network based empirical multivariate model of the methane emissions from the wetland park (Figure 2) and conducted a sensitivity analysis to the effects of using model-gap-filled methane flux data as an input for the methane model. We developed a statistical approach to use intermittent chamber measurements of fluxes to correct eddy flux measurements for the effects of inter-patch variability of fluxes within the wetland and the spatial dynamics of the eddy-flux measurement footprint.

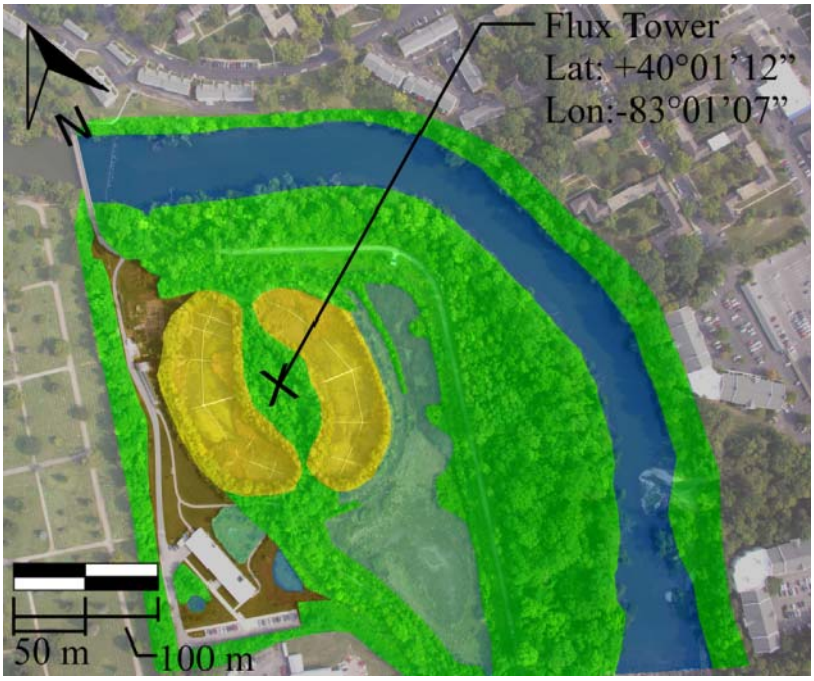

Figure 1. *The Olentangy River Wetland Research Park (ORWRP). Color shaded areas are included as components of the wetland park within the flux footprint. Yellow indicates the two experimental "kidney" wetlands, which are continuously flooded and are dominated by cattails (Typha spp.). Blue indicates permanently inundated areas which include the Olentangy River and a swale created from the southern outflows of the experimental wetlands. Green areas are forests which are periodically inundated. Blue-green indicates intermittently flooded fens where grass-like wetland vegetation dominates the plant growth. Brown areas are lawns which are never flooded but maintain a high water table. Grey shaded areas (including buildings and roads) were not counted as parts of the wetland park for the purposes of methane fluxes.*

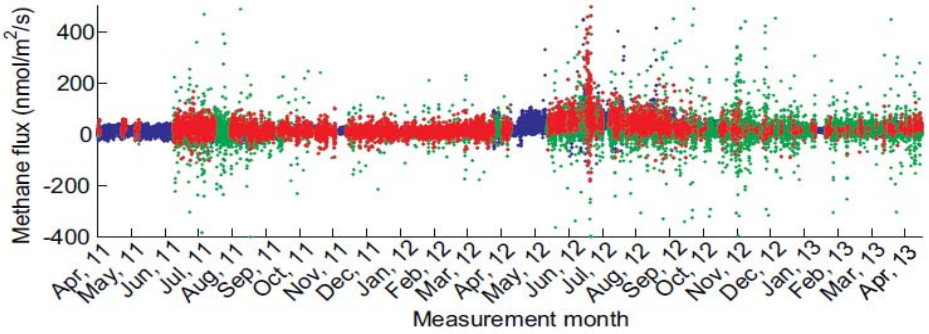

Figure 2. *Time series of methane flux from spring 2011 to spring 2013. Red points are half hourly processed flux data which gap filling was trained on. Green points were eliminated through the despike procedure, u* filter, or footprint filter and are not used for any data analysis or gap filling purposes. Blue points are gap filled by the neural network. Early data required heavy gap filling due to startup difficulties with the eddy-flux system. The large gap around April 2012 is when the tower height was adjusted.*

Findings

We determined the seasonal dynamics of methane fluxes at the wetland park as a whole (Figure 3). We found that fluxes in the winter are much lower, as expected, but sum up to about 30% of the annual emissions total. We determined the diurnal cycle of methane fluxes from the site at different seasons (Figure 4). We found that the diurnal cycle is strong in the summer than in the winter. However, even in the summer nighttime fluxes are a significant component of the diurnal total flux.

The mid-date peak flux rate during the summer may be explained at least in part by flux transport through plants, which provides an important mechanism for methane emission. The temporal patterns that are caused by transport through plants and seasonal and diurnal fluctuation in meteorological conditions must be accounted for when interpreting the results of limited-time campaigns.

We found that Peak covariences between methane and CO2 fluxes in the summer were at no lag (Figure 5), indicating that a large fraction of the relationship between methane and GPP is instantaneous and probably stomata driven. Nonetheless, the asymmetry of the covaiance structure indicates that at least some methane emission is lagged with respect to GPP and may be driven by the addition of labile carbon to the root zone. During the winters, when stomatal

control of aerenchyma transport of methane is impossible, the maximum covariance is lagged about 0.5-2 hours indicating that methane production processes in the soil respond slower to light, temperature and other environmental forcing than GPP by algae in the water. The maximal covariance between methane flux and GPP is lower in the winter than in the summer which is consistent with the plant mediation hypothesis as *Typha* spp. dies off in cold weather and leaves only dead culms, which would not be expected to affect the temporal dynamic of CH_4 fluxes.

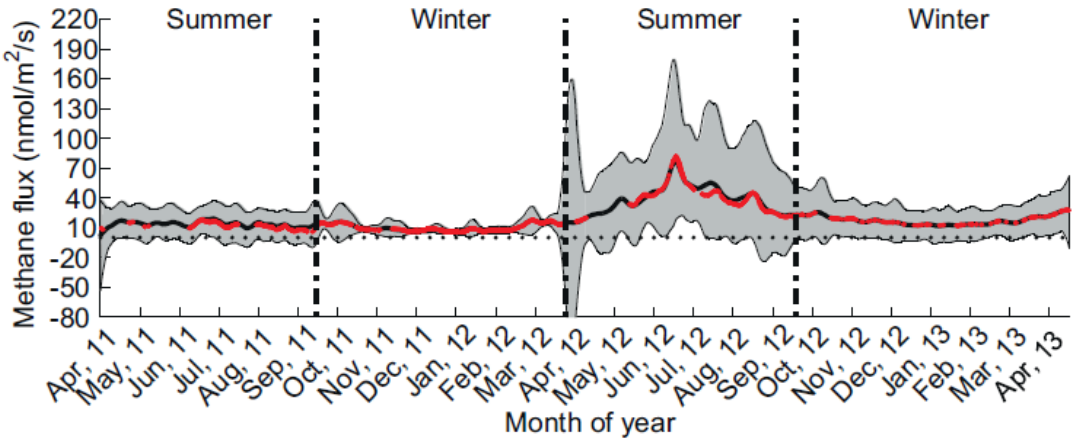

Figure 3. *2 week moving average of gapfilled methane flux data from spring 2011 through spring 2013. The light gray shading represents the 95% confidence interval given by the neural network runs. The red line with gaps shows observed methane flux data while the block continuous line shows the neural network model. When observed points were not available we used the neural network model for determining season dynamics. This shows a distinctive seasonal pattern with peaks occurring in summer months and dropping to low, but non zero, levels during the winter. Dotted line indicates the 0 nmol/m^2/s point.*

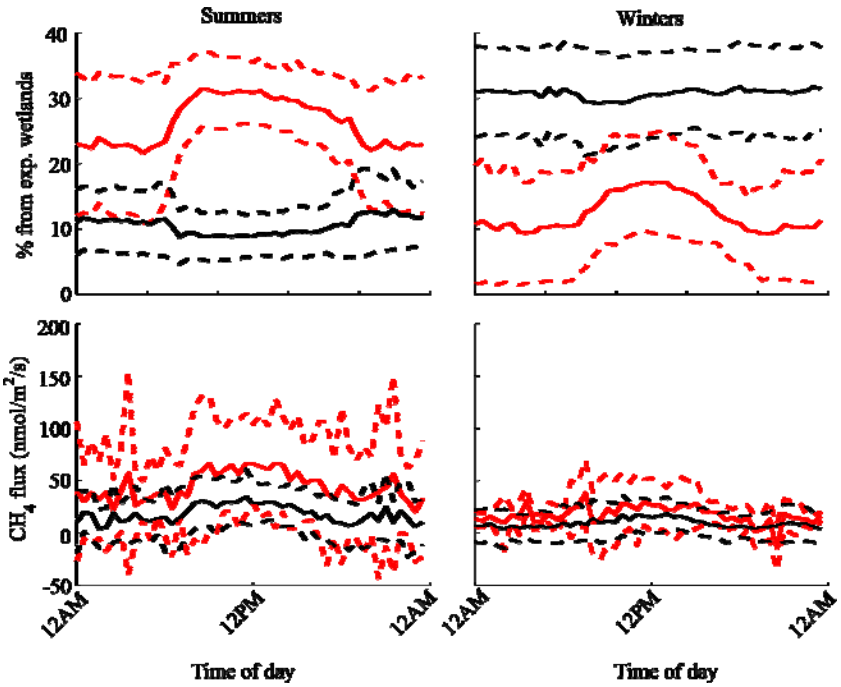

Figure 4. *Diurnal patterns of observed methane emissions from the experimental wetlands (lower panels) and the corresponding diurnal patterns of the fraction (in %) of the experimental "kidney" wetlands of the total flux source footprint (upper panels). The red lines show data for 2012, after the tower was raised while the black lines indicate the 2011 observations. Dashed lines show the standard deviation of the observations. The diurnal pattern in all seasons shows a stronger flux during the daytime and lower fluxes at night with a maximum shortly after midday.*

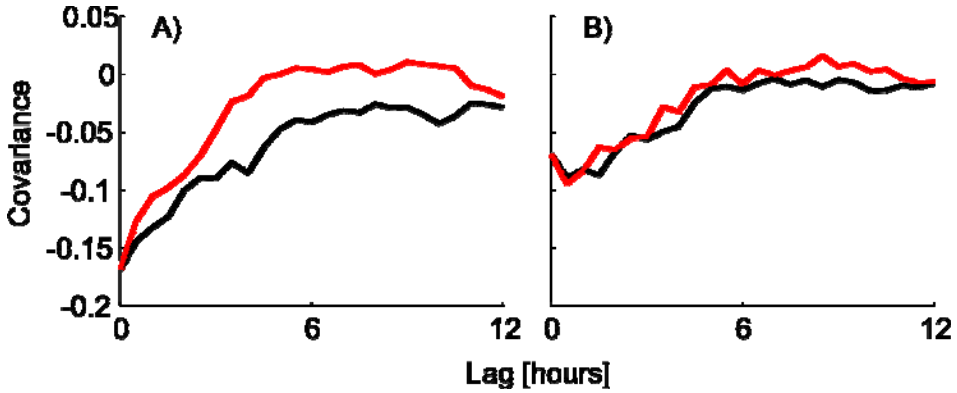

Figure 5. *The covariance between GPP and CH_4 fluxes as a function of lag time between the fluxes time series for (A) summer and (B) winter. The black line indicates the covariance as methane is lagged with respect to GPP (positive lag time, GPP happen earlier relative to methane flux) while the red line indicates the covariance as GPP is lagged with respect to methane (negative lag time, GPP happens later relative to methane). As GPP is measured as a negative flux of CO_2, a lower (more negative covariance) black curve relative to the red indicates a non-symmetric relationship with stronger lagged response of methane after GPP.*

Significance

The implications of these findings are that chamber-based and other intermittent methods of methane flux measurements must include a broad sample of all times of day and seasons in order to measure a correct annual budget of methane flux.

The plant-related influences indicate that knowledge of a wetland's plant community at high temporal resolution and their growth dynamics throughout the year, as well as the effects of these plants on methane emission mechanisms are essential for accurate quantification of its methane fluxes. Our observations provide further support for the hypothesis that plant mediated transport is responsible for a significant component of the ecosystem-level methane flux from wetlands. Further effort should target measurements that could be used to parameterize such models at an appropriately small spatial scales and high temporal resolutions.

Publications/Conference Presentations (since 3/2013)

(* - Student/post-doc/technician working for the project)

Publications

1. Morin* TH, Bohrer G, Naor-Azrieli* L, Mesi* S, Kenny WT, Mitsch WJ, Schäfer KVR. (2014) The seasonal and diurnal dynamics of methane flux at a created urban wetland. *Ecological Engineering* (in press, available on-line http://dx.doi.org/10.1016/j.ecoleng.2014.02.002).

Conference presentations

1. Naor-Azrieli* L, Morin* TH, Bohrer G, Schafer KVR, Brooker^{+} M, Mitsch WJ. Effects of environmental conditions on an urban wetland's methane fluxes. Poster, 12/2013. *American Geophysical Union Meeting 2013*, San Francisco, CA.
2. Morin* TH, Bohrer G, Vogel C. Environmental drivers influence carbon emissions and storage of a freshwater lake. Poster, 12/2013. *American Geophysical Union Meeting 2013*, San Francisco, CA.
3. Morin* TH, Bohrer G, Naor-Azrieli* L, Mesi* S, Schafer KVR, Stefanik^{+} K, Mitsch WJ. Effects of environmental conditions on urban wetland's methane fluxes. Poster, 11/2013. *42nd Annual Water Management Association of Ohio Conference, Now Trending: Innovations in Water Resource Management*, Columbus, OH.
4. Morin* TH, Bohrer G, Naor-Azrieli* L, Mesi* S, Schäfer KVR, Stefanik^{+} K, Mitsch WJ. Effects of environmental conditions on an urban wetland's methane fluxes, Poster 6/2013. *13th Annual American Ecological Engineering Society Meeting*. East Lansing, MI

Students Supported By Project 3/2013-3/2014

Two students worked on the project but none received direct support during the first project year

1. Timothy Morin – Ph. D. student in Environmental Science Graduate Program (Tuition and fees waived by CEGE department as a cost share).

Awards or Achievements

1. Ohio Water Development Authority – *Observations and modeling of wetland methane emissions* (PI-Gil Bohrer) 2013-2015, ($164,495).

Professional placement of graduates

Only one student that worked on this project graduated since the project start. Liel Naor-Azrieli. She currently does not work.

An Integrated Framework for Response Actions for a Drinking Water Distribution Security Network

Basic Information

Title:	An Integrated Framework for Response Actions for a Drinking Water Distribution Security Network
Project Number:	2012OH311O
Start Date:	8/1/2012
End Date:	7/31/2013
Funding Source:	Other
Congressional District:	1
Research Category:	Engineering
Focus Category:	Management and Planning, Solute Transport, Models
Descriptors:	
Principal Investigators:	Dominic L Boccelli

Publications

1. Rana, M. and Boccelli, D. L. (2013). “Contamination Spread Forecasting and Identification of Sampling Locations in a Water Distribution Network.” World Water and Environmental Resources Congress, ASCE, Cincinnati, OH. [oral presentation]
2. Rana, M. and Boccelli, D. L. (2013). “Contamination Spread Forecasting and Identification of Sampling Locations in a Water Distribution Network.” World Water and Environmental Resources Congress, ASCE, Cincinnati, OH. [oral presentation]
3. Rana, M. and Boccelli, D. L. (2014). “Contaminant Spread Forecasting and Confirmatory Sampling Location Identification in a Water Distribution System.” Journal of Water Resources Planning and Management, ASEC (in preparation)

An Integrated Framework for Response Actions for a Drinking Water Distribution Security Network

Problem and Research Objectives

The use of non-specific water quality sensors have provided the foundation for developing contamination warning systems (CWS) for drinking water distribution systems to protect public health from (un)intentional intrusion events. These non-specific water quality sensors (e.g., chlorine, pH, conductivity, etc.) can be linked with data driven event detection algorithms to determine when anomalous water quality conditions occur. The ability to detect water quality events has led to the development of forensic tools, such as contaminant source identification, and response strategies to mitigate the impact on the population. However, there has been little activity associated with translating the CWS signals and contaminant source information into predicting the future transport of a contamination event to inform response activities. Thus, there is a critical need to develop an integrative framework that can propagate the impacts of contaminant source uncertainty through distribution system transport to provide more information for utilizing response tools. The objective of this project, which is the next step towards developing an integrated real-time security application, is to develop a framework that will forecast contaminant spread throughout the distribution system based on the current estimated state of potential contaminant sources, which will then be utilized to inform confirmatory sampling locations to improve our estimates of contaminant spread and source location.

Methodology

Our central hypothesis is that contaminant source identification algorithms can be utilized to assess the potential contaminant spread, and provide needed information to select confirmatory sampling locations to improve our estimates of contaminant source identification and spatial distribution of an event. The rationale for developing this framework is to better utilize the information generated via CWS for assessing the overall impact throughout the distribution system and provide more appropriate response actions. We will test our central hypothesis and associated objectives by pursuing the following: 1) implement a forecasting algorithm to propagate probabilistic information associated with potential contaminant source locations to assess contaminant spread; 2) develop an approach for identifying confirmatory sampling locations that seeks to maximize new information associated with a contamination event; and 3) create an output format conducive for visualization purposes.

Forecasting Algorithm. For a given sensor network design, the forecasting algorithm will rely on the probabilistic contaminant source identification (PCSI) algorithm of Yang and Boccelli (2013) and the EPANET distribution system modeling software (Rossman, 2000) – to identify and characterize the probability of a specific location as a potential contaminant source. As sensors report positive or negative alarms (i.e., indicating an event has occurred or safe conditions exist, respectively), the PCSI algorithm utilizes the backtracking algorithm (Shang et al., 2002) to determine the upstream location-time pairs that are hydraulically connected to the observed sensor signal. Then, a Bayesian updating procedure – a Beta-Binomial conjugate pair – is used to update the probability that the location-time pair was the source (a positive alarm increases the probability; a negative alarm decreases the probability). For large networks, the PCSI algorithm will identify multiple potential source locations. The backtracking algorithm, in conjunction with hydraulic information, will be used to efficiently forecast the short-term (e.g., up to 6 hours) spread of contaminant from the individual sources represented as a "conservative tracer." For each of the downstream nodes, the flow-weighted probabilities from the

potential source locations will be assumed to characterize the probability of a contaminant being at the downstream location.

Identifying Confirmatory Sampling Locations. The following sections first introduce the metric used to quantify the information associated with sampling locations, and then how the best sampling location is determined.

Entropy as Information. Within the area of Information Theory, "entropy" is provided as a metric of information – more specifically, entropy represents the average information contained within a specific distribution (Reza, 1961). For example, if we are provided a discrete distribution of n classes, where each class has an associated probability p_i, $\sum p_i = 1$, the entropy of that distribution is defined as

$$H(P) = -\sum_{i=1}^{n} p_i \log_2 p_i$$

where P represents the overall distribution and $H(P)$ the expected information, or entropy, contained within that distribution. For a uniform distribution (i.e., p_i is the same for all classes), $H(P)$ has maximum entropy defined as $\log_2(n)$. When we have perfect information regarding one class (i.e., $p_i = 1$, $p_j = 0$ when $i \neq j$) then $H(P)$ has a minimum entropy of 0. Thus, decreasing entropy represents increased information associated with the discrete distribution.

Confirmatory Sampling Selection. The intent behind confirmatory sampling is to increase the information associated with the potential source or forecasted locations. The initial entropy estimates for the potential source and contaminant spread locations can be estimated using the probabilities developed from the PCSI algorithm. To determine the amount of information gained (or lost) by confirmatory sampling, we need to perform the following steps for each potential sampling location: i) identify the probability that the sampling location could result in a contaminant observation; ii) assume that the resulting confirmatory sample returned a positive or negative alarm and separately update the PCSI results; iii) for each set of updated source probabilities, update the probabilities of the forecasted contaminant spread; iv) calculate the updated entropies for the source and forecasted locations assuming both positive and negative alarms; and v) use the probability value associated with observing the contamination event at the sampling location (from step i) to calculate the expected entropies for the source and forecasted locations based on the updated entropies from step iv. The differences between the initial and updated entropies represent the expected amount of information gained (or lost) by performing confirmatory sampling at that individual location. Confirmatory samples with the largest information differences indicate the locations that would provide the most new information.

The benefit to this approach is that an increase in information can occur by either selecting locations that would reinforce higher probability source locations, or, vice-versa, that would reinforce lower probability source locations. In either case, the overall information would be increased by generating a distribution such that the probability of the most likely candidate location(s) also increased. Computationally, this approach is also attractive because updating the probabilities is relatively straightforward since all of the necessary hydraulic and water quality simulations have been performed leaving only the algebraic calculations to update the probabilities. The relative ease of computation will allow an enumeration approach to be utilized to identify confirmatory sampling locations rather than using a formalized optimization algorithm (e.g., a mixed-integer non-linear programming approach) that would likely be more computationally intensive.

Principal Findings and Significance

In order to test and evaluate the forecasting and sampling algorithm, two example networks were utilized: 1) a small test network (the Net 3 example) included with EPANET (Rossman, 2000), and 2) a large network most recently utilized in the "Battle of the Water Sensor Networks" (Ostfeld et al, 2008).

Small Network. Figure 1 presents the small test network model as well as the placement of five water quality sensor locations (blue symbols). A 1-hour contaminant injection was simulated at node 10 starting at the 3rd hour of the simulation. The first detection of the contaminant occurs at the 5th hour at the water quality sensors located at Node 193.

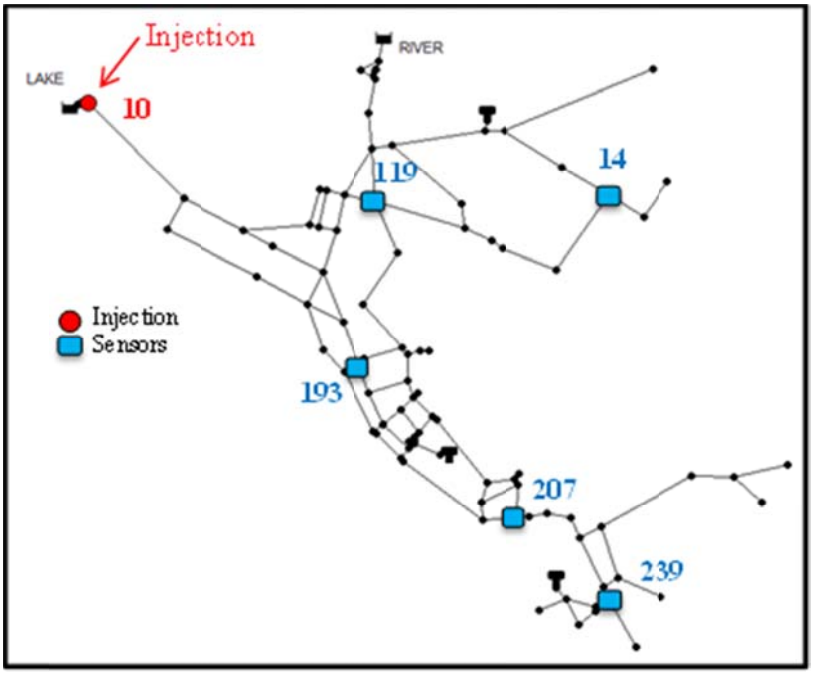

Figure 1. Small example test network for evaluating the forecasting and sampling algorithm.

Once the contaminant reaches a water quality sensor, the detection of the contaminant along with the hydraulics can be utilized with the PCSI algorithm to determine the probabilities of the upstream nodes. Figure 2 presents the upstream locations that have probabilities of greater than [red] or less than [green] a 50% probability of being a source, as determined by the PCSI algorithm.

Figure 3 presents classification results associated with data collected up until hour 6. Prior to hour 6, the data represents the classification results from the PCSI algorithm (solid lines). After hour 6, the data represents the forecasted classification performance (dashed lines). The performance of the PCSI algorithm decreases until, at the current time (hour 6), both the percent correct and incorrect identifications for the PCSI reach zero because there are no hydraulically connected nodes at the current time. With respect to the forecasted data, the increased percentage of correct identification occurs because the results are dependent upon hydraulic connections with previously connected nodes, not current connectivity with the sensors. The performance of the spread forecasting algorithm decreases as the forecasting horizon increases, which is to be expected.

Figure 4 [top] shows the forecasted change in entropy for all of the 97 possible sampling locations; a line plot (instead of a scatter plot) is used to more clearly show the results [the Node Index is an internal EPANET variable; the Node ID shown in the graph is the identifier of the actual location]. The peaks within each box are associated with the Node ID value provided, and represent the larger changes in entropy (remember, decreasing entropy suggests more information). For Nodes 1 (the biggest change), 40, and 179, these locations are either the tank or associated with the pipe to/from the tank. Node 237 is potentially downstream of contamination spread. In addition to Node 237, Nodes 206, 208, 209, 211, and 213 all have similar drops in entropy as these are all hydraulically "close" to Node 237.

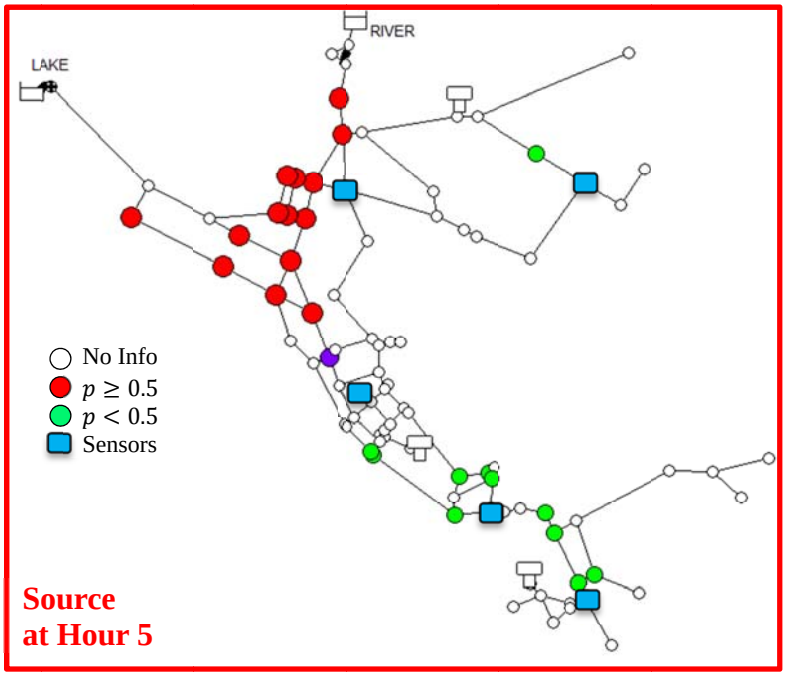

Figure 2. Estimated source probabilities at hour 5 of the simulation; red symbols represent locations with probabilities of being a source greater than 50%, green symbols represent locations with probabilities of being a source greater than 50%.

Figure 5 [top] shows the resulting change in entropy for all of the 97 possible sampling locations *after* the simulation is moved ahead one hour; a line plot is used to more clearly show the results [the Node Index is an internal EPANET variable; the Node ID shown in the graph is the identifier of the actual location]. These results provide information associated with the "true" information of the system at the next hour. The peaks within each box are associated with the Node ID value provided, and represent the larger changes in entropy (remember, decreasing entropy suggests more information). The nodes near the tank (1, 40, 179 and 271) would have provided the greatest decrease in information. The approach correctly identified Node 1 as the best sampling location and, with the exception of Node 271, also identified Nodes 40 and 179 as sampling locations with more significant decreases in entropy (Figure 4). Additionally, Nodes 199, 201 and 202, which are just downstream of Tank 1, also appear to be significant during the next hour. For the forecasted sampling, Nodes 206, 208, 209, 211, 213, and 237 were all shown to have similar impacts on entropy (Figure 3). While Nodes 211, 213 and 237 show a slightly less drop in "actual" entropy relative to the forecasted entropy, these locations were still identified. However, Nodes 206, 208 and 209 did not appear to have as significant an impact on entropy

as forecasted, but Node 241 appears to have been a good place to sample that was not one of the higher locations identified in the forecasting portion of the algorithm.

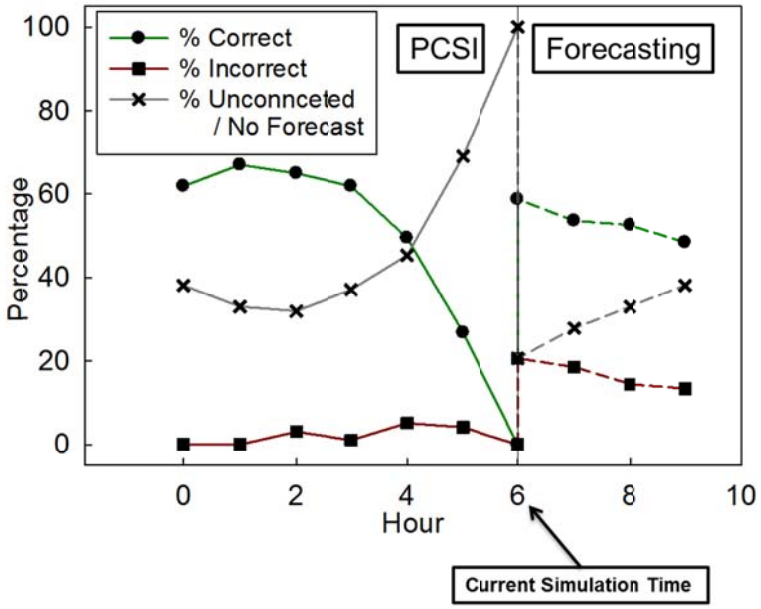

Figure 3. Spread forecasting summary for Net 3. PCSI results (solid lines) up to hour 6 are shown along with forecasting results (dashed lines) for hours 6 through 9; sensor data up to hour 6 was used for this forecasting.

Figure 6 shows the change in the PCSI results when sampling at nodes 1 or 2 along with the baseline case (no sampling). The shaded region shows the range of changes for sampling at all other locations. Sampling at nodes 1 and 2 produced the greatest increases in percent correct identification and greater decreases in percent unconnected. The percent incorrect classifications were not impacted by sampling at nodes 1 and 2. With respect to the forecasting, there was little improvement in forecasting accuracy via confirmatory sampling.

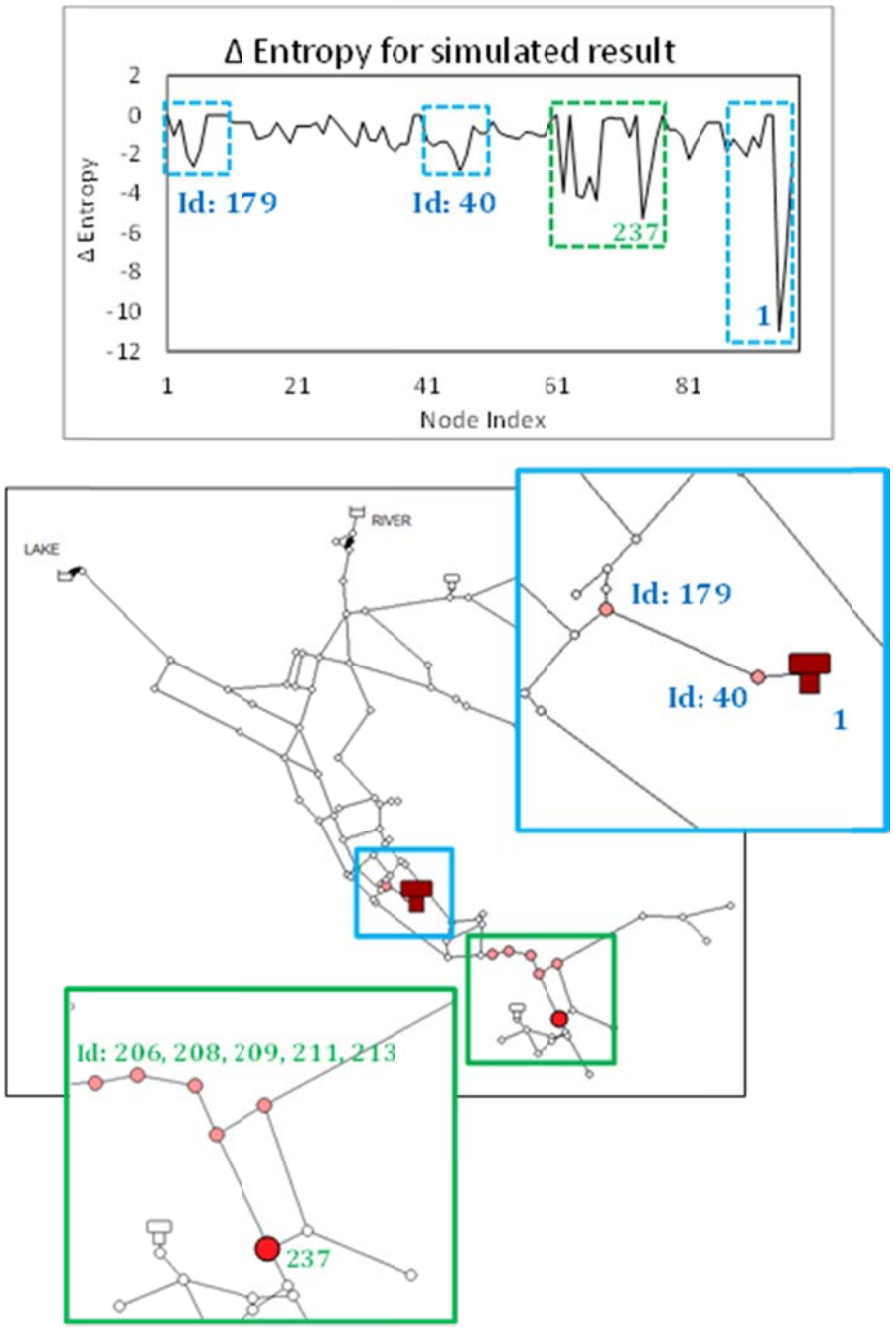

Figure 4. Plots of the forecasted change in entropy for each potential sampling location [top], as well as the spatial location of the sampling nodes that result in the greatest decrease in entropy (i.e., largest increase in information).

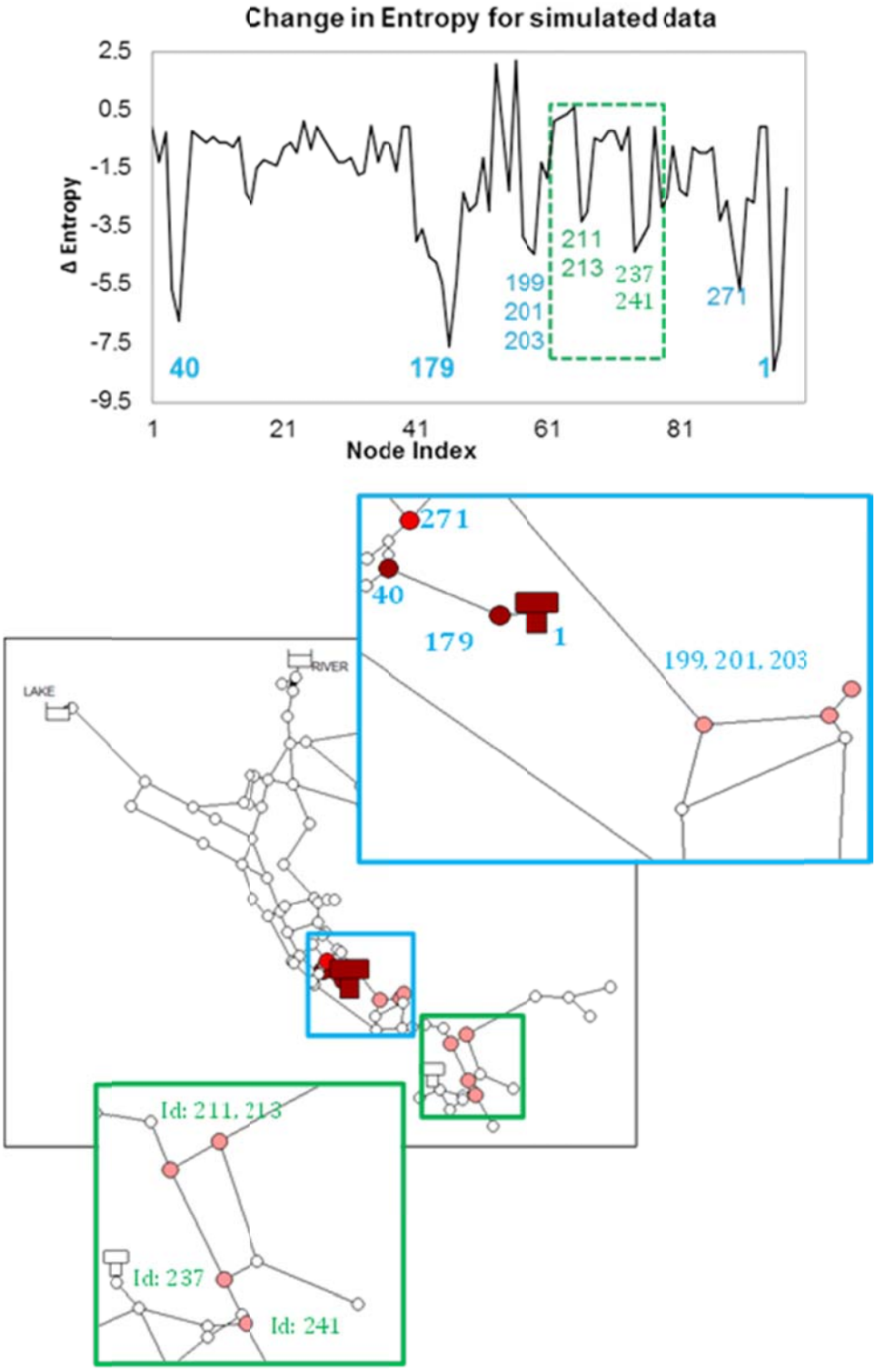

Figure 5. Plots of the forecasted change in entropy for each potential sampling location [top], as well as the spatial location of the sampling nodes that result in the greatest decrease in entropy (i.e., largest increase in information).

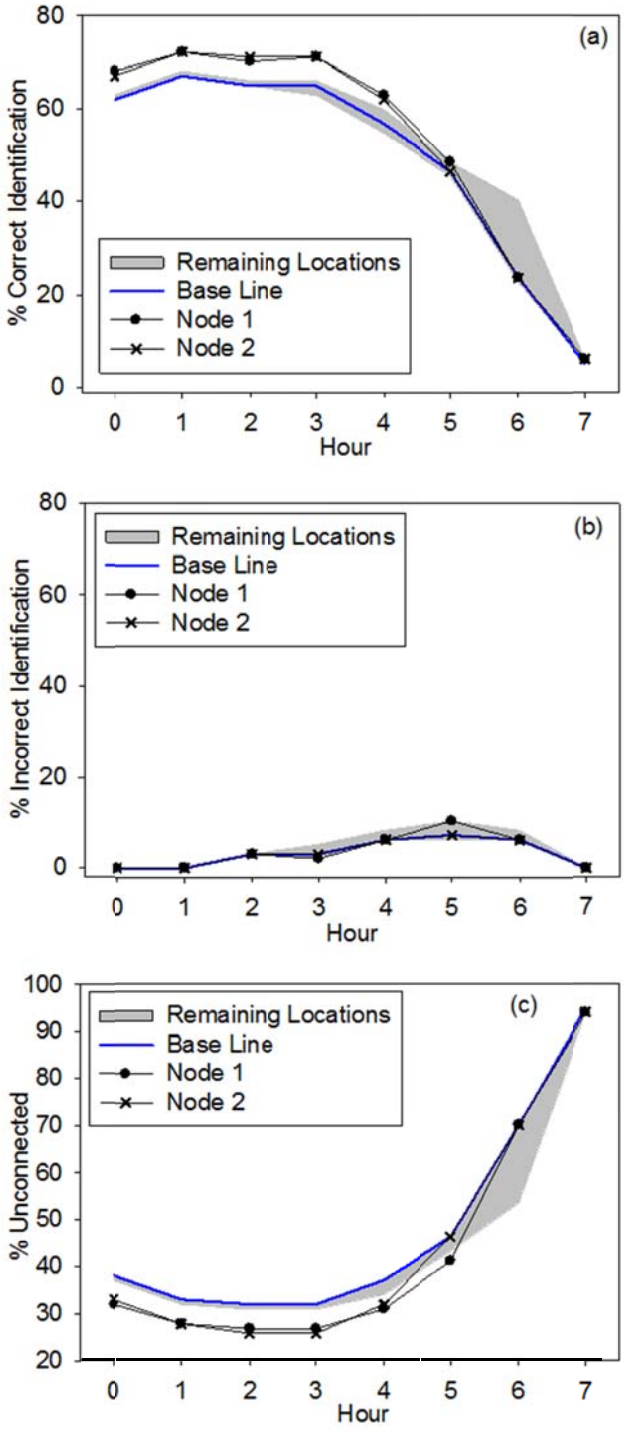

Figure 6. Changes in: (a) % correct identification; (**b**) % incorrect identification; and (c) % unconnected, in the PCSI results for Net 3 from a single grab sample during hour 7.

Large Network. Figure 7 presents the large network model as well as the placement of five water quality sensor locations (blue symbols); additional studies were performed with 10, 20 and 50 sensors. A 1-hour contaminant injection starting at the 3rd hour was simulated at node 5416 (shown by the star), which was close to the source and a high-impact node. The first detection of the contaminant occurs at the 11th hour.

Figure 7. Layout of the large test network with the injection location indicated by a star and the five sensor locations indicated by the rectangles.

Figure 8 shows the accuracy results from the PCSI algorithm and spread forecasting. These results are similar to those shown for the small network except that the percentage of correctly identified nodes and unconnected nodes are significantly decreased and increased, respectively, relative to the small network. This is due to placing the same number of sensors within a much larger network. Increasing the number of sensors improved both metrics (not shown).

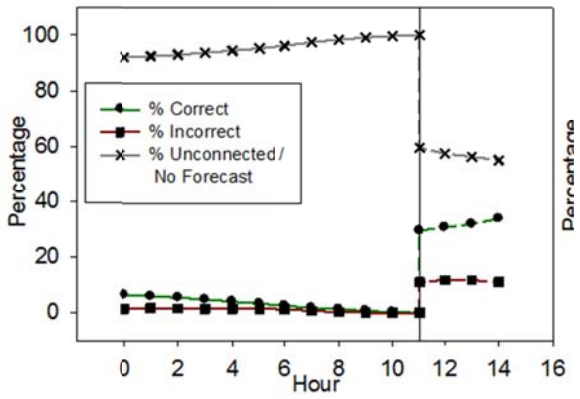

Figure 8. PCSI and spread forecasting results for the large network including the perfect correct, incorrect, and unconnected/no forecast for the 5 sensor case.

When using the forecasted results to identify the sampling locations, the sampling location that resulted in the greatest decrease in network entropy did not always result in the greatest decrease in actual network entropy once the simulations were continued. However, the locations associated with the best performance using the expected and actual network entropies were always shown to be in the top 1% of possible nodes. Figure 9 shows the top 1% of estimated confirmatory sampling locations. The circle represents the sampling location that provides the most information using the forecasted data; the triangle represents the best sampling location using perfect information (i.e., the actual hydraulic conditions, not forecasted). As can be seen in the inset, while the two possible sampling locations are not located at the same spatial locale, the sampling locations are in a similar spatial region. This observed spatial similarity occurred for all of the results if the two locations were not identical.

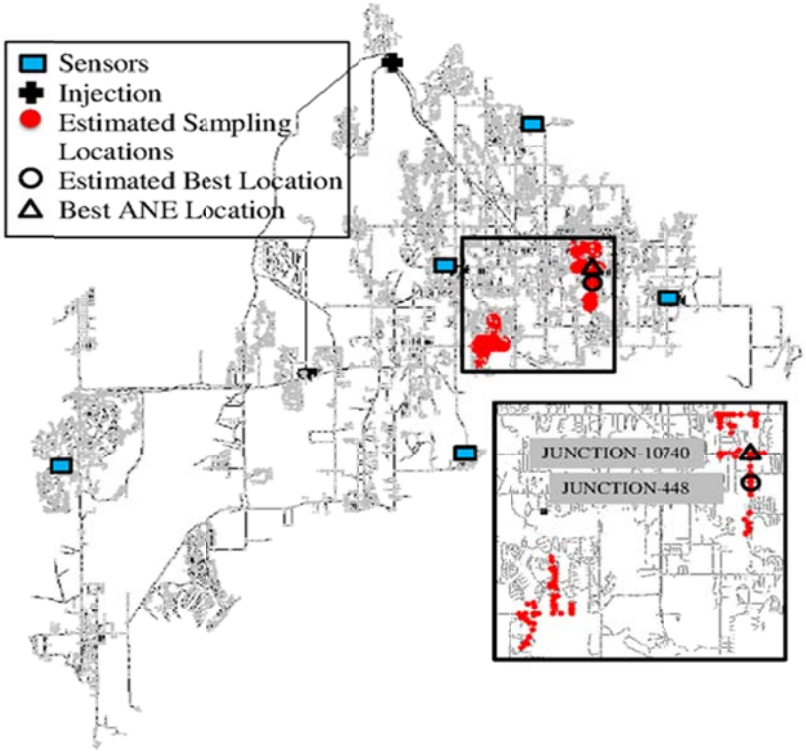

Figure 9. Spatial locations of the top 1% of the estimated sampling locations for the 5 sensor scenario in the large network; the circle represents the best sampling location based upon forecasted information and the triangle represents the best sampling location under perfect information.

Figure 10 illustrates the changes in the percentage of correct and incorrect identification and percentage of unconnected nodes in the large network for the sampling location based upon the forecasted data (JUNCTION-448), perfect information (JUNCTION-10740), and all other possible nodes (grey shaded area). While the sampling locations based on the forecasted and perfect information were not located at the exact same spatial locations, both locations provided the greatest improvement in the PCSI results relative to the other locations. In general, the confirmatory sampling algorithm identified locations that would increase the percentage of correctly identified nodes, and reduce percentage of incorrectly identified and unconnected nodes.

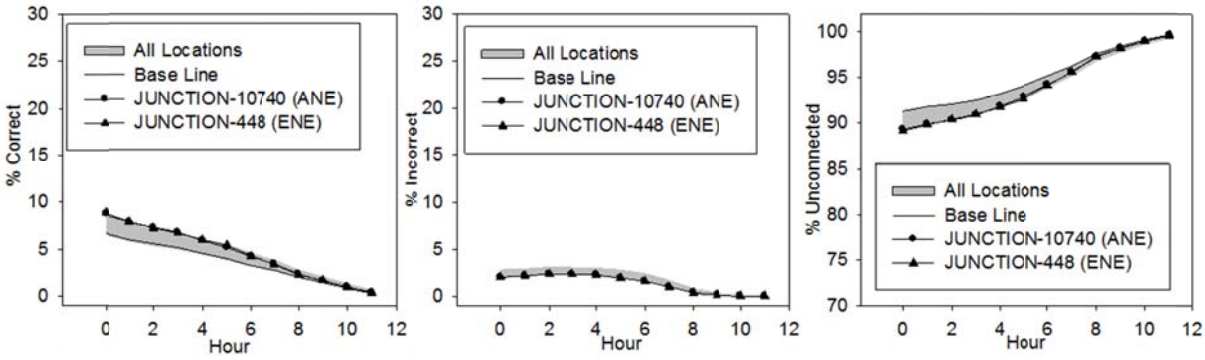

Figure 10. Changes in % correct identification (left), % incorrect identification (middle) and % unconnected (right), in the PCSI results for the large network with 5 sensors.

Figure 11 shows the future classifications without confirmatory sampling and with the confirmatory sampling locations based upon the forecasted and perfect information. For all three categories, the confirmatory samples improved our forecasted estimates. Interestingly enough, the confirmatory sampling location based on forecasted information had a greater impact on the performance of the three categories than if we had perfect information, even though the overall entropy was less. When investigating this result, the confirmatory sampling locations based upon the forecasted data tended to "uncover" more of the unconnected network whereas the sampling locations based upon the perfect information sought to identify and strengthen existing hydraulic pathways. Thus, while the latter improved the information along a given hydraulic path, not as much new information was generated

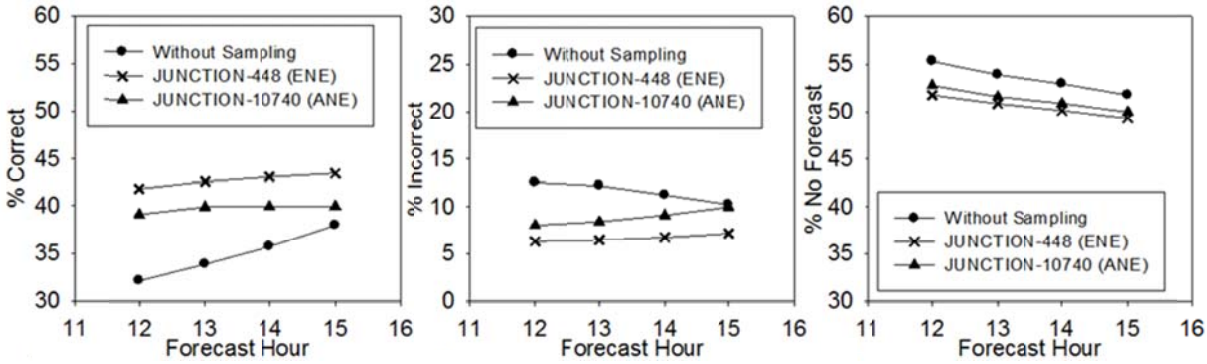

Figure 11. Change in % correct identification (left), % incorrect identification (middle) and % unconnected (right), in the forecasted spread results for the large network with 5 sensors.

about the remainder of the network.

Significance. The contribution of this research is significant as this study is effectively the first research that bridges the gap between the information generated from a contaminant warning system (via sensor response and contaminant source identification) and the initial phases of response (via confirmatory sampling). The forecasting and confirmatory sampling is particularly important for larger networks that cannot adequately cover the spatial scale of large networks with costly sensor systems.

Long-term, these results will provide the foundation for developing more robust response activities when attempting to mitigate the impact of an intrusion event.

Publication Citations

Rana, M. and Boccelli, D. L. (2013). "Contamination Spread Forecasting and Identification of Sampling Locations in a Water Distribution Network." *World Water and Environmental Resources Congress*, ASCE, Cincinnati, OH. [oral presentation]

Rana, M. and Boccelli, D. L. (2014). "Contaminant Spread Forecasting and Confirmatory Sampling Location Identification in a Water Distribution System." *Journal of Water Resources Planning and Management*, ASEC (in preparation)

Number of Students Supported

The research has funded one MS student (Masud Rana) in Environmental Engineering.

Awards or Achievements

N/A

Professional Placement of Graduates

Mr. Rana graduated with his M.S. degree in the Fall of 2013 and is currently pursuing his Ph.D. at Virginia Tech.

References

Ostfeld, A., Uber, J. G., Salomons, E., Berry, J. W., Hart, W. E., Phillips, C. A., Watson, J.-P., Dorini, G., Jonkergouw, P., Kapelan, Z., di Pierro, F., Khu, S.-T., Savic, D., Eliades, D., Polycarpou, M., Ghimire, S. R., Barkdoll, B. D., Gueli, R., Huang, J. J., McBean, E. A., James, W., Krause, A., Leskovic, J. Isovitsch, S., Xu, J., Guestrin, C., VanBriesen, J., Small, M. Fischbeck, P., Preis, A., Propato, M. Pillier, O., Trachtman, G. B., Wu, Z. Y., and Walski, T. (2008) "The Battle of the Water Sensor Networks (BWSN): A design challenge for engineers and algorithms." *Journal of Water Resources Planning and Management*, 134(6), 556-568.

Reza, F. M. (1961) *An Introduction to Information Theory*. McGraw-Hill, New York.

Rossman, L. A. (2000) *EPANET2 User's Manual*. Cincinnati, OH: Risk Reduction Engineering Laboratory, U.S. Environmental Protection Agency.

Shang, F., Uber, J. G., and Polycarpou, M. M. (2002) "Particle Backtracking Algorithm for Water Distribution System Analysis." *Journal of Environmental Engineering*, 128(5), 441-450.

Yang, X. and Boccelli, D. L. (2013) "A Bayesian Approach for Real-Time Probabilistic Contaminant Source Identification." *Journal of Water Resources Planning and Management*, (under review).

Source tracking of Microcystis blooms in Lake Erie and its tributaries

Basic Information

Title:	Source tracking of Microcystis blooms in Lake Erie and its tributaries
Project Number:	2013OH292B
Start Date:	1/3/2013
End Date:	2/28/2015
Funding Source:	104B
Congressional District:	5th
Research Category:	Biological Sciences
Focus Category:	Water Quality, Toxic Substances, None
Descriptors:	
Principal Investigators:	George Shepley Bullerjahn

Publications

1. Bullerjahn, G. S.; Davis, T. W.; Watson, S. B.; Rozmarynowycz, M. J.; McKay, R. M. Linking the genetics, toxicity and physiology of Planktothrix blooms to increased nitrogen and phosphorus concentrations in a eutrophic embayment of Lake Erie, Joint Aquatic Sciences Meeting, Portland OR, USA, May 2014.
2. Davis, T.W., Watson, S.B., Rozmarynowycz, M.J., Ciborowski, J., McKay, R.M., Bullerjahn, G. Molecular and taxonomic characterization of potential microcystin-producing cyanobacteria in Lake St. Clair during a late summer bloom, International Association for Great Lakes Research, Hamilton, ON, May 2014.
3. Davis T.W., Watson, S.B., Schulte, S., Tuttle, T., Wagner, A., Bullerjahn, G. Factors influencing Planktothrix bloom formation in the Lake Erie watershed. Water Management Association of Ohio Annual Meeting, November 2013. Invited Presentation
4. Davis, T.W., Watson, S.B., Rozmarynowycz, M.J., Ciborowski, J., McKay, R.M., Tuttle, T., Bullerjahn, G., submitted. A toxic continuum: Evidence that Lake St. Clair is a source of microcystin-producing cyanobacteria in Lakes Erie and Ontario. PLOS ONE, April 2014.

1) Progress report to Ohio Water Resources Center

Source Tracking of *Microcystis* Blooms in Lake Erie and its Tributaries

George S. Bullerjahn, PI, Bowling Green State University

The objective of this study is to determine the source of the diverse *Microcystis* that comprise the annual Lake Erie cyanobacterial blooms. Whereas some toxic and nontoxic forms may arise within Lake Erie sediments, the diversity of *Microcystis* detected in blooms may reveal genotypes that originate in sites physically removed from the lake. Understanding the origins of toxic and nontoxic forms can inform management strategies in the Great Lakes that may limit the expansion of *Microcytis* blooms in Lake Erie. Our methodology involves sequencing target genes from *Microcystis* populations to determine the toxic genotypes present, and the sites upstream from Lake Erie in which they may originate. Phylogenetic analysis of ribosomal 16S genes, toxin (*mcy*) genes and the N-responsive *ntcA* gene has provided fine-structure analysis of cyanobacterial populations that occur in the Lake Erie drainage basin. One result of our work described below is that while Lake Erie *Microcystis* genotypes are found in abundance upstream in Lake St. Clair, nearshore sites in Lake Erie (Sandusky Bay and Maumee River) are dominated by microcystin-producing *Planktothrix*. This latter finding has led to a future study on *Planktothrix* ecophysiology that has recently been funded by Ohio Sea Grant.

We proposed to monitor *Microcystis* genotypes from the Laurentian Great Lake Basin using archives of DNA from across the Great Lakes and tributaries/connecting channels, together with parallel measurements of nutrients, chlorophyll and physico-chemical parameters. The results will establish the diversity and geographic origins of the bloom-forming genotypes. Analysis of focal cyanobacterial harmful algal bloom (cHAB) species diversity from physically remote sites and Erie blooms has been conducted for one full bloom season and will be completed in continuing work during summer 2014.

Progress to date: During the summer of 2013 we conducted a spatial and temporal survey of Lake St. Clair (LSC). Three sites around the southeast corner of LSC where the Thames River enters LSC were monitored from June through September for CHAB genetic and phytoplankton community composition. In late August, a high biomass event occurred. During this event a spatial survey was conducted from Mitchel's Bay to the mouth of the Detroit River (17 sites; see Figure 1). We collected samples for DNA, dissolved and total nutrients, phytoplankton community composition and toxicity. We targeted the *mcyA* gene, part of the microcystin synthetase gene operon, to investigate the

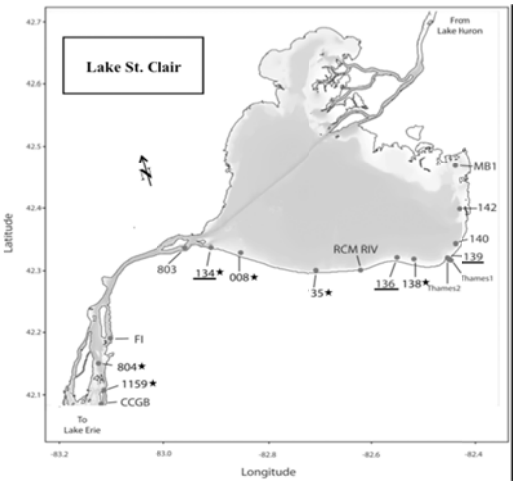

Figure 1: Map of Lake St. Clair indicating sampling sites. The underlined sites were the seasonal monitoring sites; starred sites where DNA was extracted and sequenced for genetic diversity.

phylogenetics of potential microcystin producers in LSC and the Detroit River. The *mcyA* primers we used amplify the gene segment from *Microcystis*, *Planktothrix* and *Anabaena* provided a robust picture of the potential microcystin producers in LSC and helped determine whether those strains were similar to strains found in the lower Great Lakes. We found that *Microcystis* was the predominant microcystin producer and that all toxic *Microcystis* strains found in Lake St. Clair clustered with toxic strains found in samples previously collected from Lakes Erie and Ontario, demonstrating extensive genetic connectivity between the three systems and establishing Lake St. Clair as an important immediate and historical source of toxic *Microcystis* to lakes Erie and Ontario. Also, we found that *Microcystis* blooms in Lake St. Clair can produce microcystin at levels that could negatively affect human health. These data will be presented at the 2014 International Association for Great Lakes Research and have been incorporated into a manuscript submitted to the international peer-reviewed journal PLOS ONE.

Bullerjahn's work is also informed by metagenomic and metatranscriptomic analyses provided through an approved project DOE-Joint Genome Institute ("Metagenomics and metatranscriptomics of the Lake Erie 'dead zone': a seasonal source of greenhouse gases," PIs McKay, Bullerjahn and Bourbonierre). Sampling pelagic Lake Erie and nearshore sites, we currently have metagenomes from Sandusky Bay and metagenomes and metatranscriptome data from the Erie central basin. The N-responsive regulator gene *ntcA* is unique to cyanobacteria, and we have used *ntcA* sequences as a measure of cyanobacterial diversity and relative abundance at these sites. The expression of ntcA in the metatranscriptome is also a measure of nitrogen bioavailability, as high levels of *ntcA* mRNA is diagnostic for N-limited cyanobacteria. For example, the recent availability of the Sandusky Bay metagenome has allowed us to examine total cyanobacterial diversity and diversity of microcystin producers through phylogenetics of *ntcA* and *mcyA*. Regarding total cyanobacterial diversity, toxic *Planktothrix,* not *Microcystis,* dominates in nearshore environments such as Sandusky Bay, with heterocystous cyanobacteria present as minor members of the community. Importantly, the metagenome indicates that the number of *Planktothrix* genotypes is very low, allowing the design of some fairly straightforward experiments to test mechanisms of bloom formation and toxigenicity. Given that Sandusky Bay often experiences N limitation (see below), and that *Planktothrix* is not an N fixer, we speculate that *Planktothrix* is particularly successful at scavenging nitrogen, likely provided from nitrogen fixing taxa present. We hypothesize that N scavenging by *Planktothrix* is responsible for this genus outcompeting *Microcystis* in nearshore waters. Examining the diversity of N fixers by binning all *nifH* reads from the metagenome, only about one-third of the nitrogen fixers are cyanobacteria, the remainder being heterotrophic proteobacteria.

Collectively, these data sets on Erie and Sandusky Bay have allowed the development of RT-PCR primers specific for endemic *Microcystis* and *Planktothrix ntcA*, *mcyA* and cyanobacterial/bacterial *nifH*. qRT-PCR will be employed in field samples and laboratory experiments to assess the nutrient regimes (N speciation/SRP/organic P) that promote *Microcystis* and *Planktothrix* growth and toxigenicity. Additionally, in work stemming from genomic analysis of the nitrogen fixation genes, we are currently measuring nitrogen fixation rates from sediment and planktonic microbes to determine

inputs of new N into the bloom sites. These genomic data in concert with the source tracking work described will be presented at the May 2014 Joint Aquatic Sciences Meeting in Portland, OR.

2) Publication citations

Publications in refereed journals

Davis, T.W., Watson, S.B., Rozmarynowycz, M.J., Ciborowski, J., McKay, R.M., **Tuttle, T., Bullerjahn, G.**, *submitted*. A toxic continuum: Evidence that Lake St. Clair is a source of microcystin-producing cyanobacteria in Lakes Erie and Ontario. *PLOS ONE*, April 2014.

Invited presentation:

Davis T.W., Watson, S.B., Schulte, S., **Tuttle, T.,** Wagner, A., **Bullerjahn, G.** Factors influencing *Planktothrix* bloom formation in the Lake Erie watershed. Water Management Association of Ohio Annual Meeting, November 2013.

National/international conference presentations

Davis, T.W., Watson, S.B., Rozmarynowycz, M.J., Ciborowski, J., McKay, R.M., **Bullerjahn, G.** Molecular and taxonomic characterization of potential microcystin-producing cyanobacteria in Lake St. Clair during a late summer bloom, International Association for Great Lakes Research, Hamilton, ON, May 2014.

Bullerjahn, G. S.; Davis, T. W.; Watson, S. B.; Rozmarynowycz, M. J.; McKay, R. M. Linking the genetics, toxicity and physiology of *Planktothrix* blooms to increased nitrogen and phosphorus concentrations in a eutrophic embayment of Lake Erie, Joint Aquatic Sciences Meeting, Portland OR, USA, May 2014.

3) Students supported by the project

Funds from this OWRC award covered supplies and travel costs for sampling, DNA sequencing and genetic analyses. Additionally, some funds were used for travel research sites and to confer with colleagues. **Taylor Tuttle**, MS student in the PI's lab, and **Dr. Timothy Davis,** postdoctoral fellow with collaborator Sue Watson (Environment Canada) were direct beneficiaries, as the available funds supported all their experimental work during the 2013 bloom season.

4) Awards or Achievements, additional funding for this project

Regarding the genetic work showing the dominance of *Planktothrix* in Sandusky Bay and other nearshore sites, we applied for funds to Ohio Sea Grant to explore the factors that favor *Planktothrix* in these waters. The award was funded with a start date of February 2014:

NOAA – Ohio Sea Grant College Program, R/ER-104. $103,833. "Source tracking and toxigenicity of *Planktothrix* in Sandusky Bay." Funded for period 02/01/14 – 01/31/16.

Regarding Profession Placement of Graduates including sector (if known and applicable) and Teaching Assistantship, the student conducting much of the research (Taylor Tuttle) has not yet graduated (she will graduate Spring 2015). She was supported as a Teaching Assistant with BGSU Departmental funds during 2013-14.

Again, thanks very much and I hope to see you al WMOA this fall.

Rural on-site waste treatment as a source of nutrients to a eutrophic watershed

Basic Information

Title:	Rural on-site waste treatment as a source of nutrients to a eutrophic watershed
Project Number:	2013OH294B
Start Date:	3/1/2013
End Date:	12/31/2014
Funding Source:	104B
Congressional District:	OH-004
Research Category:	Water Quality
Focus Category:	Acid Deposition, Nitrate Contamination, Water Quality
Descriptors:	
Principal Investigators:	Christopher Spiese, Bryan ONeil Boulanger

Publications

1. Spiese, CE, JM Berry, and B Boulanger. What caffeine tells us about nutrient source apportionment in rural watershed tile drainage. ASCE Environmental and Water Resources Institute Conference Proceeding. (Peer-reviewed & funded by WRRAA).
2. Berry, JM, CE Spiese, LM Streaker, and B Boulanger. Quantification of nitrogen and phosphorus from tile drainage in freshwater systems using caffeine as a human biomarker. Michigan State University Undergraduate Research Symposium, October 5, 2013. Funded by WRRAA, 1 student attending
3. Streaker LM, CE Spiese, and JM Berry. Using sterol biomarkers to trace a eutrophic watershed. Michigan State University Undergraduate Research Symposium, October 5, 2013. Partially funded by WRRAA, 1 student attending
4. Spiese, CE, JM Berry, LM Streaker, B Boulanger, and AG Thayer. Contribution of rural septic systems to nutrient loading in a eutrophic watershed. Water Management Association of Ohio 42nd Annual Meeting, November 13, 2013. Funded by WRRAA, 0 students attending.

2014 Progress Report: Rural on-site waste treatment as a source of nutrients to a eutrophic watershed

Problem and Research Objectives. This project aimed to determine whether or not rural septic systems contributed to nutrient and microbial loadings in the Blanchard River. The Blanchard River is a tributary to the western Lake Erie Basin and has been heavily impacted by increased phosphorus and nitrogen concentrations. While a number of factors can potentially contribute both nutrients to the river, septic systems have been targeted as an easily regulated source. This project looked at a marker of human waste streams, caffeine, and its relationship with phosphorus and nitrogen concentrations in tile drainage effluent as well as fecal coliform and *E. coli*.

Methodologies. Standards for all chemical parameters (nitrate, ammonia, and phosphorus) were created from certified reference materials or from drug standards (caffeine). Controls, field samples, and standards were determined using at least triplicate replicates. Caffeine was quantified using isotope dilution. Additional details concerning the study site and analytical methodology are presented in the proceeding sections.

Nitrogen. Two forms of dissolved nitrogen were measured: nitrate and ammonia. Both were measured *in situ* simultaneously using an YSI ProPlus meter with ion selective electrodes (ISE) for nitrate and ammonia. This method follows Standard Method (4500-NH_3 D) for ammonia (Standard Methods, 2013) and EPA Method 9210A for nitrate (US EPA, 2007). Standardization was performed using certified standards, and each ISE was calibrated prior to use. Detection limits for nitrate were 0.1 mg N/L.

Phosphorus. Phosphorus was determined using EPA Method 365.1 (US EPA, 1993). Soluble reactive phosphorus (SRP) was determined as molybdenum blue reactive substances present after filtration through a pre-combusted 0.45μm glass fiber filter. Total phosphorus was determined using the same method on unfiltered water samples after digestion with sodium persulfate. Absorbance measurements were made on a Shimadzu UV2401-PC UV-Vis spectrometer at 610 nm using either a 1 cm or 5 cm path length cuvette, depending on absorbance. Method detection limits were 5 μg P/L or lower for all phosphorous measurements.

Caffeine. Caffeine was determined following the method of Buerge, *et al.* (2003). Briefly, caffeine was extracted from 1 L of water using a solid-phase extraction (SPE) cartridge filled with silica-supported C_{18}. The caffeine was then eluted from the cartridge using methanol and dichloromethane. The methanol portion was re-extracted with dichloromethane and the combined dichloromethane layers were evaporated to dryness under a gentle stream of air. The evaporated sample was then reconstituted in dichloromethane system. Quantitation was achieved using a gas chromatography-mass spectrometry (GC-MS). An internal standard (caffeine-$^{15}N_2$) was employed prior to SPE in order to permit accurate quantification. Blank samples were periodically analyzed to control for any potential contamination. Spike recovery studies were

carried out for method confirmation. Reported detection limits for this method were approximately 10 ng/L with a reporting limit of 100 ng/L. Previously reported caffeine concentrations observed in a neighboring western Lake Erie watershed were in excess of 100 ng/L (Wu, *et al.*, 2012).

Principal Findings and Significance. At six sites across Putnam County, Ohio, tile drainage water was sampled over the course of a year. Caffeine was found at all of the sites, at varying levels (Fig. 1). Table 1 provides the mean ± standard deviation concentrations for nutrients, suspended sediment, and caffeine observed in each site over the course of the entire research. The observed water temperature at each site ranged from 16.3 to 21.8 °C , the observed pH ranged from 7.5 to 8.0, and chloride ranged from 6.2 to 13.0 mg/L. Temperature, pH, and chloride did not demonstrate any correlation to nutrient levels or caffeine levels observed within the watershed. There were also no correlations observed between caffeine and nitrate, caffeine and ammonium, caffeine and nitrite, or caffeine and total nitrogen. However, caffeine was observed to have a strong negative correlation (Pearson's r> -0.9) with total phosphorous (Figure 2).

Mean ± standard deviation caffeine concentrations across sampling sites ranged from non-detect at the control site (site #4) to 1.2±0.4 µg/L in tile drainage effluents from sites having on-site wastewater systems (site # 1-3, 5, and 6). Mean ± standard deviation concentrations observed for total nitrogen and phosphorous concentrations in all tile drains were 3.5±1.8 mg/L and 0.4±0.07 mg/L, respectively. While the overall standard deviations for all analytes were variable, the observed correlations were maintained during analysis of individual storm events. Therefore, we are confident in the observed trends indicated in the data set when taken for individual sampling events or as grouped means.

Table 1. Mean ± standard deviation concentrations for nutrients and caffeine observed in each site over the course of the entire research project.

Site number	Ammonia (mg/L)	Nitrate (mg/L)	Total Phosphorous (mg/L)	Suspended Sediment (mg/L)	Caffeine (μg/L)
1	0.62±1.0	3.21±3.87	0.47±0.4	21±25	0.45±0.7
2	0.26±0.2	2.47±2.19	0.45±0.4	8.2±6.0	0.43±0.3
3	0.30±0.5	0.92±0.72	0.4±0.3	16±12	0.82±1.7
5	0.14±0.1	5.7±5.2	0.31±0.3	10±14	1.2±1.4
6	0.48±0.4	2.1±1.4	0.5±0.3	15±10	0.26±0.13
control	0.17±0.04	7.3±8.6	0.38±0.3	14±8.6	BDL

The study results are interesting, because the observed caffeine-total phosphorous correlation indicates that septic effluents are not significant contributors to nutrient loadings within the rural watershed. Additionally, commonalities in nutrient fingerprints (total and speciated phosphorous and nitrogen) in groundwater and tile drainage highlight the complex relationships for nutrient and water quality management in irrigation drainage waters.

The observed trends in nutrient levels from each sampling site and the demonstrated inverse correlation with phosphorous led us to explore groundwater concentrations of the nutrients. Groundwater from a nearby well indicated a mean total phosphorous 0.39 mg P/L. A mean phosphorous tile drain concentration for the entire study was determined to be 0.4±0.07 mg P/L. Additionally, analysis of fifteen surface water samples from Riley Creek contained an average phosphorous concentration of 0.44±0.1 mg P/L. Additional groundwater samples are currently being explored to confirm a proposed pathway where property drinking water wells convey nutrient rich groundwater through the OSWT system, which then drains into the Creek via the tile. Therefore, efforts to control OSWT systems will likely not have a measurable effect on nutrient loadings unless groundwater can also be controlled or leach systems become more widely implemented. Evidence for the plausibility of the proposed nutrient pathway is also supplied by the earlier examination of the correlation between nutrients and river discharge.

The lack of a correlation between nitrate and SRP to river discharge points towards a source that is likely not coupled to rainfall. The constant use of wells throughout the region, may explain why phosphorous levels in the watershed have increased as efforts to manage nutrients in runoff have increased.

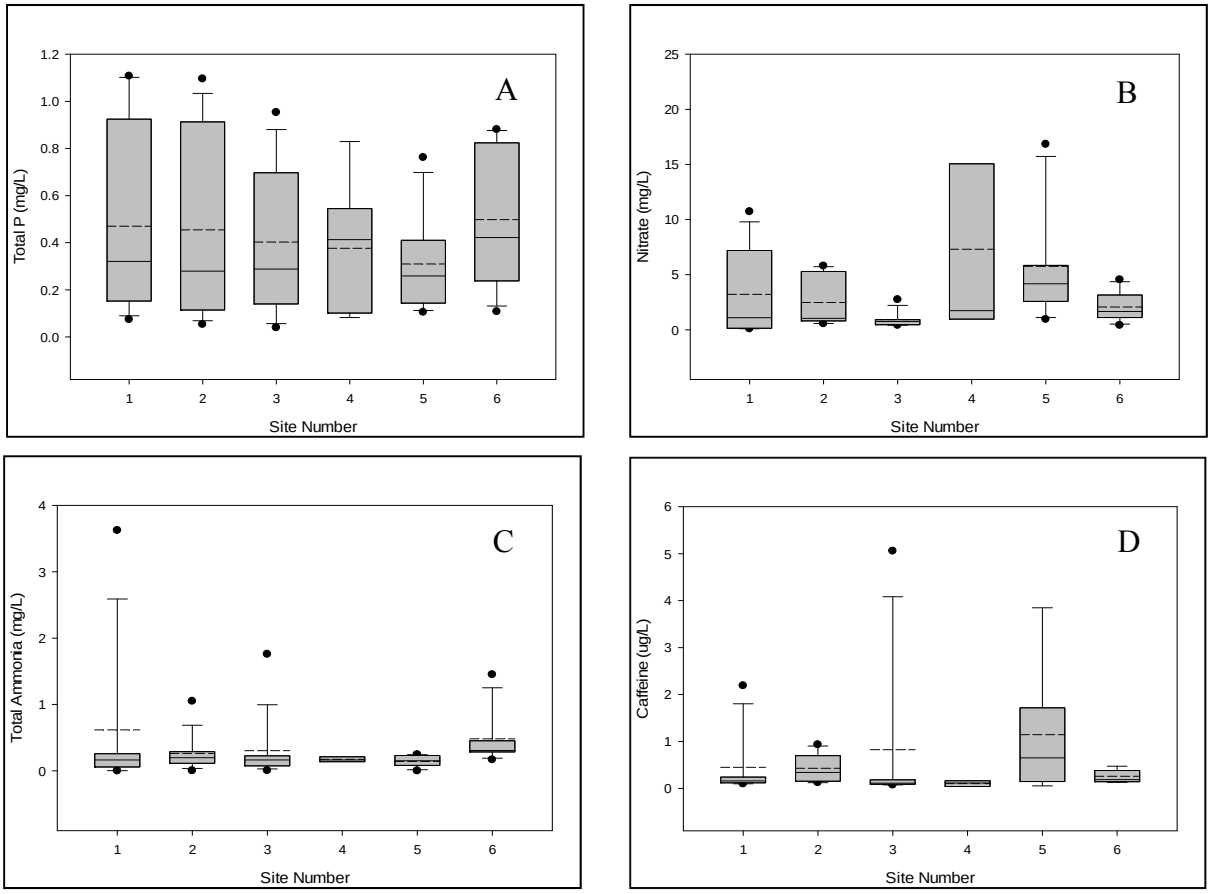

Figure 1. Compiled data for 2013 for A) total phosphorus, B) Nitrate, C) total ammonia, and D) caffeine. The boxes denote 25th through 75th quartiles, with the solid line at the median value and the dashed line at the mean. Error bars denote 95% confidence intervals and points denote outliers.

Initial results are available regarding microbial loadings tied to caffeine concentrations (Fig. 3). At nearly all sites tested, both fecal coliform bacteria and *E. coli* were detected. Both microbe types were correlated with caffeine concentration, indicating a common source. This is particularly true for *E. coli*, where the correlation is statistically significant ($p = 0.015$), and there is precedent for *E. coli* being linked directly to human waste streams (Frenzel and Couvillion 2002).

Taken together, the role of OSWT in loadings of nutrients and bacteria is complex. In this agricultural watershed, OSWT does not contribute significantly to nutrients, but do appear to be a source of bacteria. These results urge caution when making policy decisions related to nutrient reduction by targeting residential OSWT systems.

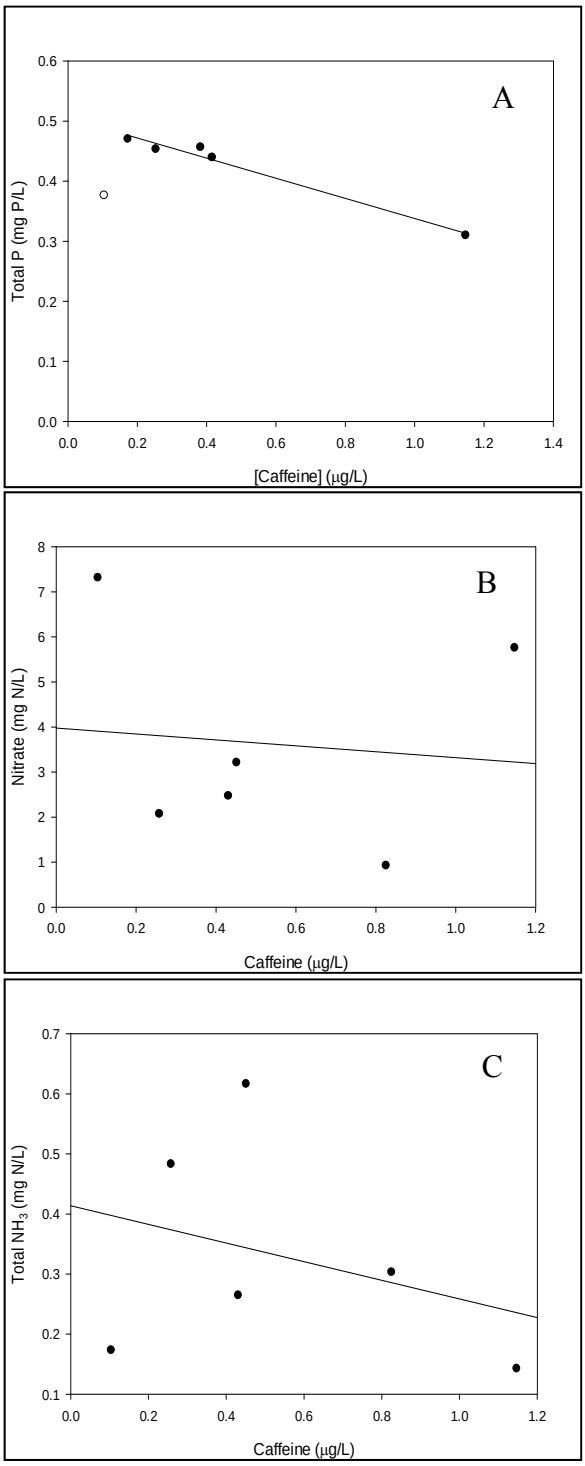

Figure 2. Correlations between caffeine and A) total P, B) nitrate, and C) ammonia. Points denote mean of all samples. Correlation coefficients were non-significant except for P ($p = 0.001$).

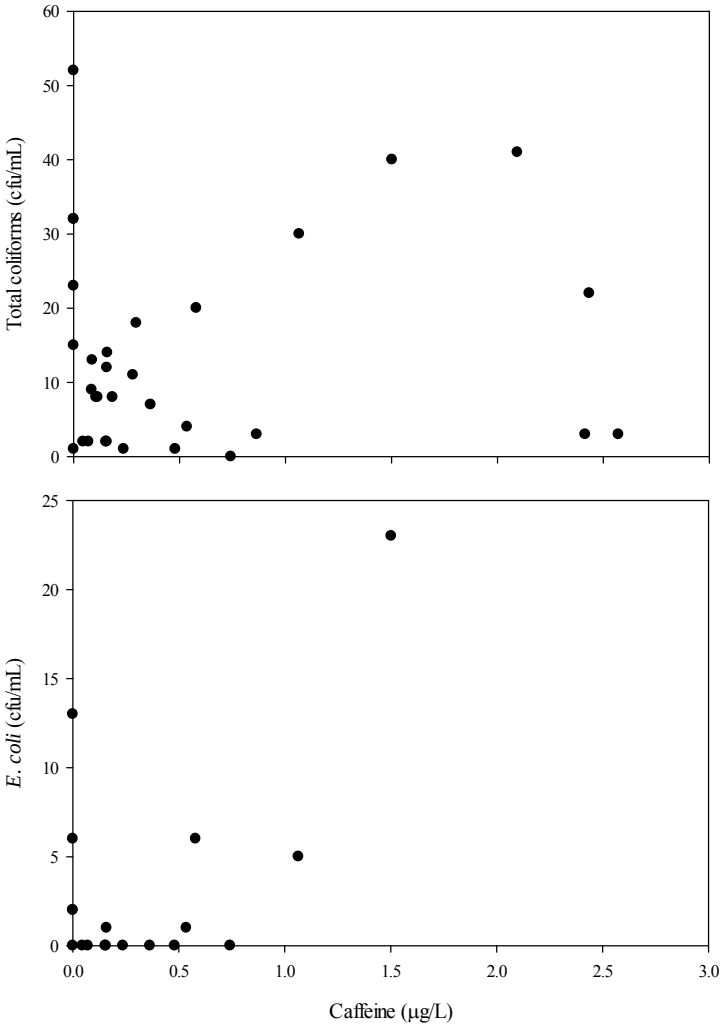

Figure 3. Correlations between caffeine and total coliform bacterial loading (upper) and caffeine and *E. coli* (lower). Correlation coefficients were significant for both microbes ($p = 0.05$ and 0.015 for coliforms and *E. coli*, respectively).

References

Buerge IJ, Poiger T, Müller MD & Buser H-R (2003) Caffeine, an anthropogenic marker fro wastewater contamination of surface waters. *Env. Sci. Tech.* **37**: 691-700.

Dolan DM & Chapra SC (2012) Great Lakes total phosphorus revisited: 1. Loading analysis and update (1994-2008). *J. Great Lakes Res.* **38**: 730-740.

Frenzel SA & Couvillion CS (2002) Fecal-indicator bacteria in streams along a gradient of residential development. *J. Am. Water Resour. Assn.* **30**: 265-273.

North RL, Guildford SJ, Smith REH, Havens SM & Twiss MR (2007) Evidence for phosphorus, nitrogen, and iron colimitation of phytoplankton communities in Lake Erie. *Limnol. Oceanogr.* **52**: 315-328.

Peeler KA, Opsahl SP & Chanton JP (2006) Tracking anthropogenic inputs using caffeine, indicator bacteria and nutrients in rural freshwater and urban marine systems. *Env. Sci. Tech.* **40**: 7616-7622.

Seiler R, Zaugg SD, Thomas JM & Howcroft DL (1999) Caffeine and pharmaceuticals as indicators of water contamination in wells. *Ground Water* **37**: 405-410.

Standard Methods (2013) Standard Method 4500-NH3 D. Ammonia-Selective Electrode Method. Standard Methods Online -- Standard Methods for the Examination of Water and Wastewater. http://standarmethods.org., last accessed Jan 16, 2014

Starr JL & Sawhney BL (1980) Movement of nitrogen and carbon from a septic system drainfield. *Water Air Soil Pollut.* **13**: 113-123.

US EPA (2013) http://water.epa.gov/infrastructure/septic/, last accessed Jan 16, 2014

US EPA (2007) EPA Method 9210A Potentiometric Determination of Nitrate in Aqueouse Samples with an Ion-Selective Electrode

US EPA (1993) EPA Method 365.1 Determination of Phosphorous By Semi-Automated Colorimetry

Wu C, Witter JD, Spongberg AL & Czajkowski KP (2012) Occurrence of selected pharmaceuticals in an agricultural landscape, western Lake Erie basin. *Wat. Res.* **43**: 3407-3416.

Research Information

1. WRC 104(b) or 104(g) or OWDA Grant including (1) Project number; (2) Number of faculty involved; (3) Number of students supported; (4) Degree type and major or specialization

Project Number: 60039770; Faculty involved: 2; Students supported: 3; Degree type: BS (Biochemistry), BS (Chemistry), BS (Chemistry & Applied Math)

2. Research Publications including (1) Complete citation; (2) Whether publication was peer-reviewed; (3) Whether publication was funded by WRRAA §104

1. Spiese, CE, JM Berry, and B Boulanger. What caffeine tells us about nutrient source apportionment in rural watershed tile drainage. ASCE Environmental and Water Resources Institute Conference Proceeding. (Peer-reviewed & funded by WRRAA).

3. Conference Presentation including (1) Complete citation; (2) Conference title; (3) Whether presentation is based on research funded by WRRAA §104 (4) Number of students attending who were sponsored by the institute

1. Berry, JM, CE Spiese, LM Streaker, and B Boulanger. Quantification of nitrogen and phosphorus from tile drainage in freshwater systems using caffeine as a human biomarker. *Michigan State University Undergraduate Research Symposium*, October 5, 2013. Funded by WRRAA, 1 student attending
2. Streaker LM, CE Spiese, and JM Berry. Using sterol biomarkers to trace a eutrophic watershed. *Michigan State University Undergraduate Research Symposium*, October 5, 2013. Partially funded by WRRAA, 1 student attending
3. Spiese, CE, JM Berry, LM Streaker, B Boulanger, and AG Thayer. Contribution of rural septic systems to nutrient loading in a eutrophic watershed. *Water Management Association of Ohio 42nd Annual Meeting*, November 13, 2013. Funded by WRRAA, 0 students attending.

4. Research Award or Other Recognition including (1) Award title; (2) Name of organization giving award; (3) Brief summary of the work that was recognized; (4) Who received the award (student name etc.)

n/a

5. Patent or Copyright including (1) Title of intellectual property; (2) Brief description of the property; (3) Whether the property is patented or copyrighted; (4) Whether property was funded by WRRAA §104

n/a

6. Profession Placement of Graduates including (1) Economic sector; (2) Number of placements

Two students supported by this grant are continuing undergraduate students. The third has graduated with a BS in Biochemistry and has accepted a position at Boston Children's Hosptial – Harvard Stem Cell Institute as a research technician.

7. Teaching Assistantship including (1) Number of assistantships; (2) number of these assistantships funded using WRRAA §104 funds
n/a

Assessment of a Novel Application of Biochar to Improve Runoff Water Quality from Vegetated Roofs

Basic Information

Title:	Assessment of a Novel Application of Biochar to Improve Runoff Water Quality from Vegetated Roofs
Project Number:	2013OH297B
Start Date:	3/1/2013
End Date:	2/28/2015
Funding Source:	104B
Congressional District:	1
Research Category:	Water Quality
Focus Category:	Hydrogeochemistry, Nutrients, Water Quality
Descriptors:	
Principal Investigators:	Ishi Buffam, Dominic L Boccelli

Publications

1. *Hochwalt, P. and I. Buffam. April 2014. “Can biochar increase nutrient binding and water holding capacity in vegetated roof growing medium?” University of Cincinnati 2014 Undergraduate Research Symposium, Cincinnati OH, USA (poster presentation).
2. *Divelbiss, D., P. Hochwalt, M. Mitchell, D. Boccelli, and I. Buffam. May 2014. “Black Is The New Green - Enhancing Green Roof Performance With Novel Substrate”. Confluence Water Technology Innovation Cluster, 2014 Water Symposium, Covington, KY, USA (oral presentation).

Progress Report 2013-14

Assessment of a Novel Application of Biochar to Improve Runoff Water Quality from Vegetated Roofs

Project G101643/G200355: 3/1/2013 – 2/28/2015 (including 12-month no-cost extension)

Ishi Buffam and Dominic L. Boccelli
University of Cincinnati

1. Summary

Vegetated (green) roofs – a type of low-impact development (LID) – have been demonstrated to improve stormwater retention and provide energy savings, but also serve as a source of inorganic nutrients through runoff. An early study using biochar – a type of activated carbon – within the green roof substrate (soil mix) suggested that an amended soil mix could improve the effluent water quality from vegetated roofs. The *overarching objective of this project* is to improve our understanding of the water quality benefits associated with the use of a biochar-amended substrate mix within vegetated roof technology. Our *central hypothesis* is that biochar can enhance the ability of vegetated roofs, which can already reduce the quantity of CSOs, to decrease nutrient loading by binding nutrients as the runoff passes through the amended green roof substrate. In this phase of the project, we carried out replicated column reactor experiments with varying proportion of biochar integrated into green roof substrate, and measured the breakthrough curves for inorganic nutrients ammonium (NH_4^+), nitrate (NO_3^-), and phosphate (PO_4^{3-}). We found that the incorporation of biochar substantially reduced and delayed the efflux of NH_4^+ and slightly delayed the passage of NO_3^-, but had little effect on PO_4^{3-}. The dynamics of sorption kinetics suggest a two-phase sorption mechanism onto biochar, the slower process taking several days to reach equilibrium. Biochar also increased the water-holding capacity of the substrate, which has important implications for the stormwater runoff reduction potential of green roofs. Our results so far indicate that biochar has excellent potential as a low-cost amendment to green roof substrate to improve downstream surface water quality. Our ongoing research in the coming year includes measuring the effect of biochar on nutrient retention, water retention, and plant vitality in green roof plots, as well as constructing a hydraulic/water quality model parameterized with the results from the lab and field experiments.

2. Problem and Research Objectives

A significant issue many urban centers face is the direct discharge of untreated sewage into receiving waters due to overburdened and antiquated combined sanitary and stormwater sewers. While conventional grey infrastructure approaches to mitigating combined sewer overflows (CSOs) tend to be disruptive and costly, the use of low impact development (LID) – generally defined to represent the application of new and innovative technologies for improving the sustainability associated within, primarily, urban areas – can mitigate overflow events and the associated deleterious impacts, while contributing other co-benefits. Green infrastructure techniques have been gaining traction for reducing urban stormwater runoff and improving water quality (e.g., NYC Department of Environmental Protection, 2011), and are one of the best management practices for CSO reduction recommended as part of the integrated green infrastructure program by Cincinnati's Metropolitan Sewer District (www.projectgroundwork.org). Vegetated (green) roofs – a type of LID – are becoming increasingly popular with for example >20% coverage of the flat roof area in cities like Stuttgart, Germany. These installations are expected to continue to proliferate in the near future with stated goals of 20% coverage of large buildings in Washington, D.C. by the year 2025 (Deutsch et al. 2005) and 50-70% coverage of city owned buildings in Toronto and Portland (Carter and Laurie 2008). Vegetated roofs have been demonstrated to improve stormwater retention (Bliss et al, 2009; Getter et al, 2007; Carter and Rasmussen, 2006, Mentens et al, 2006; Van Woert et al, 2005) and provide energy savings (van Woert et al, 2005), but also serve as a source of organic carbon, nutrients, and metals through runoff (Berndtsson et al., 2010). There is concern that the water quality benefits of green roofs related to reduced CSO events, may be offset by the direct contribution of organic carbon and nutrients in runoff from these systems. Runoff from vegetated roofs often contains very high concentrations of nutrients, particularly phosphorus but also organic carbon and sometimes inorganic nitrogen (Berndtsson et al. 2009; Berndtsson et al. 2010; Oberndorfer et al. 2007; Buffam et al. 2012; Gregoire and Clausen 2010). Thus, there is a need for further study into the potential water quality benefits and, potential, negative impacts associated with nutrient release. These are at high enough levels to contribute to eutrophication in downstream waterways, and to date no clear solution to this ecosystem disservice has been found and tested.

A novel potential solution to this problem has been identified: the integration of biochar into the vegetated roof substrate. Biochar is the term given to biomass, such as wood, which has undergone pyrolysis to generate a carbon-rich product. The production of biochar is similar to the process which creates charcoal but is distinct in that the end product is meant to be used as a soil amendment. The purpose of this soil amendment is to increase soil productivity, sequester carbon, and filter percolating water (Lehman, 2009). Adding biochar to soils has improved the ability of the soil to absorb phosphorous (Lehmann, 2002; Beaton, 1960; Downie, 2007), absorb metals by increasing cation exchange rate (Lehmann, 2009), and increase water holding capacity (Piccolo, 1996).

Biochar is a proven technology to improve water quality but it has not been extensively challenged in the treatment of green roof effluent. The multifaceted claims of biochar, specifically, improved soil fertility, carbon sequestration, and improved effluent water quality (Lehmann, 2009), suggest the technology could reduce threats to ecosystems receiving runoff, create cost savings due to reduced green roof maintenance through nutrient retention, and

increase effectiveness of green roofs to retain water. Evaluation of this application is necessary to determine the true effectiveness of this possible game changing technology for green roofs. One previous study (Beck, 2011) carried out in Portland, OR has shown that biochar is capable of improving effluent water quality (i.e. phosphorous, nitrate, organic carbon) and reducing runoff volume in green roofs. However, this study did not examine the temporal dynamics of sorption, nor the changes in performance by varying biochar concentrations in the media, instead using a fixed proportion of 7% biochar.

The *overarching objective of this project* is to improve our understanding of the water quality benefits associated with the utilization of a biochar-amended soil mix within vegetated roof technology. Our *central hypothesis* is that biochar can enhance the ability of vegetated roofs to improve water quality by binding nutrients (N and P) as the runoff passes through the amended green roof medium. While vegetated roof technology has been demonstrated to reduce rainfall runoff, additional research has demonstrated a potential degradation in the effluent water quality (Oberndorfer et al. 2007; Berndtsson et al. 2010). Recent research has shown a net leaching of dissolved nitrogen and exceptionally high levels of inorganic phosphorous in green roof runoff, both from full-scale green roofs and small-scale experimental plots (Buffam et al. 2012). The use of biochar – an inexpensive activated carbon – is expected to improve the ability of vegetated roofs to retain nutrients. The *rationale* for understanding the water quality impacts of a biochar-amended soil medium is to evaluate the benefits for use within vegetated roofs an part of an integrated stormwater management plan, which would benefit designers and planners in assessing the potential impact to water quality conditions within a regional design setting.

Our project has three associated objectives: 1) evaluating the abiotic capabilities for nutrient and stormwater runoff retention due to enhanced sorption properties of biochar-amended soil medium via column reactors; 2) evaluating biotic and abiotic capabilities for nutrient and stormwater runoff retention due to enhanced sorption properties of a biochar-amended soil medium in vegetated green roof plots; and 3) developing a computational model for representing the hydraulic and water quality performance of vegetated roofs with and without biochar. In the first year of the project we have carried out the first objective, while the remaining objectives will be carried out in the second year.

3. Methodology

3.1 Research Design. We designed and carried out column studies in order to determine the nutrient holding capacity and water-holding capacity of biochar-amended vegetated roof substrate. Pilot batch studies were also carried out to determine the sorption kinetics for nutrients in vegetated roof substrate with and without biochar.

3.2 Column Studies. Fixed bed column reactors (7 cm diameter, Figure 1) were packed with four different treatments in duplicate of combined biochar and commercial green roof media (with biochar proportions of 0%, 2%, 7%, and 14% of total weight) at 10 cm of media depth to conform to common extensive green roof construction. Biochar samples used were derived from a wood-based feedstock from chips or grounds, 3 mm minus, >70% carbon sorption >8% butane ash up to 23% but with low buffering at 500°C. The growing medium used was a proprietary aggregate based extensive blend from Tremco Roofing Inc, (Cincinnati, OH), sieved through a 2 mm sieve.

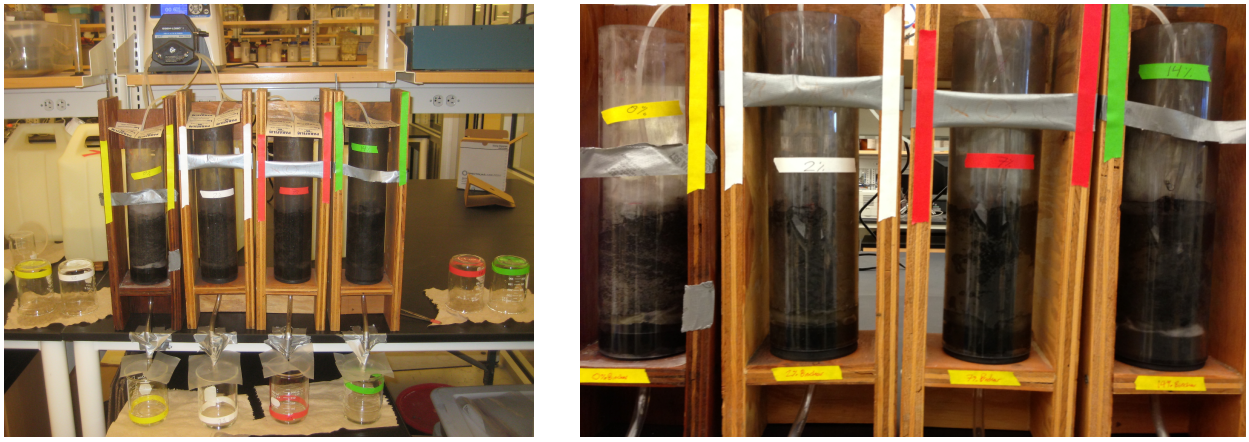

Figure 1. Left panel: Column setup showing pump, four columns varying in % biochar integrated into substrate, and beakers collecting continuous runoff water samples. **Right panel:** Column setup showing, from left to right, closeup of columns containing 400 cm^3 of 0%,2%,7%, & 14% by mass biochar/ substrate mixtures.

The columns were flushed during 24 hours with 1 year's worth of artificial rain water (ARW), equivalent to 1 meter depth, immediately prior to the beginning of the experiment. This was done so that the experiment would not be dominated by the initial release of nutrients from the substrate and would instead behave as a more established green roof. The concentrations of compounds in the ARW were determined by using the NADP precipitation averages from 2007 to present for the Oxford, Ohio station (OH09) (http://nadp.sws.uiuc.edu/NTN/ntnData.aspx). The flow rate was then reduced to 1cm/h to simulate a heavy, yet realistic, rain event. This treatment was continued for 24 hours, followed by a "heavy nutrient" mix containing ARW enriched with approximately 3 mg/L each of NH4-N, NO3-N, and PO4-P. This heavy nutrient mix was added at the same flow rate for 48 hours. This was determined to be long enough to observe the breakthrough of nutrients. This was followed by a 48h flush out using ARW. Thus, the total experiment length was 120 hours.

Water samples were collected at 1 hour intervals throughout the entire experiment, and enough samples analyzed to adequately construct the breakthrough curves (in practice, typically one sample every 4 hours). We collected a total of 120 per treatment (n=4) per trial (n=2) for a total of 960 samples.

3.3 Batch experiments. Batch experiments were run with a known ratio of biochar to growing medium in solutions with a known concentration of three nutrients - ammonium, nitrate, and phosphate. The solutions contained either artificial rainwater (ARW) containing nutrients at levels observed in local precipitation, or ARW + 20 mg/L of NH4-N, NO3-N, and PO4-P. Samples were taken periodically and analyzed for nutrient concentration.

Two sample levels were prepared per treatment, 0% biochar and 14% biochar, measured by mass. The 0% contained no biochar and 1.00 g of growing medium. The 14% contained 0.14 g biochar and 0.86 g growing medium. The mixtures were placed in 50 mL centrifuge tubes along with 40 mL of either ARW or the 20 ppm nutrient spike, depending on the treatment. Five centrifuge tubes were used per sample per treatment (20 total). Once the treatment water was added to the mixtures, the tubes were immediately placed on a shake table shaking 100 rpm at 25°C. The table was covered to ensure no light penetrated the tubes to control for any

photocatalytic activity that may ensue. Samples were taken at five time points- 10 min, 30 min, 1hr, 24 hr, and 96 hr- and vacuum filtered through a 0.45 µl filter then immediately frozen for further analysis. Nutrient concentrations of the effluent were determined using a spectrophotometer.

3.4 Water Quality Analysis. Column effluent and batch samples were collected in acid-washed high-density polyethylene containers, filtered at 0.45 µm, frozen to preserve and subsequently analyzed for the concentrations of the inorganic nutrients ammonium, nitrate and phosphate. Colorimetric techniques (Figure 2) were used at a microplate scale (Ringuet et al. 2010) for nitrate (Doane and Horwath, 2003), ammonium (Weatherburn, 1967), and phosphate (Lajtha et al., 1999). Initial pilot study samples for the concentration of metals common in the urban environment including copper (Cu) and zinc (Zn), revealed that the green roof substrate was a sink for these metals when loading occurred at a level to be expected in urban environments. Even in the absence of biochar, effluent concentrations of these metals were below the detection limit (Atomic Absorption spectroscopy). Therefore, detailed breakthrough curves were not generated for these elements, and focus was rather placed on inorganic nutrients, which have been shown to be a pervasive issue in green roof effluent.

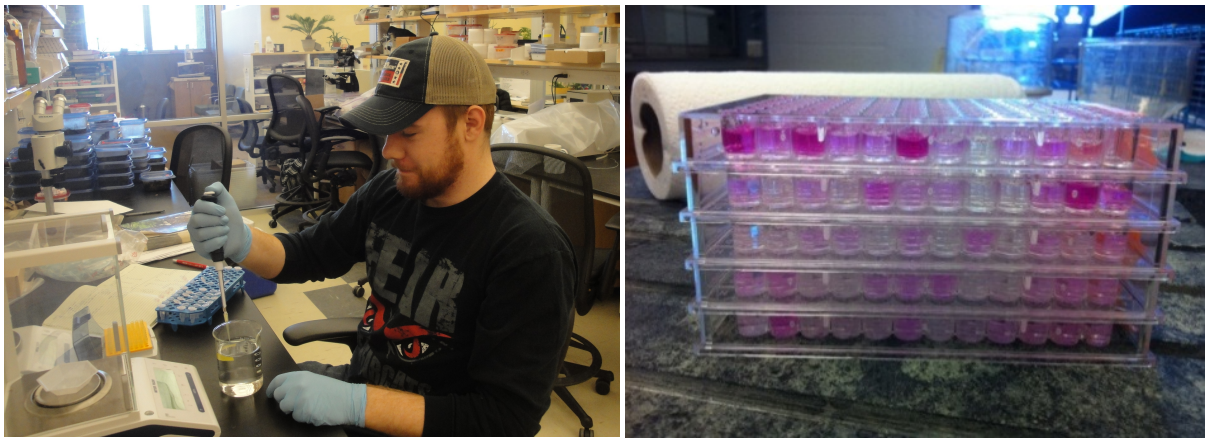

Figure 2. Left panel: Undergraduate research assistant Pat Wright pipetting out standards for use in nutrient analysis. **Right panel:** Side view of five 96-well microplates showing color development used in nitrate analysis.

4. Principal Findings

In summary, we found that the incorporation of biochar into vegetated roof substrate substantially reduced and delayed the efflux of NH_4^+ and slightly reduced and delayed the passage of NO_3^-, but had little effect on PO_4^{3-} (Figures 3-5). Biochar also increased the water-holding capacity of the substrate (Figure 6), which has important implications for the stormwater runoff reduction potential of green roofs. When averaged over the entire 5-day experiment, the volume-averaged mean concentrations (directly proportional to total flux) were reduced in the high-biochar treatment by up to 75% for ammonium and 17% for nitrate, while all columns were a slight net source of phosphate regardless of biochar amendment (Figure 7).

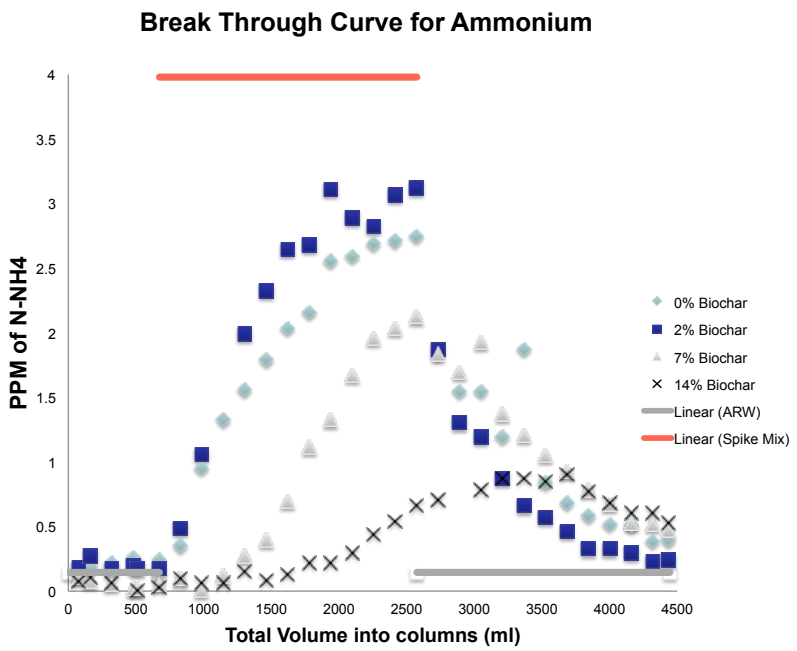

Figure 3. Nutrient break through curve of ammonium for vegetated roof substrate columns amended with 0%, 2%, 7%, & 14% by mass biochar. Each point represents an effluent sample taken every 4 hours, which was then analyzed for ammonium-N concentration. The hard lines (grey and red) represent the concentration of the input water over the length of the line (1 day with ARW, 2 days with ARW+high nutrients, and 2 days with ARW again). Increasing concentrations of biochar result in a lowering and delay in the peak ammonium concentration.

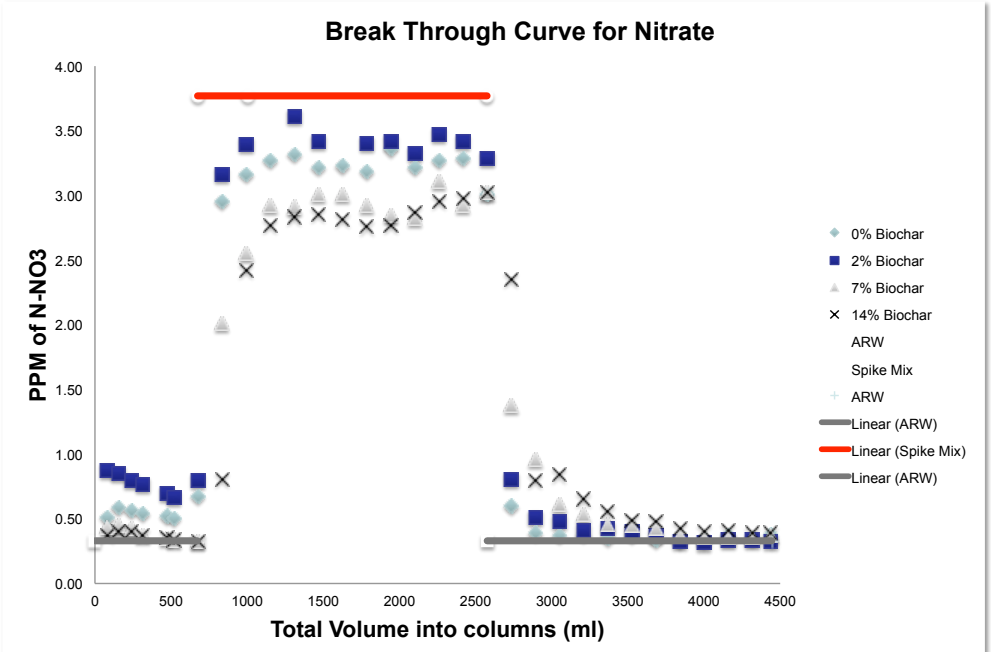

Figure 4. Nutrient break through curve of nitrate for vegetated roof substrate columns amended with 0%, 2%, 7%, & 14% by mass biochar. Each point represents an effluent sample taken every 4 hours, which was then analyzed for nitrate-N concentration. The hard lines (grey and red) represent the concentration of the input water over the length of the line (1 day with ARW, 2 days with ARW+high nutrients, and 2 days with ARW again). Increasing concentrations of biochar result in a slight lowering and delay in the peak nitrate concentration.

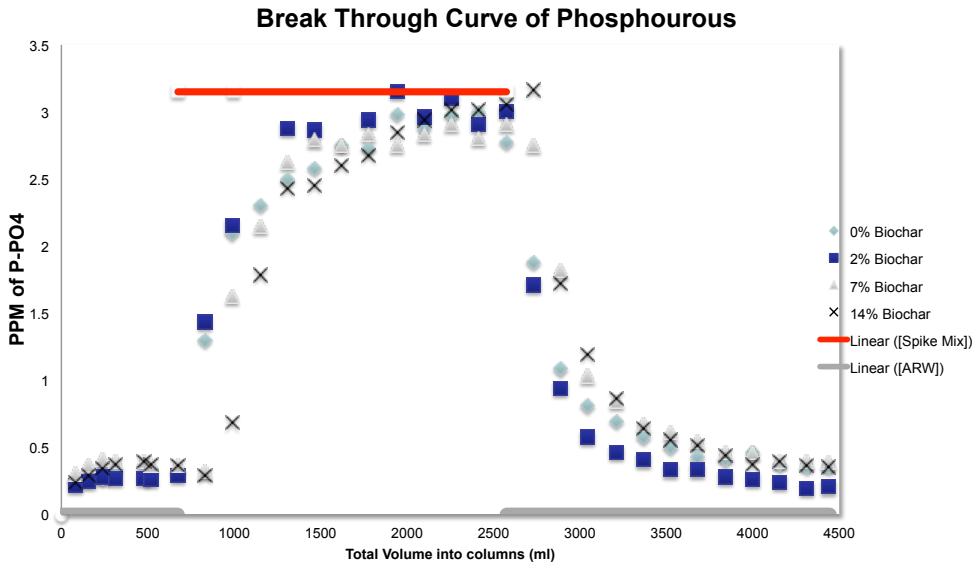

Figure 5. Nutrient break through curve of phosphate for vegetated roof substrate columns amended with 0%, 2%, 7%, & 14% by mass biochar. Each point represents an effluent sample taken every 4 hours, which was then analyzed for phosphate-P concentration. The hard lines (grey and red) represent the concentration of the input water over the length of the line (1 day with ARW, 2 days with ARW+high nutrients, and 2 days with ARW again). Increasing concentrations of biochar result in a slight delay but no apparent change in peak phosphate concentration.

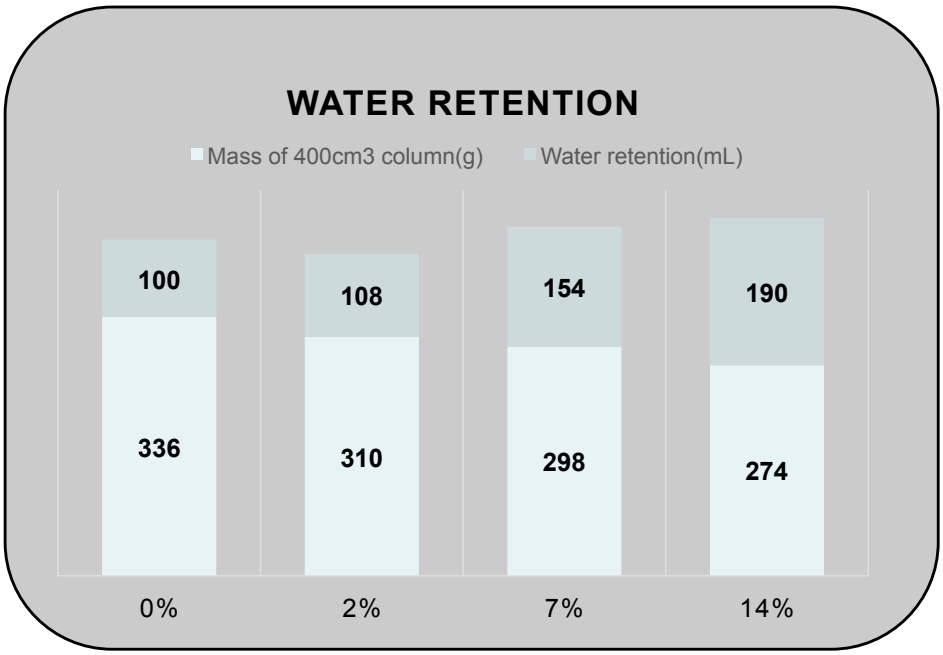

Figure 6. The water holding capacity was measured by the wet weight of the columns at the finish of the experiment. Increasing biochar had the effect of increasing water retention, with the 14% biochar treatment nearly doubling the water retention relative to the biochar-free control – this in spite of a lower initial mass for the high biochar column.

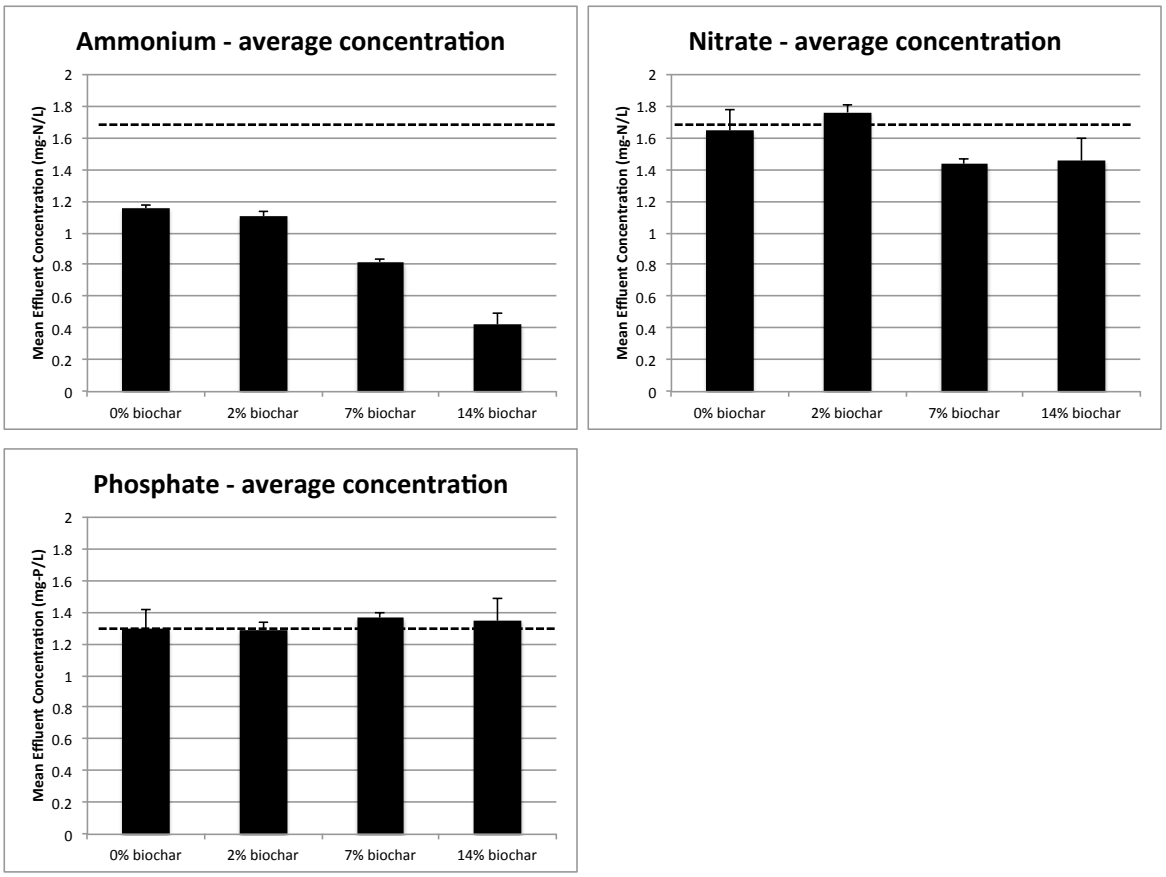

Figure 7. Volume-averaged mean effluent nutrient concentrations for the entire 5-day experiment, for columns varying in biochar % integrated into green roof substrate. Error bars represent standard error of the mean for duplicate trials. The horizontal dotted lines represent the volume-averaged influent "precipitation" concentration in the experiment. Substrate alone resulted in a 34% reduction in NH4-N, with higher biochar resulting in a reduction of up to 76% of NH4-N. NO3-N fluxes were not affected by substrate alone, but the higher biochar treatments resulted in a 17% decrease in NO3. PO4-P fluxes were not affected significantly by either substrate alone, or biochar amendments; though all columns were a slight source of PO4-P.

The objective of the batch study was to determine the kinetics and equilibrium concentrations for standard and biochar (14%)-amended substrate, subjected to two different initial nutrient concentrations in solution (ARW and 20 ppm). For the small-scale batch study, the hypothesis was that that for ammonium, nitrate, and phosphate, the concentration of nutrients in the effluent will be reduced with a higher ratio of biochar to growing medium. This was corroborated for ammonium (Figure 8), low concentrations of nitrate, and high concentrations of phosphate but rejected for low concentrations of phosphate because final concentrations were higher than initial values (data not shown). The 14% biochar amendment was quite effective at binding and reducing concentrations of ammonium from ARW- though equilibrium was not reached after 96 hours as well as reducing concentrations from a 20 ppm spike and coming to equilibrium in 1 hour (Figure 8). This conclusion is congruent to Yao et al. (2011) finding in that biochar does have the ability to bind contaminants from water. This is also supported by the effect biochar had in reducing nitrate concentrations from ARW (data not shown). With phosphate, the opposite occurred and phosphate was leached out of the substrate into the ARW, as was seen by Buccola (2008). However, when initial phosphate concentrations are increased to 20 ppm, biochar did show the capability to bind phosphate with equilibrium reached at 1 hour (data not shown).

In the batch study, the biochar appeared to come to an initial equilibrium with the water for several hours then followed by a later decrease in concentration. This may indicate that multiple equilibria exist that could include binding sites on the surface of the biochar as well as deeper within the particle. This would entail a fast and slow cycle, where the slow cycle is the binding of nutrients to the surface sites, and the slow cycle is the nutrients diffusing further into the biochar particles to inner binding sites. This would seem plausible because the diffusion process through solids takes longer than surface binding and would account for the ~23 hour period of equilibrium. As a consequence of the complicated kinetics, estimated time to equilibrium varied substantially among treatments (Table 1).

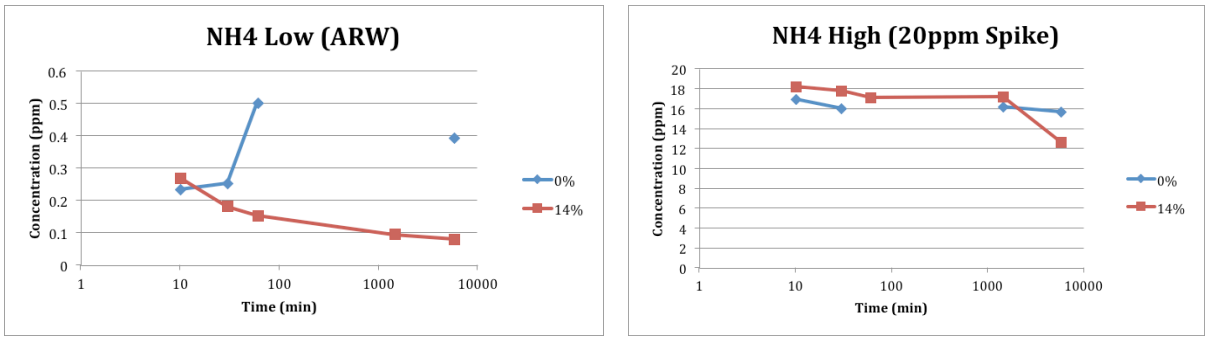

Figure 8. Left panel: The addition of 14% biochar to substrate decreases the concentration of NH_4 in ARW while substrate alone is a source of NH_4. **Right panel:** For the high ammonium spike solution, both substrate alone and substrate + 14% biochar result in a gradual decrease in ammonium over time, presumably due to sorption. A fast initial drop (within 1 hour) followed by continued gradual decline in both experiments suggests multiple mechanisms of sorption. Missing points represent missing analytical samples in this pilot study.

Table 1. Time of equilibrium reached for each analyte and treatment, in the batch kinetic study.

Analyte	0% ARW	14% ARW	0% 20ppm	14% 20ppm
NH_4	≈ 2 hrs	N/A	30 min	>24 hr
NO_3	1 hr	>24 hr	N/A	N/A
PO_4	N/A	24 hr	>30 min	1 hr

5. Significance

The integration of biochar is a potential breakthrough in reducing water quality degradation by green roof runoff, but very little is known about the sensitivity to variation in the proportion of the biochar amendment, or the dynamics of sorption kinetics or equilibria. Our project has demonstrated that a biochar amendment substantially decreases ammonium leaching from green roof substrate, by up to 75% for the high biochar (14% w/w) treatment. The high biochar treatment also doubled water holding capacity of the substrate, a finding with great significance for green roof design for stormwater runoff reduction. This is of particular note because on a per-mass basis, biochar is no more expensive than typical commercially available green roof substrate mixes. The patterns of breakthrough curves also give insight into likely

physicochemical mechanisms of nutrient binding. Specifically, the inflections in the curve suggest a dual-layer sorption mechanism for the biochar for ammonium and phosphate, with initial surficial sorption occurring within a few hours followed by a slow sorption process taking a few days, perhaps limited by diffusion into the interior of biochar particles. Follow-up work using different sorption breakthrough models and isotherms are underway, to further explore the sorption/desorption dynamics.

This study evaluates a low-cost option for improving the effluent water quality of vegetated roof technology, which is becoming increasingly more important as part of green-engineered solutions for stormwater management. The research demonstrates the water quality improvements associated with a biochar-amended green roof, but will also result in a modeling component that can be used within an integrated assessment framework both within and beyond the Ohio River Valley. As a result, the positive impact of this project will be a significant step forward in developing a more integrated infrastructure solution for storm water management by illustrating the potential impacts of biochar-amended vegetated roofs on CSO and nutrient management in urban environments.

6. Publication Citations

Journal Articles: None to date.

Presentations at Conferences *(note, includes dates in 2014 after end of accounting period)*
*Indicates student presenter

*Hochwalt, P. and I. Buffam. April 2014. "Can biochar increase nutrient binding and water holding capacity in vegetated roof growing medium?" *University of Cincinnati 2014 Undergraduate Research Symposium, Cincinnati OH, USA (poster presentation).*

*Divelbiss, D., P. Hochwalt, M. Mitchell, D. Boccelli, and I. Buffam. May 2014. "Black Is The New Green - Enhancing Green Roof Performance With Novel Substrate". *Confluence Water Technology Innovation Cluster, 2014 Water Symposium, Covington, KY, USA (oral presentation).*

7. Students Supported by the Project

This project so far has provided direct funding for one undergraduate student, Paul Hochwalt (Biological Sciences major), and has also provided research opportunities for one other undergraduate student, Pat Wright (Environmental Studies major) and one graduate student (Dan Divelbiss, Environmental Engineering program). These students participated in the design and pilot testing of the column experiments (led by Paul Hochwalt), as well as carrying out the column experiments, nutrient analysis, and data analysis. All three students have presented results of their research at local or regional conferences. Pat Wright carried out undergraduate capstone independent research associated with this project.

8. Notable Awards and Achievements

Paul Hochwalt – 2014 University of Cincinnati STEM Excellence in Research Award, Biology: This award included a $500 honorarium and was awarded based on Paul's research funded by this project.

7. References

Beaton, J.D., H.B. Peterson, and N. Bauer. (1960). "Some aspects of phosphate adsorption to charcoal." *Soil Science Society of America Proceedings*. 24:340-346.

Beck, D.A, G.R. Johnson, G.A. Spolek. (2011) "Amending greenroof soil with biochar to affect runoff water quantity and quality" *Ecological Engineering* 159:2111-2118.

Berndtsson, J.C., Bengtsson, L., and Jinno, K. (2009) "Runoff water quality from intensive and extensive vegetated roofs" *Ecological Engineering* 35: 369-380.

Berndtsson JC (2010) Green roof performance towards management of runoff water quantity and quality: A review. *Ecological Engineering*, 36, 351-360.

Bliss, D. J., Neufeld, R. D., and Ries, R. J. (2009) "Storm Water Runoff Mitigation Using a Green Roof" *Environmental Engineering Science*, 26 (2), 407-417.

Buccola, N. 2008. "A laboratory comparison of green roof runoff." A thesis submitted in partial fulfillment of the requirements for the degree of Masters of Science in Civil and Evnironmental Engineering, Portland State University, Portland, OR.

Buffam I., Townsend-Small, A., Boccelli, D. L., Russell, V., and Durtsche, R. D. (2012) "Greening the Skyline -- Biogeochemical Services and Disservices Provided by Green Roof Ecosystems" *4th International EcoSummit*, Columbus, OH.

Carter, T. L. and Rasmussen, T. C. (2006) "Hydrologic Behavior of Vegetated Roofs" *Journal of the American Water Resources Association*, 42 (5) 1261-1274.

Carter, T.; Laurie, F., Establishing green roof infrastructure through environmental policy instruments. *Environmental Management* **2008,** *42*, 151-164.

Deutsch, B.; Whitlow, H.; Sullivan, M.; Saveneau, A. *Re-Greening Washington, DC: A Green Roof Vision Based on Quantifying Storm Water and Air Quality Benefits*; 2005; p 15.

Doane, T.A., and W.R. Horwath. (2003) "Spectrophotometric determination of nitrate with a single reagent" *Analytical Letters* 36: 2713-2722.

Downie, A., V.C. Lima, G. Seehann, J. Donath, V.R. Monntoia, and T. Schwarz. (2007) "Retention properties of wood residues and their potential for soil amelioration." *Wood Science and Technology*. 41:169-189.

Getter, K. L., Rowe, D. B., Andersen, J. A. (2007) "Quantifying the Effect of Slope on Extensive Green Roof Stormwater Retention" *Ecological Engineering*, 31 (4), 225-231.

Gregoire, B. G. and Clausen, J. C. (2011) "Effect of a modular extensive green roof on stormwater runoff and water quality" *Ecological Engineering*, 37, 963-969.

Lajtha, K., Driscoll C.T., Jarell W.M., and Elliott E.T. (1999) "Soil phosphorus: characterization and total element analysis" Pages 115-142 in G.P. Robertson, D.C. Colemna, C.S. Bledsoe, and P. Sollins, editors. Standard Soil Methods for Long-Term Ecological Research. Oxford University Press, New York.

Lehmann, J. and S. Joseph. (2009) *Biochar for environmental management: Science and technology.* Stirling, VA: Earthscan.

Lehmann, J., J.P. da Silva Jr., M. Rondon, M.S. Carvo, J. Greenwood, T. Nehls, C. Stiener, and B. Glaser. (2002) "Slash-and-char – a feasible alternative for soil fertility management in the central Amazon?" *Proceedings of the 17th World Congress of Soil Science*. Bangkok, Thailand. Paper no 449.

Mentens, J., Raes, D., and Hermy, M. (2006) "Green Roofs as a Tool for Solving the Rainwater Runoff Problem in the Urbanized 21st Century" Landscape and Urban Planning, 77 (3), 217-226.

NYC Department of Environmental Protection. (2011) "NYC Green Infrastructure Plan: A Sustainable Strategy for Clean Waterways", 154 pp.

Oberndorfer, E., Lundholm, J., Bass, B., Coffman, R., Doshi, H., Dunnett, N., Gaffin, S., Kohler, M., Liu, K. K. Y., and Rowe, B. (2007) "Green roofs as urban ecosystems: Ecological structures, functions, and services" *Bioscience*, 57, 823-833.

Piccolo, A., G. Pietramellara, and J.S.C Mbagwu. (1996) "Effects of coal-derived humic substances on water retention and structural stability of Mediterranean soils." *Soil Use and Management*. 12:209-213.

Ringuet, S., Sassano, L., & Johnson, Z.I. (2010) A suite of microplate reader-based colorimetric methods to quantify ammonium, nitrate, orthophosphate, and silicate concentrations for aquatic nutrient monitoring. *Journal of Environmental Monitoring*, **13**, 370-376.

Van Woert, N. D., Rowe, D. B., Andersen, J. A., Rugh, C. L., Fernandez, R. T., and Xiao, L. (2005) "Green Roof Stormwater Retention: Effects of Roof Surface, Slope and Media Depth" *Journal of Environmental Quality*, 34 (3), 1036-1044.

Weatherburn, M.W. (1967) "Phenol-hypochlorite reaction for determination of ammonia" *Analytical Chemistry* 39: 971-974.

Yao; Gao; Inyang; Zimmerman; Cao; Yang. 2011. "Removal of phosphates from aqueous solutions by biochar derived from anerobically digested sugar beet tailings." *Journal of Hazardous Materials.* 190: 501-507.

Characterizing the influence of surface chemistry and morphology on biofilm formation of ceramic membranes in wastewater treatment

Basic Information

Title:	Characterizing the influence of surface chemistry and morphology on biofilm formation of ceramic membranes in wastewater treatment
Project Number:	2013OH300B
Start Date:	3/1/2013
End Date:	2/28/2015
Funding Source:	104B
Congressional District:	OH-12
Research Category:	Engineering
Focus Category:	Treatment, Acid Deposition, Water Quality
Descriptors:	
Principal Investigators:	Paula J Mouser, Hendrik Verweij, Linda Kay Weavers

Publications

There are no publications.

Progress Report 2013 – 2014

Contract Information

Title	Characterizing the influence of surface chemistry and morphology on biofilm formation of ceramic membranes in wastewater treatment
Project Number	60039765
Start Date	6/1/2013
Proposed End Date	9/1/2014 (including a no-cost extension)
Focus Category	Water and wastewater treatment membranes
Keywords	Ceramic membrane, biofouling, ultrasound
Lead Institute	The Ohio State University
Principal Investigators	Paula Mouser; Linda Weavers

Abstract

The commercial use of manufactured membranes for water and wastewater treatment has been steadily growing for decades, and is now considered a cost-effective alternative for new treatment facilities when compared to conventional treatment systems. The state of Ohio alone has dozens of large-scale water and wastewater treatment facilities utilizing membranes; many of which have begun operation within the last ten years. Although there are many advantages to utilizing membranes, their major disadvantage is their susceptibility to fouling – and particularly biological fouling. Many membrane treatment facilities, including those operating in Ohio, experience severe biological fouling, which is currently not well understood. In some cases the extent of biological fouling can be irreversible in that a costly replacement or extreme cleaning measures are required to partially recover the membrane performance. Given the severity and longevity of the problem, extensive research involving characterizing and preventing biological fouling of polymeric membranes (i.e. cellulose acetate, polyvinylidine fluoride, etc.) has been performed. However, very little attention has involved investigating biological fouling of membranes manufactured from ceramic materials. Full-scale installations of polymeric membranes have dominated over ceramic membranes in the past due to lower material cost. However, ceramic costs are trending downward in recent years. Consequently, although ceramic membranes have been in existence for decades, they are still considered an emerging technology in the water treatment industry due to their limited implementation. Considering the differences in characteristics such as surface chemistry and morphology of polymeric and ceramic membranes, it is not known whether or not biological fouling processes will be similar when comparing the two. One purpose of this research is to therefore be one of the first studies involving characterizing biological fouling of ceramic membranes. Secondly, this study is investigating the effectiveness of implementing ultrasonic cleaning techniques to remove biological fouling layers. Previous studies have documented that the use of ultrasound has proven to be effective at cleaning inorganically-fouled ceramic membranes. There has been no apparent published research investigated ultrasonic cleaning effectiveness for biologically fouled ceramic membranes, which this study is currently investigating.

Methodology and Materials

This study aims to identify the major components of biological fouling layers (i.e. proteins, polysaccharides, nucleic acids, phospholipids, etc.) that accumulate on ceramic membranes and determine which layers are more readily removed through ultrasonic cleaning techniques. Our experimental design includes in-line ceramic membranes (0.2 μm effective pore size) set in a duplicate, parallel system connected to a feed pump, control valves, and pressure gauges (Figure 1). Flow recorders and sampling ports measure the physical membrane performance and membrane flux decline due to biological fouling. Wastewater used for this research is collected from the primary clarifier effluent at the City of Columbus's Jackson Pike Wastewater Treatment plant, which treats municipal wastewater. Samples of wastewater are collected intermittently and kept biologically active by continuously aerating, mixing, and amending with carbon and nutrients. Biological assessment of the membrane surfaces, influent, and effluent quality has been performed with total proteins and polysaccharides assays, analysis of phospholipid fatty acid content, Fourier Transform Infrared Spectroscopy (FT-IR), and fluorescent staining of fouling layers. Components of the ultrasonic cleaning equipment used for these experiments are manufactured by L3 Communications Elac Nautik and consists of a water-cooled cleaning vessel, ultrasonic generator, and ultrasonic transducer.

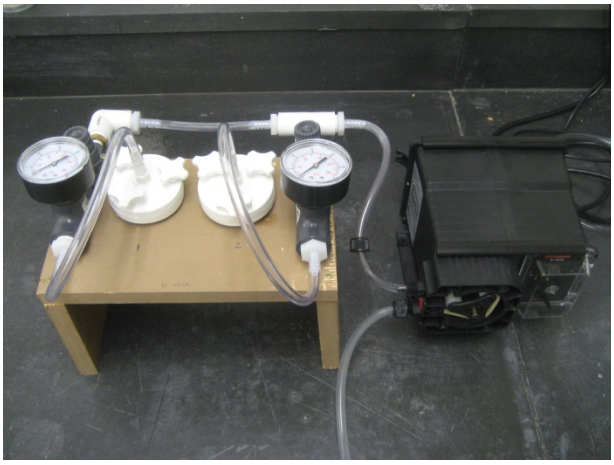

Figure 1. Experimental apparatus constructed to test ceramic membranes.

Preliminary Results and Ongoing Experiments

Previous studies involving biological fouling of polymeric membranes suggest the two major components of fouling layers are proteins and polysaccharides. Biotechnology tools are being applied to identify the microbial communities that persist on these membranes, and identify the organic and inorganic components present within fouling layers. Although most of the experiments involved with this research are currently on-going; some preliminary findings have yielded promising and repeatable results. Measurements indicate that only 10% of total proteins pass through the membrane, with 90% retention on the membrane surface and within the pores. Polysaccharides, on the other hand, more readily pass through the membrane, with only about 50% of these being retained by the membrane. This indicates that proteins may primarily be attributing the decline in membrane flux. Results of preliminary ultrasonic cleaning experiments indicate biologically-fouled layers are effectively cleaned from ceramic membranes, although some remnant matter remains on the membrane following cleaning (Figure 2). Ongoing studies are underway to determine if the amount of polysaccharides retained by the membrane change significantly as the membrane becomes more fouled, to perform more detailed characterizations of the protein and polysaccharide composition, and to further quantify how effectively biological fouling layers are removed through ultrasonic cleaning.

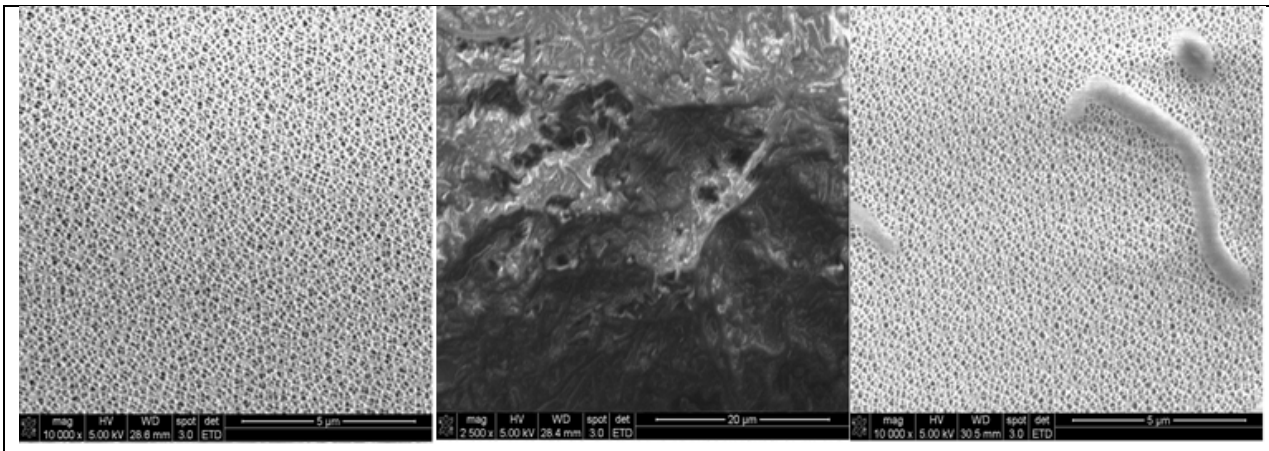

Figure 2. Scanning electron microscope (SEM) images of a clean ceramic membrane surface (left), a fouled membrane after wastewater filtration (middle), and the surface of a ceramic membrane following cleaning with ultrasound at 620 kHz for 30 seconds (right).

Although initial cleaning of ceramic membrane surfaces by means of ultrasonic cavitation looks promising, there are considerations for long-term cleaning effectiveness to be made. Certain components of biological fouling layers may persist and be difficult to remove with ultrasonic cleaning. This hypothesis has become evident based on experiments assessing repeated fouling and cleaning procedures. Initial cleaning recoveries are typically 90% or higher, with subsequent cleanings declining in their initial membrane flux when compared to a clean membrane surface (Figure 3). The key aspect of this research is therefore to determine which components of the biological fouling layers are most difficult to remove from the surface and within the pores of ceramic membranes. To determine this, the microbial analysis techniques described previously are being used to study membrane surfaces following cleaning. It is expected that these components will be identified and characterized prior to the fall of 2014.

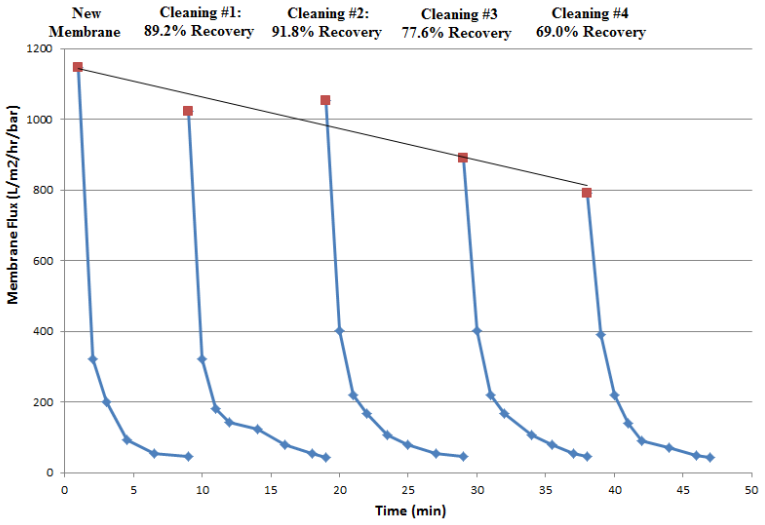

Figure 3. Decline in ceramic membrane flux after multiple fouling and cleaning events using ultrasonication.

Significance of Findings

Our preliminary findings suggest that although ultrasonic cleaning of biologically-fouled membranes is effective, certain components of the biologically-sourced layers may persist on the membrane surface and within the membrane pores after cleaning. Our goal will be to better quantify these biological components in order to develop cleaning or preventative maintenance

strategies to specifically target these constituents. Developing such methods would have the ultimate goal of being implemented in full-scale treatment system applications to combat the persistent problem of biological fouling of membranes.

Publications and Conference Presentations

No publications or conference presentations have been completed to date. The preliminary findings of this research were submitted in an abstract for oral presentation at the 2014 Ohio American Water Works Association, Water Environment Federation One Water Conference, occurring in August, 2014 in Columbus, Ohio. At the time of this report, the abstract has not been accepted or rejected for a presentation. At least one publication is expected to be submitted by Fall 2014 following completion of the above described experiments.

Students Supported By the Project

One student has been working on this project since it began. John Krinks is currently a PhD student in the Civil, Environmental and Geodetic Engineering Graduate Program. His tuition and fees were provided by CEGE toward the required 2:1 cost share.

Awards or Achievements

Work that is closely related to this project is continuing through a new $200,000 grant awarded by the Ohio Water Development Authority to PI Linda Weavers in the Department of Civil, Environmental and Geodetic Engineering (CEGE), and co-PIs Paula Mouser (CEGE) and Henk Verweij in Material Sciences at Ohio State.

Professional Placement of Graduates

No students that have worked on this project have graduated.

High-performance biologically inspired membranes for water treatment

Basic Information

Title:	High-performance biologically inspired membranes for water treatment
Project Number:	2013OH435O
Start Date:	5/1/2013
End Date:	2/28/2015
Funding Source:	Other
Congressional District:	9th
Research Category:	Engineering
Focus Category:	Treatment, Water Quality, Waste Water
Descriptors:	Membrane separations; water treatment; biomimetic
Principal Investigators:	Isabel Escobar

Publications

1. Wagh P. and I.C. Escobar (2013). “Synthesis of Biomimetic Polybenzimidazole Nanofiltration Membranes,” 2013 AIChE Annual Meeting, San Francisco, CA, November 3-8, 2013.
2. Escobar (2014). “Development of Biomimetic Nanofiltration Membranes Using Aquaporins,” 2014 NAMS Annual Meeting, Houston, TX, May 31-June 4, 2014.

Title. High-performance biologically inspired membranes for water treatment

PI. Isabel C. Escobar, The University of Toledo.

Problem and Research Objectives, Methodology, and Principal Findings and Significance

This project relies on the idea of combining the ultra-efficient functioning of biological molecules with the productivity of synthetic membranes. Aquaporin is a bidirectional water channel protein present in the cells, which regulates the flow of water in and out of the cells. It allows water molecules to pass through in single file while the transport of ions, salts is prevented by electrostatic tuning mechanism of channel interior. Larger molecules are rejected due to size exclusion. Aquaporin is well-known for its potential to form biomimetic membranes.

Problem –

Challenges involved in the incorporation of the Aquaporin proteins in the membranes limit their applicability. One challenge is to attach aquaporins to membranes without chemically altering or damaging the aquaporin during chemical binding. The second challenge is to design and prepare an assembly that will allow biomimetic membranes with aquaporins to sustain high hydraulic water pressure gradients without losing their integrity and performance.

Research objective –

The objective of the project is to make a new class of biomimetic nanofiltration membranes by modifying their surface and making them chemically and mechanically stable. We propose that aquaporins can be treated with polysaccharides to protect them, and then can be embedded in amphiphilic PVA-alkyl matrix. The PVA-alkyl with embedded aquaporins will be used as the nanofiltration membrane active layer.

Methodology –

1. PBI membranes casting -

The dope polymer that was used to cast the membranes was Polybenzimidazole (PBI). PBI is stable polymer, which has robust mechanical strength with thermal stability for a wide range of high temperature applications and it also provides chemical stability over a wide range of pH. PBI membranes are hydrophobic. They are strong but brittle. The structure of PBI molecule is shown in Figure 1. Within the imidazole group of PBI, the heterocycle has two nitrogen atoms. One is attached to the hydrogen atom as a site to form hydrogen bond while other nitrogen has a lone pair, which can act as a proton acceptor.

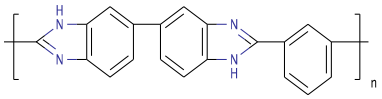

Figure 1. PBI molecule structure

The solvent used to make the dope solution was N, N-Dimethylacetamide. Commercially 26% w/w dope solution is available which contains 26% PBI polymer, 72% N, N- Dimethylacetamide (DMAc) and 2% Lithium chloride (LiCl). LiCl served the function of preventing PBI polymer from phasing out of the solution. Hence, it imparts long shelf life to the solution. The dope solution was diluted to 21% PBI by adding solvent to it, and the solution was sealed with parafilm in order to prevent the air bubbles from being trapped inside the solution affecting its homogeneity. Because of very high viscosity of the solution, the solution needed to be kept in the sonicator and degassed for 2 days in order to ensure complete mixing of the solvent and the solute and make the solution homogeneous. After sonication, the solution was allowed to come to room temperature and then the solution was ready to make the membranes. The membranes were cast using phase inversion process. Phase inversion is the phenomenon whereby the phases of a liquid-liquid dispersions interchange such that the dispersed phase spontaneously inverts to become the continuous phase. The non-solvent phase that is used in this process is water.

A casting knife or doctor's blade was used to make flat sheet membranes. A clean glass mirror was used as a hydrophobic surface to make sure that the solution would not become stuck to the membrane. The solution was placed in an even line on the surface and the casting knife was used to push the solution across the glass surface to make a thin film. The thickness of the membranes was kept between 150µm and 200µm. A water coagulation bath was used to induce phase inversion subsequent pore formation within the membranes. Once the phase inversion had taken place, the membrane came out of the surface of the membrane. The membrane was thoroughly washed with water and kept in a 50/50 glycerol-DI water solution. Glycerol was added to DI water due to possibility of water evaporation. If the membranes get dry, they become brittle and susceptible to breakage. The membranes were kept in the solution at least one day before they were analyzed.

2. Surface activation of the membranes –

The PBI membranes prepared are hydrophobic. Hence, for subsequent modifications, the surface of the membranes needed to be activated. It was achieved by way of reaction of highly reactive chlorine atom of 4-chloromethyl benzoic acid (CMBA) with the secondary amine group in the imidazole ring of repeat unit in PBI backbone. CMBA added a carboxylic group to the surface. This served two purposes: 1) It imparted negative charge on the membrane surface 2) It acted as a platform for subsequent functionalization of the membrane. There are two secondary amine sites in PBI molecule. Hence, after the reaction, carboxylic group was added on both sites on the molecule. For simplicity, reaction at only one site is shown in the diagram below. Overall reaction is as follows:

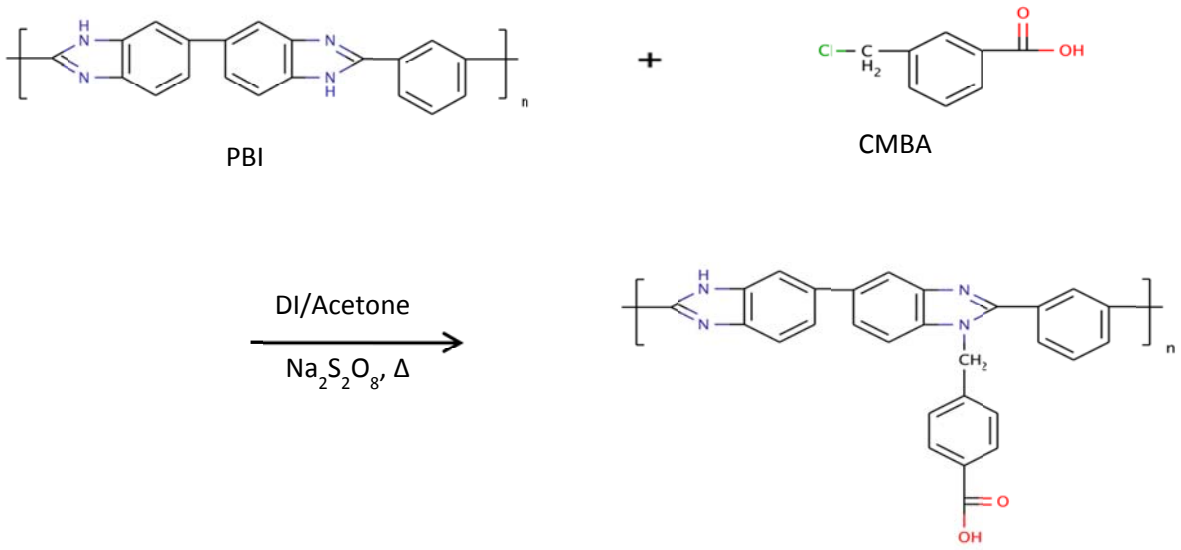

For the reaction, 1 wt% solution of sodium persulphate in water was prepared. Sodium persulphate was used as a free radical initiator for the reaction. 200 ml DI water was taken in a 500mL beaker with a stir bar. 2.02g sodium persulphate was added to the water and the solution was stirred on hot plate. The temperature was set at 40°C. 2 membranes were added to the solution and it was made sure that the membranes are fully submerged and were not stuck under the stir bar. In a second beaker, 0.5 wt% solution of CMBA in acetone was prepared. 0.788 g CMBA was added to 200 mL acetone and was stirred until all CMBA was dissolved. Then acetone/ CMBA solution was slowly added to the beaker on hot plate and stirring was done at a slow rate. This was done in order to prevent the precipitation of CMBA as it is insoluble in water. After complete addition of the solution, it was covered with parafilm. The final solution had 50/50 mixture of both solutions. The temperature of the solution was kept at 40°C and it was stirred for 24 hours. The temperature was chosen to keep all the reactants in solution and prevent the evaporation of CMBA. Once the reaction was done, the membranes were washed with copious amounts of DI water to remove excess sodium persulphate and placed in glycerol/water bath as soon as possible.

3. Preparation of PVA–alkyl:

PVA-alkyl is polyvinyl alcohol carrying long alkyl side chains. It is amphiphilic as it has both hydrophilic and hydrophobic elements present in it. PVA has hydrophilic properties and long alkyl chains account for the hydrophobicity of the molecule. PVA-alkyl was prepared in the lab in two steps.

a) Preparation of carboxy-methyl PVA (PVA-COOH):

Initially, 50mL water was taken in a 100 mL beaker and 1g PVA was added to it and the beaker was kept on a hot plate. The temperature of the water was maintained at 70°C. The mixture was stirred for 1 hour continuously with stir rod to prevent PVA from sticking to the bottom of the beaker. The stirring was continued until PVA was completely dissolved in water. The solution was transferred to a 500mL beaker and 50g sodium monochloroacetate was added to it. The solution was then covered with aluminium foil and was incubated at 4°C for 24 hours.

After that, 42mL water was taken in a 100mL beaker and 42g sodium hydroxide was added to it. The mixture was stirred until sodium hydroxide was completely dissolved in it.

NaOH/water solution was added to the incubated solution and it was kept stirring at room temperature for 24 hours. Then it was neutralized using hydrochloric acid. For that, 6M solution of hydrochloric acid with water was prepared in separate beaker and benchtop pH meter was used to continuously monitor the pH of the final solution. This neutralized solution was dialyzed against deionized water. The molecular weight cut-off for the dialysis was 12-14 kDa. The dialysis tubing used was soaked in water for 3 hours in order to open it and fill it with the solution and was sealed with dialysis locking membrane clamps. A 2000mL beaker with a stir bar in it was filled with DI water. The tubing was attached to foam to keep it suspending in water. It was kept stirring and the water was changed after every 4-5 hours to make sure that the driving force for the dialysis is high. The procedure was continued for 3 days. Remaining solution in the tube was taken out and stored in another beaker.

Then, it was deionized using ion-exchange resins. DOWEX 1X8 was used for negatively charged ions and DOWEX 50WX8 was used for positively charged ions. The output solution after the ion exchange was lyophilized using freeze dryer. For that, the solution was kept in centrifuge tubes and was allowed to freeze dry for 3 days. PVA-COOH was obtained as a white solid after freeze drying. The weight of the product was 0.45 g and the yield was 39%. The overall reaction is as follows:

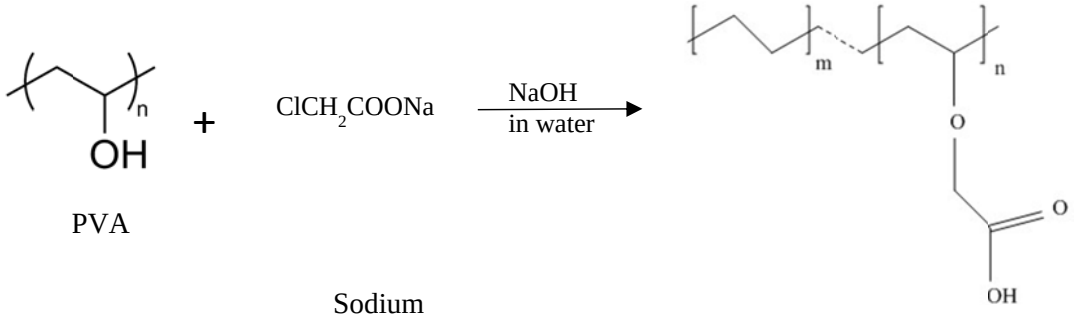

PVA

Sodium monochloroacetate

PVA-COOH

b) Preparation of PVA-alkyl:

First part of making PVA-alkyl was synthesis of hexadecanal. Chemicals used for the preparation were celite, pyridinium chlorochromate and 1-hexadecanol. Dichloromethane was used as the solvent. 11.2mL dichloromethane was taken in a 50mL beaker with stir bar in it. 0.95g celite, 0.95g pyridinium chlorochromate and 0.5 g 1-hexadecanol were added to the beaker. The addition was done under fume hood. The solution was sealed with aluminium foil and kept on stir plate. It was stirred for 6 days at room temperature. After that, the reaction mixture was diluted by adding 40mL diethyl ether to it. Florisil columns were used to remove excess celite, pyridinium chlorochromate and 1-hexadecanol. Then the mixture was evaporated. Hexadecanal was obtained as a white solid.

PVA-COOH obtained after first reaction was dissolved in DMSO. The mixture was prepared in 100mL beaker with stir bar. Hexadecanal and 200µm of 12M hydrochloric acid were added to the solution and it was kept on hot plate. The temperature was maintained at 70^{o}C

and kept stirring for 25 hours. The reaction mixture was extracted with diethyl ether. The mixture was then neutralized with 1M sodium hydroxide.

Neutralized solution was dialyzed against DI water using dialysis tubing of 12-14kDa. Same procedure as described above was used for dialysis. Then the solution was desalted with ion exchange resins mentioned above and lyophilized using a freeze dryer for 3 days. PVA-alkyl was obtained as a white solid with yield of 49%. Final weight of the product was 0.22g. The overall reaction for the second step of the process is as follows:

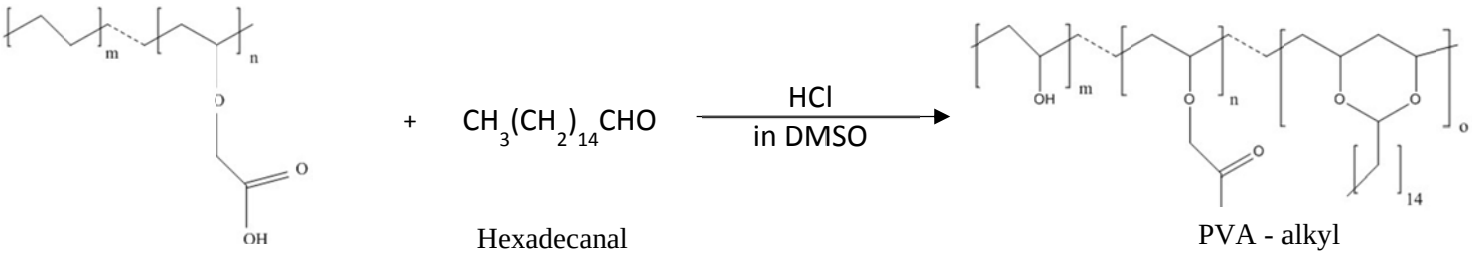

PVA-COOH Hexadecanal PVA - alkyl

4. Surface modification of PBI membrane using PVA-alkyl:

PVA-alkyl was attached to the membrane using carbodiimide chemistry. Carbodiimide chemistry is used for the reaction between carboxylic group and a nucleophile. The nucleophile that is used in this case is hydroxide group present in PVA-alkyl molecule. For the reaction, N-(3-dimethylaminopropyl)-N'-ethylcarbodiimidehydrochloride (EDCH) and N-hydroxysuccinimide (NHS) were used. The reactions were performed in 2-(N-morpholino) ethanesulfonic acid (MES) buffer.

400mL water was taken in a 500mL beaker and 7.85g MES buffer was added to it. The solution was stirred until MES was completely dissolved in water. 11.75g NaCl was added to the solution and stirred until dissolved. The solution was titrated to pH 6 using NaOH. Benchtop pH meter was used to monitor pH with addition of NaOH. 0.23g NHS and 0.153g EDCH were added to the solution and stirred well. CMBA modified membrane was added to the solution and was stirred for 15 minutes. After 15 minutes, the reaction mixture was titrated to pH 7 using NaOH as soon as possible. PVA-alkyl was added to the solution and it was kept stirring for 24 hours. After 24 hours, membrane was taken out of the solution and rinsed well with DI water and stored in a beaker filled with DI water. The membrane was stored for 24 hours before using it for analysis. Overall reaction is as follows:

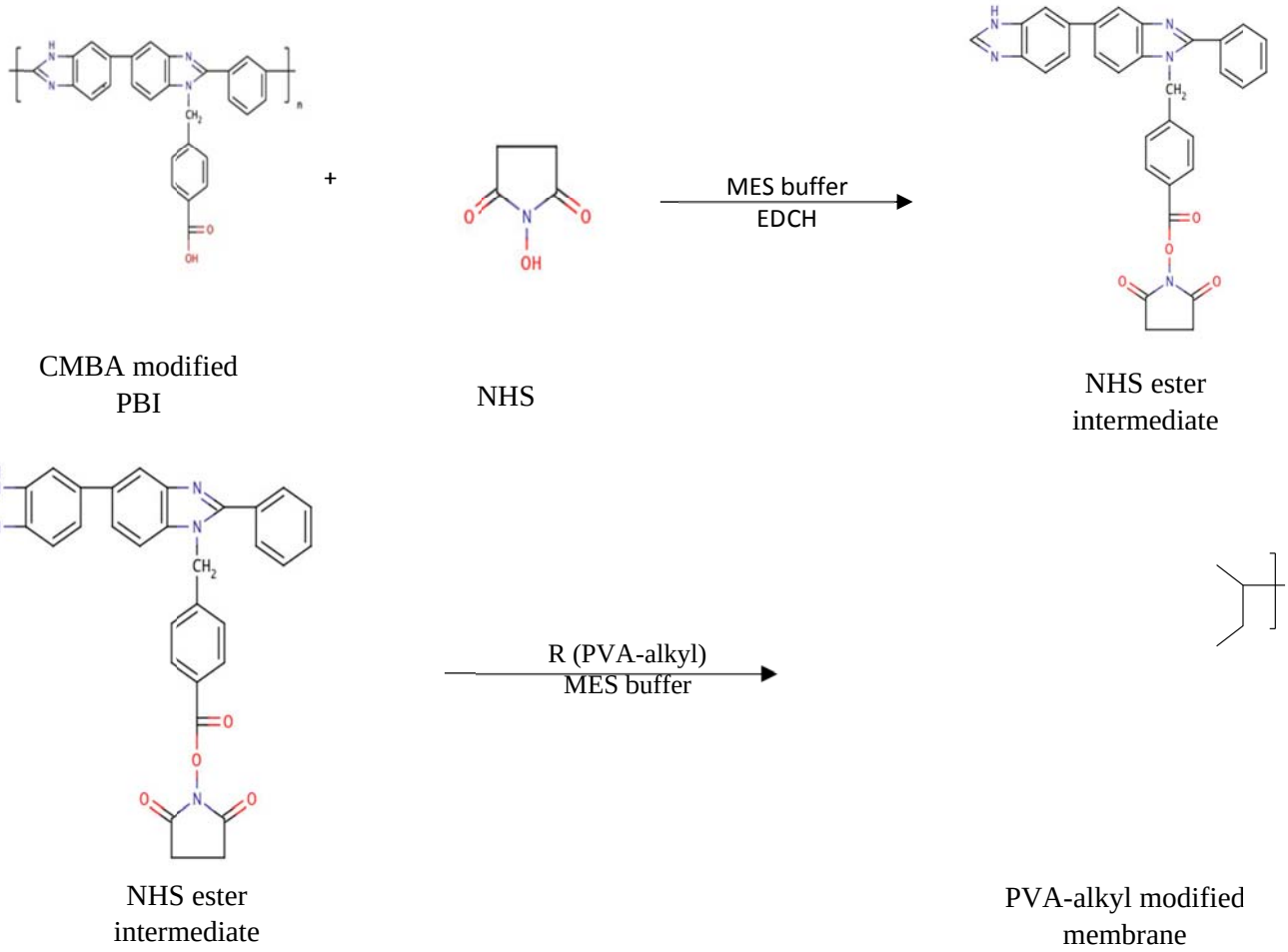

CMBA modified PBI

NHS

NHS ester intermediate

NHS ester intermediate

PVA-alkyl modified membrane

Preliminary Results –

Virgin PBI and CMBA-modified membranes were tested using Fourier Transform Infrared Spectroscopy in attenuated total reflectance mode (FTIR-ATR). The difference in the FTIR curves of both the membranes can be seen in Figure 2. The appearance of peak 1 in the curve for the CMBA-modified membrane was associated with the presence of a C-O bond in the molecule. Peak 2 corresponded to carbonyl group, while peak 3 was associated with the presence of an O-H bond. Secondary amine groups, present in the PBI molecule, displayed peaks in the same region as carbonyl groups (1620-1640 cm^{-1}).

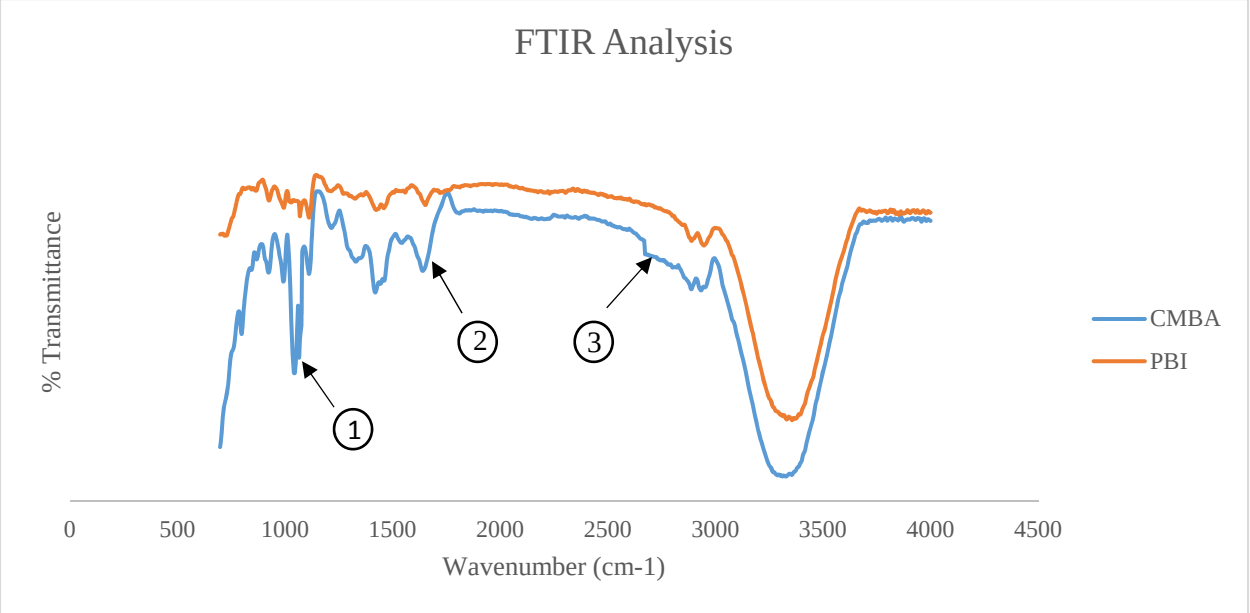

Figure 2 FTIR Spectra of virgin PBI and CMBA-modified membranes

Virgin PBI membranes were analyzed to determine the flux decline during operation. The decrease in the permeate flux over the time period of operation was measured using membranes prepared using 21% dope solution. A10-mL Amicon dead-end filtration cell was used for this purpose. A constant pressure of 70 psi was maintained for all the tests and the membranes were supported with a filter paper. The time required to collect 2mL of permeate was measured, and the flux was calculated. The first step of filtration was precompaction, during which deionized water was filtered through the membrane, and the flux decline with time was measured. Filtration experiments were also performed using bovine albumin serum (BSA) and lipase protein solutions after precompaction. The concentration of feed for both solutions was kept 10 mg/L. After BSA filtration, the membrane was backwash for one hour. For this purpose, the membrane was flipped and then DI water was filtered through the membrane under the same operating conditions as above. Flux recovery of the membrane was measured after backwash. Flux decline is shown in Figure 3.

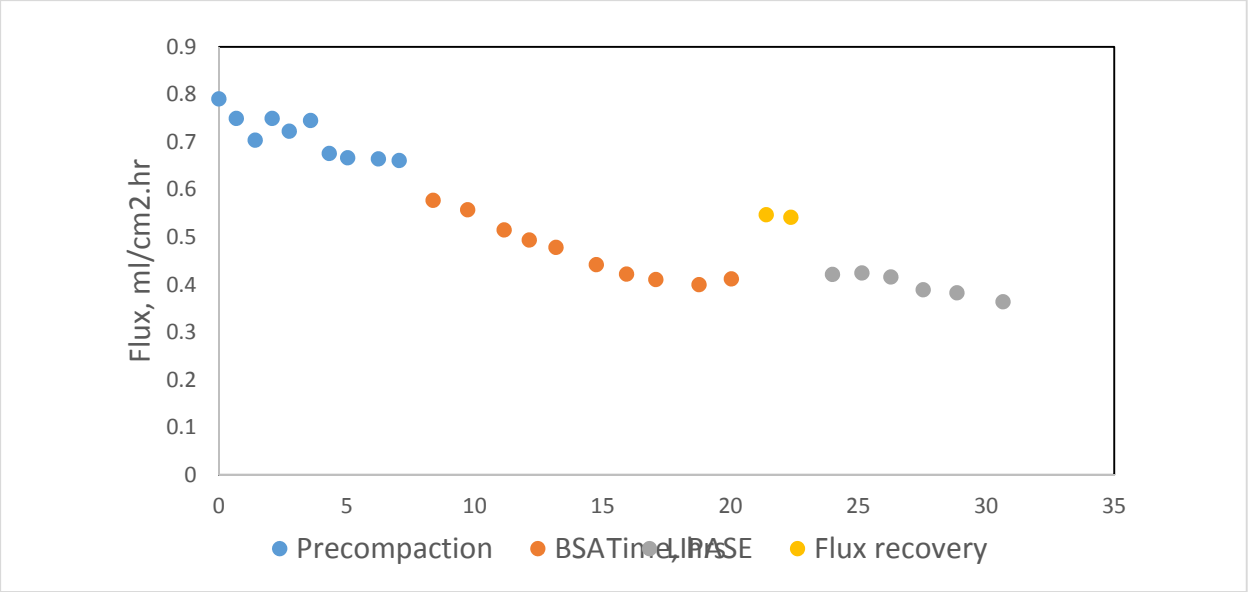

Figure 2 Flux analysis of PBI membrane

Ongoing Studies –

The following tasks are underway:

- Produce AqpZ, treat it with GA, and incorporate it in amphiphilic PVA-alkyl.
- Use chemical surface modifications to polymerize the AqpZ-GA in PVA-alkyl to the PBI membrane to form biomimetic membranes.
- Characterize the biomimetic membranes chemically and structurally.
- Characterize the biomimetic membranes with respect to flux and solute rejection.

Publication citations (all journal articles, proceedings and presentations at conferences)

So far, one conference presentation was given at the American Institute of Chemical Engineers, and in early June, another conference presentation will be given at the North American Membrane Society:

- Wagh P. and I.C. Escobar (2013). "Synthesis of Biomimetic Polybenzimidazole Nanofiltration Membranes," 2013 AIChE Annual Meeting, San Francisco, CA, November 3-8, 2013.
- Wagh P. and I.C. Escobar (2014). "Development of Biomimetic Nanofiltration Membranes Using Aquaporins," 2014 NAMS Annual Meeting, Houston, TX, May 31-June 4, 2014.

Number of students supported by the project (MS/PhD/undergraduate/post docs) as well as their majors

One undergraduate and one PhD students have been supported by the grant:

- Priyesh Wagh, PhD, chemical engineering
- Kayla Nagle, undergraduate, chemical engineering

Awards or Achievements (patents, copyrights), additional funding for this project

N/A

SEPARATION OF PHOSPHORUS- AND NITROGEN-NUTRIENTS FROM AGRICULTURAL DEGRADED WATERS USING PERVIOUS FILTER MATERIAL DEVELOPED FROM INDUSTRIAL BY-PRODUCTS

Basic Information

Title:	SEPARATION OF PHOSPHORUS- AND NITROGEN-NUTRIENTS FROM AGRICULTURAL DEGRADED WATERS USING PERVIOUS FILTER MATERIAL DEVELOPED FROM INDUSTRIAL BY-PRODUCTS
Project Number:	2013OH436O
Start Date:	9/1/2013
End Date:	8/31/2014
Funding Source:	Other
Congressional District:	OH-12
Research Category:	Engineering
Focus Category:	Treatment, Agriculture, Water Quality
Descriptors:	Industrial by-rpoducts, filter material, nutrients
Principal Investigators:	Linda Kay Weavers, ChinMin Cheng

Publications

There are no publications.

SEPARATION OF PHOSPHORUS- AND NITROGEN-NUTRIENTS FROM AGRICULTURAL DEGRADED WATERS USING PERVIOUS FILTER MATERIAL DEVELOPED FROM INDUSTRIAL BY-PRODUCTS

Progress Report

Submitted to:

Ohio Water Resources Center

Submitted by:

Principal Investigator:
Linda Weavers, Ph.D., P.E., BCEE.
Professor
Department of Civil, Environmental, and Geodetic Engineering
e-mail: weavers.1@osu.edu; Telephone: 614-292-8263; Fax: 614-292-3780

Co-PI:
Chin-Min Cheng, Ph.D., P.E.
Research Associate II-Engineer
Department of Civil, Environmental, and Geodetic Engineering

ABSTRACT

End-of-tail filtration has been suggested as a more aggressive and effective approach to reduce losses of nutrients from crop lands compared to current best management practices (BMPs) focusing on source reduction and minimizing transportation. A number of industrial by-products, e.g., coal combustion by-products and bauxite leaching residual, have been proven chemically effective in trapping P- and/or N-nutrients, and therefore, are potential low-cost nutrient sorbents for the end-of-tail filtration approach. However, the application of these industrial by-products as the filtration media is limited due to unfavorable hydraulic properties, as well as unknown associated environmental impacts. In this proposed study, pervious filter materials owning both reactivity to nutrients and adequate hydraulic properties are developed using fly ash, stabilized FGD materials, and bauxite leaching residual as the feedstock. By modifying the composition of these industrial by-products, the pervious materials are expected to have selective nutrient-sequestrating capabilities, which can be used to separate and recycle phosphorus- and nitrogen-nutrients from agricultural drainage waters (ADWs). This study is carried out in three tasks to (1) investigate the adsorption efficiency and service lifetime of selected pervious materials with synthetic ADW; (2) evaluate the physical and chemical integrity of the pervious materials before and after service; and (3) study the interactions between the prepared filter materials and emerging pollutants commonly found in ADW (e.g., estrone). The goal of this study is to demonstrate the feasibility of applying a low-cost and environmentally-sustainable approach to ADW handling and treatment. This alternative to current BMPs is able to convert agricultural and industrial wastes to value-added products containing concentrated and specific nutrients. Currently, the project is still on going. Results obtained from this study will be used to develop a competitive proposal for external funding.

1. Introduction

Eutrophication of water bodies, a result of release of excessive phosphorous (P) and nitrogen (N) from soil to drainages[1], has been an increasing environmental issue in the US, especially in the Midwest, northeast, and Gulf coast area where the watersheds of major freshwater bodies involve rapid growth and intensification of crop and livestock farming[2]. Not only eutrophication posts unpleasant aesthetic characteristics to water bodies, accumulation of toxic, volatile chemicals produced by algae can cause neurological damage in people and animals being exposed to them. Consequently, eutrophication of water resources results in losses of biodiversity, as well as their amenities and services[3]. For example, the recent outbreaks of Cyanobacteria, or blue-green algae, in the Grand Lake at St. Mary's area in Ohio has led to state officials to issue water contact and fish consumption advisories.

The major cause of many eutrophication incidents can be directly correlated to fertilizer application[4]. To prevent accumulation of nutrients in surface waters, reduction of nutrients present in the agricultural degraded waters (ADW, i.e., livestock wastewater overflow, subsurface drainages, and surface runoffs from cropland) is perceived as necessary approach[5]. Although many best management practices (BMPs) focusing on source reduction and minimizing transportation have been implemented to reduce losses of nutrients from crop lands, these approaches have shown no control on dissolved phosphorus losses[6,7], which is the most readily available form of phosphorus to aquatic organisms[8]. Instead, end-of-tail filtration has been suggested as a more aggressive and effective approach[6]. However, the application is limited. Ideal filter materials, i.e., material with both favorable nutrient-sequestrating capability and hydraulic property, have yet been identified[9].

In this study, low-cost pervious sorption materials prepared from a self-geopolymerization process using agricultural wastes and industrial by-products are tested for their potential as an alternative to current BMPs. The self-geopolymerization process enchains agricultural wastes with chemically-effective, nutrient-sorbing industrial by-products (e.g., coal ash, flue gas desulfurization materials, and bauxite residual) and forms pervious materials. By modifying the composition, the pervious materials are expected to have selective sorption capabilities to nitrogen (N-) and phosphorus (P-) nutrients with adjustable hydraulic properties, which can be used to separate and recycle nutrients from ADWs.

2. Objectives

In this study, a geopolymerization procedure is developed to convert coal combustion by-products (i.e., fly ash and flue gas desulfurization (FGD) material) and alkaline bauxite leaching

residual (bauxite red mud) to pervious filter materials. The materials are tested in a bench-scale setting for their effectiveness and capacity on removing nutrients from simulated agricultural drainage waters. The specific objectives of this proposed project are to:

(1) Assess the performance of the industrial by-product-derived pervious filter materials with respect to their nutrient removal efficiencies, service lifetime, and hydraulic properties;
(2) Evaluate the chemical and physical integrity of the materials; and
(3) Study the interactions between the prepared filter materials and other pollutants contained in ADWs (i.e., estrogens).

3. Materials and Method

The work of this proposed study is divided into three tasks. In summary, the first task focuses on preparing and characterizing the pervious filter materials. At least three sets of P-type (i.e., materials selectively adsorb P-nutrients) and N-type (i.e., materials adsorbed nitrate and/or other N-nutrients) are prepared. In the second task, a series of column experiments are setup to (1) evaluate the adsorption efficiency and capacity of the selected pervious materials with a simulated ADW and (2) study the interactions between estrogens and filtration materials. In addition, the physical and chemical integrities of the pervious filter material during and after service are evaluated. The release of metals and metaloids (e.g., mercury, arsenic, selenium, thallium, and boron), as well as sulfate, from the filter materials during filtration are monitored. In addition, surface characterization techniques, such as X-ray diffraction (XRD) and scanning electron microscopy (SEM), are applied to investigate the transformations of mineral composition and surface morphology before and after the filtration materials are exhausted.

Pervious Filter Material Preparation and Characterization

Coal combustion by-products (i.e., fly ash and stabilized FGD materials) and bauxite leaching residue (i.e., red mud) are used in the preparation of the nutrient-selective pervious filtration materials (Figure 1). Two different types of pervious filtration materials (i.e., P- and N-types) are prepared using a method modified from Cheng et al.[10] and Jin[11]. Class F fly ash and sulfite-rich stabilized FGD material provided by coal combustion power plants located in eastern Ohio are used to prepare the phosphorous-capture (P-type) filtration materials. Quick lime

(Carmeus USA, Pittsburg, PA), CaO, is added to provide required alkalinity. The nitrogen-capture materials are prepared from red mud, fly ash, and stabilized FGD material. No quick lime is used in the preparation of N-type filter materials. The bauxite red mud provided by a bauxite processing plant located at southeast Texas is oven-dried before use. In one batch, manganese oxide (MnO_2) is also added in the preparation of N-type material. Woodchip is used in the preparation of both N and P-type filter mixtures to modify the hydraulic properties. The prepared mixtures are then cured in a humidity chamber.

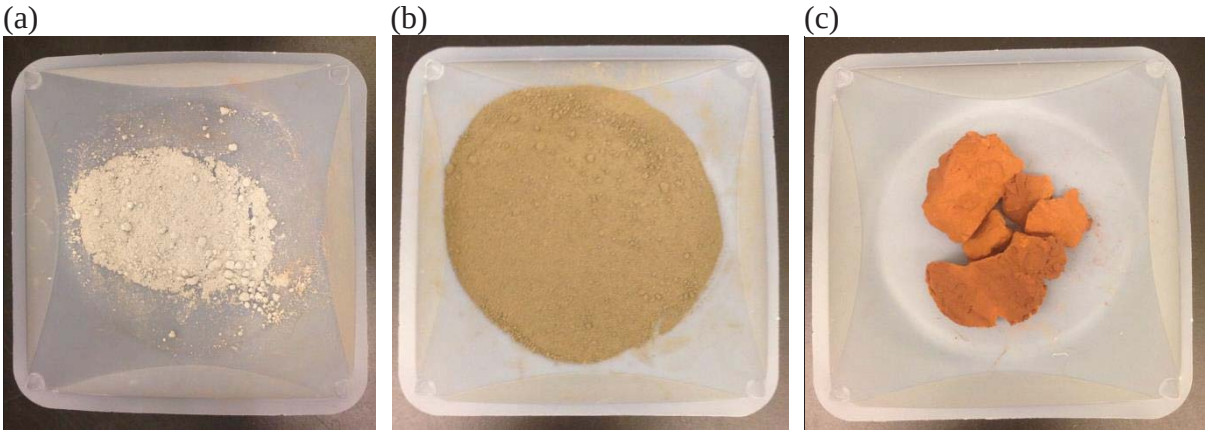

Figure 1. (a) Stabilized FGD material, (b) fly ash, and (c) bauxite red mud used in the preparation of pervious filtration materials.

The cured filter materials are tested for their chemical (i.e., elemental and mineral compositions), physical (density and surface morphology), and engineering (i.e., permeability (k) and/or hydroconductivity (K)) properties as per standard testing protocols. Details on the chemical and physical characterizations of the filter materials are described in the "*Physical and Chemical properties Integrity Evaluation*" section.

Bench-Scale Column Test

A series of column tests are carried out to measure the adsorption capacity and efficiency of prepared pervious materials for P- and N-nutrients with a simulated ADW. In addition to the prepared filter materials, two reference columns, packed separately with granular activated carbon (GAC) and top soil from the OSU's Waterman Farm Complex, are also included in the column study. A control column, i.e., without packing medium, is included to evaluate the adsorption of nutrients and compounds on the experimental apparatus.

The setup of the column test is illustrated in Figure 2. The ADW used in the column test is synthesized based on formula listed in Table 1. In addition to the constituents listed in the table, one estrogen, e.g., estrone (E1) or 17α-Estradiol (17α-E2), commonly found in dairy wastewater[12] is added in selected experimental batches. A peristaltic pump delivers the synthetic ADW to the inlet of a series of two vertically-oriented columns at a constant feed rate (Figure 2). The ADW sequentially passes through the column containing P-type filter material (P-type column) and then the N-Type column. For a given set of filter materials, the column test is carried out under a saturation condition demonstrated in Figure 2.

Table 1. Composition of synthetic dairy wastewater used in this study

Component	Amount (mg/L)
Urea	115.7
NH_4Cl	250.0
$Na_2PO_4 \cdot 12H_2O$	385.7
$KHCO_3$	257.1
$NaHCO_3$	668.6
$MgSO_4 \cdot 7H_2O$	257.1
$FeSO_4 \cdot 7H_2O$	10.3
$MnSO_4 \cdot H_2O$	10.3
$CaCl_2 \cdot 6H_2O$	15.4

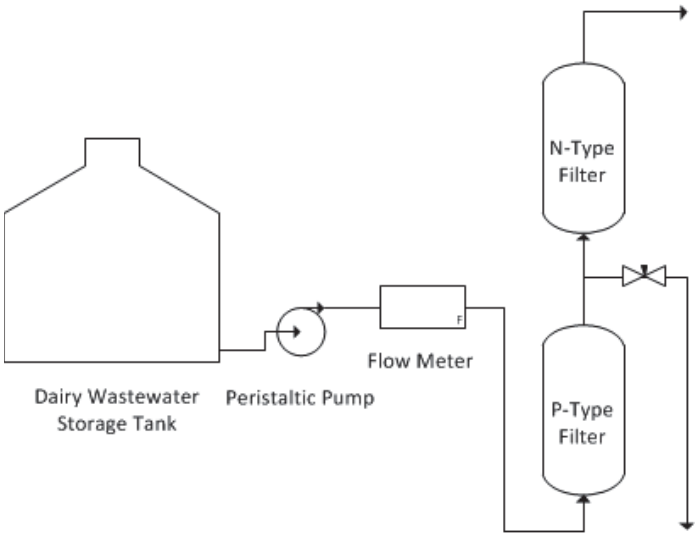

Figure 2. Setup of bench-scale column test

Effluent samples are collected periodically from the outlets of P-type and N-type columns for a list of chemical analyses shown in Table 2. After collection, sample is immediately separated into four sub-samples. The first sub-sample is for pH, conductivity, and redox potential measurements. In the selected batches when estrogen is included in the synthetic ADW, an aliquot of the first subsample is filtered with 1.2μm glass fiber and concentrated by solid-phase extraction for estrogen analysis. Any compounds remained on the sample collection bottle or filter is desorbed by rinsing the bottle and filter with methanol. The concentrated sample is analyzed using a high-performance reverse-phase liquid chromatography tandem electrospray ionization mass spectrometry (HPLC/MS/MS). Deuterated internal standards is added to the samples to correct the interferences caused by the matrix of the sample.

The second sub-sample is filtered and analyzed for alkalinity, total dissolved solids, Cl-, SO_4^{-2}, PO_4^{-3}, total Kjeldahl nitrogen, ammonia, and NO_3^-. The third sub-sample is preserved with 5% HNO_3 and analyzed for "total" elements in the solution. The final sub-sample is filtered through a 0.45-μm syringe filter and preserved with 5% HNO_3 before being analyzed for "dissolved" elements.

Table 2. List of monitoring parameters and respective analytical methods for aqueous samples

Subsample	Parameter	Detection Methods	Instruments	Locations
Subsample I	Conductivity	AWWA Sec. 2510	Thermo Orion 1234	*in-situ*
	pH		Thermo Orion 1234	*in-situ*
	Redox Potential		Thermo Orion 1234	*in-situ*
	Estrogen[c]	HPLC/MS/MS	Micromass Q-TOF II	CCIC[b]
Subsample II	Alkalinity	AWWA Sec. 2310	-	CEGE EER Lab/ OARDC STAR Lab
	Total dissolved solid	AWWA Sec. 2540	-	
	Chloride (Cl)	AWWA Sec. 4110C	Dionex 2100	
	Sulfate (SO_4^{-2})	AWWA Sec. 4110C	Dionex 2100	
	Phosphate(PO_4^{-3})	AWWA Sec. 4110C	Dionex 2100	
	Nitrate (NO_3^-)	AWWA Sec. 4110C	Dionex 2100	
	Ammonia (NH_4^+)	AWWA Sec. 4110C	Dionex 2100	
	Total Kjeldahl Method	AWWA Sec. 4500 N_{org}	-	
Subsample III/ Subsample IV	Mercury (Hg)	CVAFS	Varian CVAAs,	
	Selected Elements[a]	AWWA Sec. 3120B	Varian VISTA-AX	
	Arsenic (As)/ Thallium(Tl)	AWWA Sec. 3120B	Varian GFAAs, Varian 880Z	
	Selenium (Se)	AWWA Sec. 3120B	Varian GFAAs, Varian 880Z	

[a] Aluminum (Al), arsenic (As), barium (Ba), beryllium (Be), boron (B), cadmium (Cd), copper (Cu), chromium (Cr), iron (Fe), lead (Pb), magnesium (Mg), manganese (Mn), nickel (Ni), phosphorous (P), sodium (Na), silver (Ag), zinc (Zn).
[b] Campus Chemical Instrument Center at The Ohio State University
[c] On selected experimental batches

Chemical and Physical Integrity Evaluations

The exhausted filter materials are preserved using liquid nitrogen and freeze-dried before being analyzed for the mineral and chemical compositions, surface morphology, and forms of adsorbed phosphorus by the methods listed in Table 35. The mineral compositions and morphology of the selected N- and P- type filters materials before and after service are characterized using X-ray diffraction (XRD) and scanning electronic microscopy (SEM), respectively. A Bruker D8 Advance X-ray diffractometer or equivalent is used to identify the mineral composition. The mineral patterns in the diffractograms are matched using the DIFFRACplus EVA software with ICDD Power Diffraction File (PDF2+) database. The complete elemental composition analysis is measured with the assistance of the digestion procedure described in EPA method 3052. A reference coal fly ash, 1633b, provided by the National Institute of Standards and Technology (NIST), is included for analytical quality control. A list of the analyses performed on the materials can be seen in Table 4.

The release potential of trace elements from filter materials before and after service will also be characterized. Standard protocols, i.e., EPA Standard Method 1311, Toxicity Leaching Characteristic Procedure (TCLP), the EPA Standard Method 1312, Synthetic Precipitation Leaching Procedure (SPLP), are used.

Table 3. Physical, mineral, and chemical analyses for selected pervious filter materials

	Method	Instrument	Location
Permeability	ASTM D4525-08		CEGE Soil Lab
Hydraulic Conductivity	ASTM D7100-06		
Morphology	Scanning Electron microscopy	Hitachi S-3000 SEM	OSU Nanotech West Lab
Mineral Composition	X-ray Diffraction	Bruker D8 Advance X-ray diffractormeter	SENR Soil Lab[c]
Selected Elements[a]	ASTM D-6357	Milestone Microwave Digestor/ Varian VISTA-AX	CEGE EER Lab[b]
Mercury	ASTM D-6414	Varian CVAAs, Varian 880Z	CEGE EER Lab
Selenium	ASTM D-4606	Varian CVAAs, Varian 880Z	CEGE EER Lab
Arsenic, Thallium	ASTM D-3683	Varian GFAAs, Varian 880Z	CEGE EER Lab

[a] aluminum (Al), barium (Ba), beryllium (Be), boron (B), cadmium (Cd), chromium (Cr), lead (Pb), magnesium (Mg), manganese (Mn), nickel (Ni), phosphorous (P), sodium (Na), sulfur (S), and zinc (Zn).
[b] Environmental Engineering Research Laboratory at Department of Civil, Environmental, and Geodetic Engineering of The Ohio State University
[c] Soil Lab at School of Environment and Natural Resources of The Ohio State University

4. Current Progress and Tasks to be completed

Characterizations of Industrial By-products

The chemical compositions of fly ash, stabilized FGD material, and bauxite red mud are first characterized and the results are summarized in Table 4. As shown in the table, calcium (Ca) and sulfur (S) are the two most abundant elements in the stabilized FGD material, which is associated with the presence of hannebachite ($CaSO_3 \cdot 0.5H_2O$), portlandite ($Ca(OH)_2$), and enttringite ($Ca_6Al_2(SO_4)_3(OH)_{12} \cdot 26H_2O$) in the material. The X-ray diffractogram and mineral composition of stabilized FGD material can be seen in Figure 3. Iron (Fe), aluminum (Al), sulfur (S), and silicon (Si) are the major elements in fly ash. Based on XRD analysis, the fly ash used in this study is comprised of amorphous glass, aluminum silicates (e.g., mullite), and iron oxides (hematitem, magnetite, and maghemite). Bauxite red mud is consisted of Al, Fe, and Ca. The X-ray diffractograms of fly ash and red mud are not shown.

By properly coalescing fly ash, stabilized FGD material, and red mud under high alkaline environment, fly ash acts as an inorganic polymer binder to enchain active ingredients through a geopolymerization process. After being alkali-activated, the Si-O-Si or Al-O-Si bonds in fly ash and stabilized FGD material are disassociated and subsequently form network-like crystalline and/or amorphous alkaline aluminosilicates with structural framework similar to zeolite[13]. In a previous project, it has been demonstrated that a geotextile material derived from the geopolymerization process with a mixture of fly ash and stabilized FGD material, has effective phosphorus sorption capability by forming Ca- and Fe-precipitates[10,14,15]. However, the fly ash/stabilized FGD material mixture did not show observable effect on nitrate mitigation[10].

The addition of bauxite red mud is to enhance the nitrogen-nutrients adsorption capability of the fly ash/FGD mixture. Bauxite red mud contains minerals, e.g., iron (III) (hydr)oxides and hydrous aluminum oxides, that have high affinities for nitrate[16]. As a result, the material has been shown to be an effective nutrient sorbent[17]. Cengeloglu et al[17] used original and acid-treated bauxite red mud to remove nitrate from aqueous solution and reported 70% and over 90% of removal, respectively. They found the alkaline property of bauxite red mud hindered the adsorption performance.

In this study, bauxite red mud is used as the sole alkalinity source in the geopolymerization process, which might promote the nitrate adsorption capacity. During geopolymerization, the OH- ions from bauxite red mud is consumed (eq. 1) and redistribute the electron density around the silicon atom in fly ash, which weaken the strength of Si-O-Si bond[18]

and progress the polymerization process. The reaction neutralizes the negative surface charge of red mud particles, and therefore, might promote the nitrate sorption.

$$\equiv Si - O - Si \equiv + OH^{-} \Rightarrow \equiv Si - OH + {}^{-}O - Si \equiv \quad (1)$$

Preparation of P- and N-type pervious filtration

A series of P- and N-type pervious filtration materials have been prepared based on the formulas listed in Tables 5 and 6. Currently, the prepared materials are undergoing a 21-day curing process. The images of two selected prepared materials can be seen in Figure 4. The hydraulic property of the filtration materials are adjusted by the addition of woodchip. Two different sizes of woodchip, i.e., <2.3mm and 2.3-3.6mm, are used. The addition of woodchip creates larger capillary routes for water to pass through. During the geopolymerization process, active ingredients are coated on the surface of woodchip, which allows the nutrients in ADW to react with the active ingredients while passing through the void space.

Table 4. Chemical compositions of fly ash, stabilized FGD material and bauxite red mud used in this study

		Fly Ash	Stabilized FGD material	Red Mud
Phosphorus	P	531	177	1054
Potassium	K	2986	1307	310
Calcium	Ca	9836	172906	33055
Magnesium	Mg	1528	10026	227
sulfur	S	11827	85746	2867
Aluminum	Al	27050	9705	62817
Boron	B	531	313	<3
Copper	Cu	42	<0.4	<0.8
Iron	Fe	59824	18855	240960
Manganese	Mn	85	73	139
Molybdenum	Mo	22	<13	<0.5
Sodium	Na	18851	5296	32412
Zinc	Zn	109	40	22
Arsenic	As	143	36	28
Barium	Ba	177	137	61
Beryllium	Be	<0.18	<0.11	<0.18
Cadmium	Cd	2	6	5
Cobalt	Co	23	4	15
Chromium	Cr	74	25	1397
Lithium	Li	167	106	55
Nickel	Ni	48	7	6
Lead	Pb	28	8	46
Antimony	Sb	<1.5	17	<1.5
Selenium	Se	20	18	1
Silicon	Si	4771	1481	184
Strontium	Sr	229	212	117
Thallium	Tl	129	38	871
Vanadium	V	2	<1.1	<0.6
Mercury	Hg	NA	0.318	NA

NA:Not Available
Unit: mg/kg

Table 5. Formulas of Prepared P-type Filtration Materials

	P-Control	P-type I	P-type II	P-type III
Fly Ash	10.0	10.0	10.0	10.0
Stabilized FGD material	6.0	6.0	6.0	6.0
Quick Lime (CaO)	1.2	1.2	1.2	1.2
Deionized Water	10.5	10.5	10.5	10.5
Wood Chip (<2.3 mm)	0	2.5	5.0	0
Wood Chip (2.3-3.6 mm)	0	0	0	2.5

Unit: g

Table 6. Formulas of Prepared N-type Filtration Materials

	N-type I	N-type II	N-type III	N-type IV
Fly Ash	10.0	10.0	10.0	10.0
Stabilized FGD material	6.0	6.0	6.0	6.0
Red Mud (dried weight)	8	8	8	8
Deionized Water	10.5	10.5	10.5	10.5
Wood Chip (<2.3 mm)	0	2.5	5.0	2.5
MnO_2	0	0	0	2.0

Unit: g

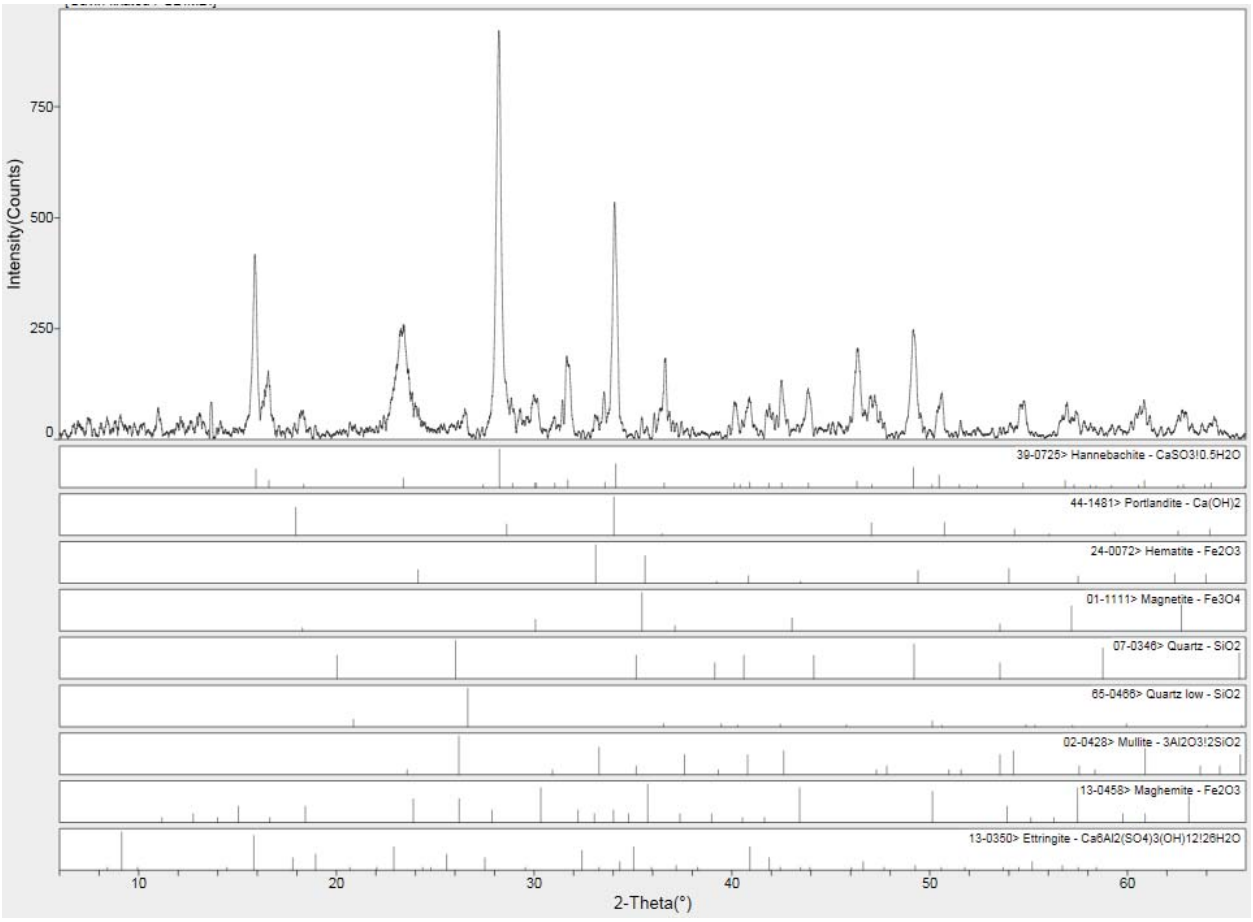

Figure 3. Mineral composition of stabilized FGD material

(a) (b)

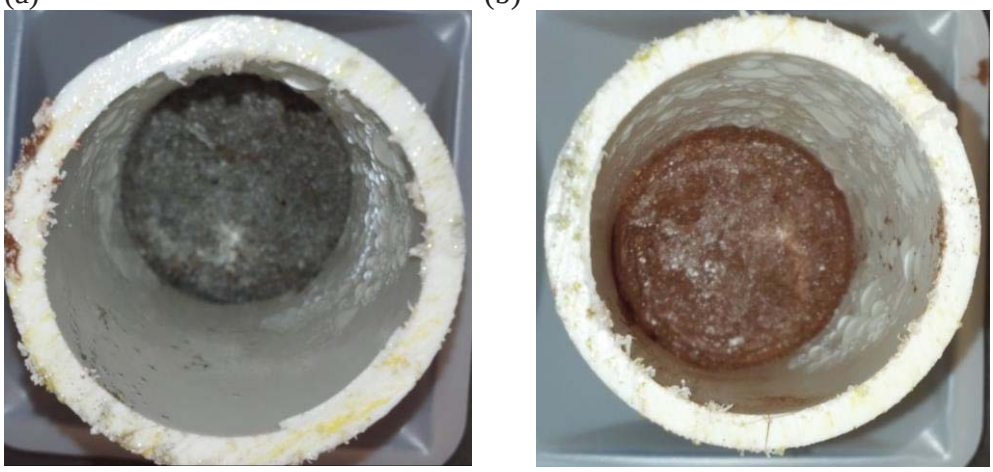

Figure 4. Prepared Pervious filtration materials. (a) P-type and (b) N-type.

These two types (i.e., P- and N-types) of pervious materials are expected to have selective sorption capacity, which can be used to sequentially separate and recover soluble phosphorous and nitrogen in agricultural drainage waters. In practice, two different pervious filter materials can be used in series. The dissolved phosphorous is expected to be selectively retained in the first pervious material (P-type) containing only fly ash and FGD material while allowing nitrate to pass through. Nitrate is captured in the second pervious material (N-Type) containing bauxite red mud, fly ash, and stabilized FGD material.

Tasks to be completed

The bench scale column test described in the "*Materials and Methods*" section is to be carried out soon after the curing of pervious filtration materials is completed. In addition, the integrities of physical and chemical properties of the pervious materials after adsorption will be evaluated.

Despite the great potential for the proposed filtration application, the major concern of reutilizing these by-products is the release of trace elements contained in the materials after being contacted with water. Cheng et al.**Error! Bookmark not defined.** investigated the water quality impacts associated with using stabilized FGD material as a low permeability liner for a swine manure storage pond. Based on five-year worth of field monitoring data, the concentrations of arsenic (As), boron (B), chromium (Cr), copper (Cu), and zinc (Zn) were consistently found lower in the water passing through the liner than the water collected from the pond. Other trace elements, such as Cd, Se, and Hg were often below the analytical detection limits. Ruyter et al.[19] investigated the red mud accident occurred on October 4th 2010 in Ajka, Hungary by testing the

plant toxicity and trace element availability with mixtures of red mud and non-contaminated soil. They observed the concentrations of trace elements in the leachate of red mud were either non-detectable or less than 20μg/L. In addition, Peters and Basta[Error! Bookmark not defined.] added bauxite red mud directly to soil to reduce the bioavailable phosphorus. No excessive soil pH and increases of soil salinity, extractable Al, or heavy metals in soils were found in their study. Based on available field data, the application of coal combustion by-products and bauxite red mud has not been suggested to post adverse impacts on the environments.

However, to comprehend the overall benefits of reusing these by-products, it is vital to understand the leaching properties of the prepared pervious materials under different application scenarios.

Expected Outcomes and Significances

The outcome of this study is expected to provide:

(1) Initial feasibility evaluation of a potential beneficial utilization for by-products produced from coal combustion and aluminum production processes
(2) Insights regarding the interaction between nutrients and an agricultural emerging pollutant (i.e., estrogen) of FA zeolite-like material and the properties of biopolymers, and
(3) Results to be transferred in forms of peer-reviewed publications and conferences, and be based upon in preparing competitive proposal for external funding.

The advantage of using selective sorption materials in the filtration approach is the potential to recycle and reutilize nutrients and industrial by-products, which promotes agricultural production to be in accord with the principles of sustainability. FGD gypsum and stabilized FGD material have shown to improve the yield of crops by providing necessary elements (e.g., calcium), changing soil physical properties, and increasing water infiltration and storage when they are applied as soil amendments[20,21]. Hylander et al.[22], used different filter materials (i.e. limestone, Polonite®, and sand) to capture soluble phosphorus and evaluated the subsequent suitability for plant production. They observed some of recycled phosphorus achieved 76% of the yield increased by commercially available P-fertilizer. As demand for food increases, which results in more land to be used for agricultural purpose and a requirement for increased crop yields, the fertilizer demand have been projected to increase faster than world population[23]. With foreseeable increase in demand and depletion in reserve, use of recycled nutrients rather than a raw material is important step toward sustainable agricultural

development. Currently, the majority of phosphate rock from mining goes into artificial fertilizer production[24]. It estimates that sources of high-grade phosphate ore deposits could disappear within the next 100 years at current use rates[25].

5. References

[1] Alexander, R. B., Smith, R. A., Schwarz, G.E., Boyer, E.W., Nolan, J.V., Brakebill, J.W. (2008) Differences in phosphorous and nitrogen delivery to the Gulf of Mexico from the Mississippi River Basin. *Environ. Sci. Technol*., 42, 822-830.

[2] Mueller, D.K., Helsel, D.R., Nutrients in the Nation's Waters--Too Much of a Good Thing?. U.S. Geological Survey Circular 1136, http://pubs.usgs.gov/circ/circ1136/circ1136.html#PUBS, accessed 2/4/2011.

[3] Smith, V.H., Tilman, G.D., Nekola, J.C. (1999) Eutrophication: impacts of excess nutrient inouts on freshwater, marine, and terrestrial ecosystems, *Environ. Poll.*, 100, 179-796.

[4] Smil, V. *Enriching the Earth: Fritz Haber, Carl Bosch, and the Transformation of World Food*. The MIT Press, 2001, Cambridge, U.K.

[5] Sharpley A, Foy B, Withers P (2000) Practical and innovative measures for the control of agricultural phosphorus losses to water: An overview. *J. Environ. Qual.*, 29, 1-9.

[6] Kleinman P.J.A., Sharpley, A.N., Buda, A. R., McDowell, R.W., Allen, A.L. (2011) Soil controls of phosphorus in runoff: Management barriers and opportunities. *Can. J. Soil Sci.* 91, 329-338.

[7] Sharpley A., Kleinman, P., and Weld J. (2010) Assessment of best management practices to minimize the runoff of manure-borne phosphorous in the United States, *New Zealand J. Agric. Res.*, 47, 461-477.

[8] Sonzogni, W.C., Chapra, S.G., Armstrong, D.E., Logan, L.T. (1982) Bioavailability of phosphorus inputs to lakes. *J. Environ, Qual.*, 11, 555-563.

[9] King, k.W., McDonald, J., Moore, J.F., Agrawal, S.G., Fischer, E.N., Balogh, J.C. (2010) Nutrient and pesticide removal from laboratory-simulated tile drainage discharge, *Trans. ASABE*,53, 769-777.

[10] Cheng, C.-M., Tu, W., Behrad, Z., Tarunjit B., Wolfe, W., Walker, H. (2007) Beneficial Reuse of FGD Material in the Construction of Low Permeability Liners: Impacts on Inorganic Water Quality Constituents, *J. Environ. Eng.*, 133, 523-531.

[11] Jin, N. fly ash Applicability in Pervious Concrete, Master Thesis, The Ohio State University, Columbus, OH 2010.

[12] Gall, H. E., Sassman S.A., Lee, L.S., and Jafvert, C.T., Hormone discharges from a Midwest tile-drained agroecosystem receiving animal wastes. Environ. Sci. Tech., 2011, 45, 8755-8764.

[13] Buchwald A., Dombrowski, k., and Weil, M. Influence of geopolymer binder composition on conversion reactions at thermal treatment, in Developments in porous, Biological and Geopolymer Ceramics: A collection of Papers Presented at the 31st international conference on advanced Ceramics and Composites, eds. Brito, M., Case, E., Kriven, W.M., Ceramic Engineering and Science Proceedings Volume 28. 257-271. Florida 2007,

[14] Allred, B. (2010) Laboratory batch test evaluation of five filter materials for removal of nutrients and pesticides from drainage waters. *Transactions of the ASABE*, 53, 39-54.

[15] Bryant, R.B., Buda A.R., Kkeinman, P.J.A., Church, C.D., Saporite, L.S., Folmar, G.J., Bose, S., Allen, A. (2012) Using fluegas desulfurization gypsum to remove dissolved phosphorus from agricultural drainage waters. *J. Environ. Qual.* 41, 664-671.

[16] Yao, W., Millero, F.J. (1996) Adsorption of phosphate on manganese dioxide in seawater, *Environ. Sci. Technol,* 30, 536-541.

[17] Cengeloglu, Y., Tor, A., Ersoz, M., Arslan, G. (2006) Removal of nitrate from aqueous solution by using red mud. *Sep. Purif. Technol,* 51, 374-378.

[18] Duxson P, Lukey G.C., Separovic F. van Deventer J.S.J., (2005) Effect of alkali cations on aluminium incorporation in geopolymeric gels, *Ind. Eng. Chem. Res.*, 44, 832-839.

[19] Ruters, S., Merten, J., Vassilieva, E., Dehandschutter, B., Poffijn, A., Smolders, E. (2010) The red mud accident in Ajka (Hungary): plant toxicity and trace metal bioavailability in red mud contaminated soil. *Environ. Sci. Technol.*, 45, 1616–1622.

[20] Chen L., Dick W., Nelson S., (2001) Flue Gas Desulfurization by-product additions to acid soil: Alfalfa productivity and environmental quality, *Environ. Poll.*, 114, 161-168.

[21] Punshon T., Adriano D.C., Weber, J.T. (2001) Effect of flue gas desulfurization residue on plant establishment and soil and leachate quality, *J. Environ. Qual.*, 30, 1071-1080.

[22] Hylander, L.D., Kietlinska, A., Renman, G., Siman, G. (2006) Phosphorus retention in filter materials for wastewater treatment and its subsequent suitability for plant production**.** *Biores. Technol.*, 97, 914-921.

[23] Haar, A. The Reuse of Phosphorus. Eureau Position Paper EU2-04-SL09, 2005; http://eureau.org/sites/eureau.org/files/documents/2005.02.21_recovery_of_phosphorus_from_sludge.pdf. Accessed 10/6/2012.

[24] Jasinski S.M., Phosphate rock, 2006 Minerals Yearbook. United States Geologci Survey, 2007, http://minerals.usgs.gov/minerals/pubs/commodity/phosphate_rock/myb1-2006-phosp.pdf, accessed 10/2/2012.

[25] Christen, K. (2007) Closing the phosphorus loop, *Environ. Sci. Technol.*, 41, 2078.

2) Publication citations (all journal articles, proceedings and presentations at conferences)

Not available. The study is still on going.

3) Number of students supported by the project (MS/PhD/undergraduate/post docs) as well as their majors

None.

4) Awards or Achievements (patents, copyrights), additional funding for this project

Not available. The study is still on going.

Characterizing methane in geologic formations of Ohio Phase 1: Seed grant to investigate natural biogenic methane from domestic wells unaffected by oil and gas production

Basic Information

Title:	Characterizing methane in geologic formations of Ohio Phase 1: Seed grant to investigate natural biogenic methane from domestic wells unaffected by oil and gas production
Project Number:	2013OH437O
Start Date:	3/1/2013
End Date:	7/31/2013
Funding Source:	Other
Congressional District:	OH-12
Research Category:	Water Quality
Focus Category:	Groundwater, Hydrogeochemistry, None
Descriptors:	Methanogenesis, Groundwater
Principal Investigators:	MaryAnn Thomas, Paula J Mouser

Publications

There are no publications.

Progress Report 2013-2014

Contract Information

Title	Characterizing methane in geologic formations of Ohio Phase 1: Seed grant to investigate natural biogenic methane from domestic wells unaffected by oil and gas production
Project Number	N/A
Start Date	3/1/2013
End Date	7/31/2013
Focus Category	Methanogenesis, Groundwater
Keywords	Carbon, Microbial Ecology
Lead Institute	The USGS, The Ohio State University
Principle Investigators	Mary Ann Thomas and Paula Mouser

Abstract

One of the public concerns associated with shale-gas development in Ohio is stray methane—the unintentional migration of methane from hydrocarbon-producing horizons to water-supply wells or homes. Investigating stray methane complaints can be challenging for regulators/scientists because methane has multiple potential sources in addition to shale-gas development. A significant percentage of water-supply wells in Ohio likely produce methane naturally. Methane is a relatively common gas that forms in multiple environments and at a range of depths. In general, methane is derived from organic matter by thermogenic or microbial processes. Thermogenic methane is generated when deeply buried organic matter is subjected to heat and pressure, which causes complex organic compounds to be broken down into simpler molecules (the simplest of which is methane). Thermogenic methane is associated with hydrocarbon reserves, coal deposits, and organic-rich shale. Microbial methane (also referred to as biogenic or bacteriogenic methane) is formed at relatively shallow depths by the microbial metabolic processes of acetate fermentation or carbon dioxide reduction. In general, microbial methane forms in peat bogs, lakes sediments, landfills, sewers, glacial deposits, and some Paleozoic sediments. The composition and isotopic characteristics of methane and related constituents (CO_2 and H_2O) can make an important contribution to stray gas investigations because these measures can carry information about the origin, mixing, and (or) transport history of methane in subsurface formations. Age dating methods can contribute to the understanding of methane in groundwater. The overall objective is to begin the process of compiling “baseline” information about methane in geologic formations of Ohio. Funds will be used to collect methane-related information from domestic wells in areas unaffected by shale-gas development.

Methodology

We plan to collect methane-related data from a subset of the domestic wells being sampled this summer as part of an arsenic-related study in southwestern and central Ohio. Methane concentrations, composition of dissolved gases, and microbial communities in water samples will be collected and analyzed from 15 wells. For a subset of wells with the highest arsenic concentrations, we will determine characteristics of carbon and hydrogen isotope ratios of

methane, water, and carbon dioxide. Data from southwestern and central Ohio will be compared to published data from other States. The sampling will be used to develop a proposal for documenting baseline methane in other formations and geographic areas of Ohio.

Major Activities
In April and June, 2013, 11 domestic wells in southwestern and central Ohio were sampled as part of a study funded by the Miami Conservancy District and the USGS Ohio Water Science Center (Project D5W0027). Raw and treated water was collected following USGS protocols and analyzed for major ions, trace elements, nutrients, total organic carbon, and arsenic speciation at the USGS National Water Quality Laboratory (NWQL). For wells with sufficient methane, samples will also be analyzed for isotopic ratios of methane, water, and dissolved inorganic carbon. For quality assurance purposes, replicates, field blanks and source solution blanks were submitted. Water samples for analysis of microbial communities were also collected at this time. DNA has been isolated from cells concentrated on 0.2 mm filters, amplified using the 16S rRNA gene, and sequenced at OSU's Plant Microbe Genomics Facility. Data reduction is currently underway.

Principal Findings
Methane was detected in all 11 raw water samples from domestic wells. The volume percent of methane was 0.03-0.7 percent for 7 samples and 61-92 percent for 4 samples. Methane concentrations were directly related to arsenic concentrations. The isotopic signature of methane was determined for the 4 samples with higher methane concentrations, and results were consistent with biogenic methane.

Significance

The study serves as a starting point for compiling information about "baseline" methane in Ohio subsurface formations. This information could ultimately be used to assist investigations of stray gas complaints. Results of the study will be used to develop a more comprehensive proposal to assess methane in other geologic formations and geographic areas of the State. Results of the study will also contribute to our understanding of arsenic occurrence. If isotopic signatures from the domestic wells areas are not consistent with microbial drift gas, the hypothesis guiding arsenic studies in Ohio may need to be revised. This study addresses 2 goals of the USGS Water Resources mission area: (1) to effectively manage groundwater and surface-water resources for domestic, agricultural, commercial, industrial, recreational, and ecological uses, and (2) to contribute to the wise physical and economic development of our Nation's resources.

Publications/Conferences (since 1/2013)
The methane results are included in a USGS Scientific Investigations Report, which is currently in preparation.

Students Supported By Project (since 1/2013)
None to date

Awards or Achievements
None to date

Professional Placement of Graduates
None to date

Information Transfer Program Introduction

The Ohio WRC conducted a number of activities to transfer water related information to a wide range of state, federal, county, and municipal agencies, to the academic community, students, and to private citizens throughout Ohio. Specific activities included:

1) Preparation of information for the Ohio WRC website and maintenance of the website.

2) Responding to questions from the public regarding water resources issues in the State of Ohio.

3) Creating a statewide database of water related investigators in Ohio universities and sorting their research interests.

4) In collaboration with our sponsored researchers we developed one-page summaries of completed or in-progress sponsored research projects. The summaries include the importance and impact of the project's results for the State of Ohio. We disseminated these one page summaries to State Agency representatives and our Advisory Board members

5) Publishing research project summaries in the Ohio Water Table, which is the quarterly newsletter for the Water Management Association of Ohio. In this newsletter WMAO prints the Ohio WRC prepared one page research summaries (see activity (4)) that highlight specific completed research projects. These summaries include the importance of the research to the State, the most important research impacts and results, and investigator background. During the reporting period the highlighted researchers and projects were: Dr. Ethan Kubatko's project #2011OH239B, Dr. Paula Mouser's project #2011OH205B and Dr. Xioazhen Mou's project #2012OH254B. This newsletter is distributed to about 575 people in Ohio in the water resource industry from private sector (33%), universities (8%), nonprofit/citizens (17%) and state and local government agencies (42%).

6) Co-organized quarterly Ohio WRC-WMAO luncheon seminars, which includes assisting with luncheon administration and securing speakers. This past year the four luncheons were attended by approximately 112 water professionals from government, academia, NGOs and industry. The speakers and topics in this reporting period were: Stacia Eckenwiler (City of Columbus): "Creating Value from Waste: Results of a Nutrient Recovery Pilot for the City of Columbus"; Dan Mecklenburg (Ohio DNR): "Stream Restoration by Fluvial Biogeomorphic Succession"; Chad Hammerschmidt (Bowling Green State University): "Anthropogenic Unintended Consequences: Phosphorus and Alum in Grand Lake St. Marys, Ohio"; Nestor Mancipe-Munoz (University of Cincinnati): "Green-Gray Decentralized Detention Infrastructure to Control Combined Sewer Overflow".

7) Hosted and organized joint Ohio WRC-USGS mini-symposium on April 5th, 2013 to engender researcher partnerships between The Ohio State University and USGS Ohio Water Science Center researchers. Six USGS researchers and 15 OSU researchers participated in the mini-symposium, where both researchers from USGS and some from OSU presented and discussed their research interests and possible collaborations.

8) Sponsored Environmental Professional Network seminar and networking event on July 9th, 2013 entitled: "Vexing, Wicked, Intractable & Emerging Water Issues in Ohio – yes, we may have a few!, with moderator Steve Grossman, Executive Director of the Ohio Water Development Authority and panelists Mike Baker (Chief, Division of Drinking & Ground Waters, Ohio EPA), George Elmaraghy (Chief, Division of Surface Water, Ohio EPA), Ted Lozier (Deputy Chief, Division of Soil and Water Resources, Ohio DNR) and Jim Morris (Director, USGS Michigan & Ohio Water Science Centers)

9) Participation in Central Ohio Children's Water Festival on May 7th, 2013 that entailed organizing an educational booth about buoyancy. This included a hands on activity for the 4th graders where we built paper boats, which they sank using washers. We specifically worked with 6 school groups, with about 25 children in each group, but the event was attended by over 760 children. The event, now in its sixth year, aims to promote environmental awareness of our valuable water resources through interactive displays, hands-on activities and fun workshops.

10) Writing a short summary of Dr. Senko's research on acid mine drainage and bacteria that was highlighted in the publication of National Institute of Water Resources as an example model partnership between NIWR and USGS

11) Participating in quarterly meetings of the Ohio Water Resources Council, which is a partnership permanently established in 2001 by Ohio law that is designed as a forum for policy development, collaboration and coordination among state agencies, and strategic direction with respect to state water resource programs. The membership is comprised of an Executive Assistant to the governor and the heads of nine state agencies: the Ohio Departments of Agriculture, Development, Health, Natural Resources and Transportation; the Ohio Environmental Protection Agency; Ohio Public Works Commission; Ohio Water Development Authority; and the Public Utilities Commission of Ohio.

12) Continued administrative support for the Water Management Association of Ohio (WMAO) and associated WMAO meetings, conferences, and division activities. We participated in the WMAO Board meetings, encouraged participation of Ohio WRC sponsored researchers at the annual WMAO conference (6 presenters out of 50 presented research that was directly sponsored by Ohio WRC). We also provided a booth at the conference to discuss Center activities with interested researchers and practitioners.

13) Presenting at a workshop for Boat of Knowledge in Science Classroom (BooKS, http://books.ohio.edu) Professional Development organized by the Ohio River Basin Consortium and Education attended by 9 high school teachers, 12 graduate students and 5 BooKS staff members, November 9th, 2013 at Ohio University, Athens, Ohio.

14) Led the Ohio State University Shale Water Management Network faculty group to promote research surrounding water impacts as a result of shale gas exploration and production activities. The network consists of 25+ faculty that span between colleges/departments and fields, with experts from Ecology, Veterinary Health, Public Health, Environmental Engineering, Public Affairs, Environmental and Natural Resources, Agricultural Engineering, Mechanical Engineering and others. Arranged monthly meetings and their schedules, organized large proposal writing, participated in designing environmental monitoring studies etc.

USGS Summer Intern Program

None.

Student Support					
Category	**Section 104 Base Grant**	**Section 104 NCGP Award**	**NIWR-USGS Internship**	**Supplemental Awards**	**Total**
Undergraduate	6	0	0	1	7
Masters	6	0	0	1	7
Ph.D.	4	0	0	1	5
Post-Doc.	1	0	0	0	1
Total	17	0	0	3	20

Notable Awards and Achievements

The WMAO President Service Award presented to Ohio Water Resources Center, November 2013, for their continued service to WMAO through their co-sponsorship of topical water resources seminars and the Ohio Water Education Project WET. Peter W. Soltys

2012OH259B Ohio Water Development Authority, “Observations and modeling of wetland methane emissions”. PI Gil Bohrer. Funded for period 2013-2015. $164,495.

2011OH205B Department of the Interior, USDA, “An integrated approach to foster science-based management of agricultural drainage channels in the Western Lake Erie basin”. PI Jon Witter, co-PI Paula Mouser. Funded for period: 2013-2016. $659,979.

2013OH292B NOAA – Ohio Sea Grant College Program, R/ER-104. “Source tracking and toxigenicity of Planktothrix in Sandusky Bay.” PI George Bullerjahn. Funded for period: 2014 – 2016. $103,833.

2013OH300B Ohio Water Development Authority, PI Linda Weavers in the Department of Civil, Environmental and Geodetic Engineering (CEGE), and co-PIs Paula Mouser (CEGE) and Henk Verweij in Material Sciences at Ohio State. Funded for period: 2013-2015. $200,000.

2013OH297B Paul Hochwalt – 2014 University of Cincinnati STEM Excellence in Research Award, Biology: This award included a $500 honorarium and was awarded based on Paul’s research funded by this project. PI Ishi Buffam.

Publications from Prior Years

1. 2010OH157B ("Nitrogen Removal by Microbial-Mediated Processes Under Hypoxic Conditions in Lake Erie") - Articles in Refereed Scientific Journals - Xiaozhen Mou, Jisha Jacob, Xinxin Lu, Steven Robbins, Shulei Sun, and Joseph D. Ortiz. (2013) “Diversity and distribution of free-living and particle-associated bacterioplankton in Sandusky Bay and adjacent waters of Lake Erie Western Basin”, Journal of Great Lakes, 39: 352-357
2. 2009OH89B ("MONITORING THE ROLE OF BIOFILM BIOPOLYMERS AGAINST DISINFECTANTS IN WATER DISTRIBUTION SYSTEMS") - Articles in Refereed Scientific Journals - Zheng Xue, Christopher M. Hessler, Warunya Panmanee, Daniel J. Hassett, and Youngwoo Seo (2013) “Pseudomonas aeruginosa inactivation mechanism is affected by capsular extracellular polymeric substances reactivity with chlorine and monochloramine”, FEMS Microbial Ecology, 83: 101-111